2022

AN ANTIMICROBIAL POLYDOPAMINE SURFACE COATING TO REDUCE BIOFOULING ON TELEMETRY TAGS USED IN MARINE CONSERVATION PRACTICES

Ariana Smies
Michigan Technological University, agtyo@mtu.edu

AN ANTIMICROBIAL POLYDOPAMINE SURFACE COATING TO REDUCE BIOFOULING ON TELEMETRY TAGS USED IN MARINE CONSERVATION PRACTICES

By

Ariana G. Smies

A DISSERTATION

Submitted in partial fulfillment of the requirements for the degree of

DOCTOR OF PHILOSOPHY

In Biomedical Engineering

MICHIGAN TECHNOLOGICAL UNIVERSITY

2022

This dissertation has been approved in partial fulfillment of the requirements for the Degree of DOCTOR OF PHILOSOPHY in Biomedical Engineering.

Department of Biomedical Engineering

Dissertation Co-Advisor: *Sean J. Kirkpatrick, Ph.D.*

Dissertation Co-Advisor: *Rupak M. Rajachar, Ph.D.*

Committee Member: *Smitha Rao Hatti, Ph.D.*

Committee Member: *Alexandre Zerbini, Ph.D.*

Committee Member: *Jooke Robbins, Ph.D.*

Committee Member: *Bruce P. Lee, Ph.D.*

Department Chair: *Sean J. Kirkpatrick, Ph.D.*

Table of Contents

List of Figures

CHAPTER 4

List of Tables

CHAPTER 2

CHAPTER 3

Preface

This dissertation describes the development and characterization of an antimicrobial polydopamine surface coating to be used to reduce the chances of biofilm formation and subsequent tissue infection in cetacean conservation applications. Several chapters are either in preparation for or published in open-source scientific journals.

Chapter 1 is a literature review. This review explores the use of satellite telemetry tags in marine conservation applications, current antibiotic and antimicrobial-based solutions used to reduce chances of infection, and how polydopamine (pDA) can act as an antimicrobial through the release of H_2O_2. This chapter also includes the rationale, hypotheses, and specific aims for this work.

Chapter 2 contains the creation and characterization of the pDA-based surface coatings. The data in this chapter is published in Frontiers in Chemistry (2019). I performed a majority of the work with help from Maureen Hennenfent to characterize release profiles and Fatemeh Razaviamri to evaluate the hydrophilicity of the surfaces. The conclusions of this work are my own and I am the main author of this work.

Chapter 3 explores the antimicrobial character of pDA coatings. The data in this chapter was obtained by both myself and Jeremy Wales. Part of this work is published in Frontiers in Chemistry (2019) while the rest is in preparation for publication in Frontiers in Marine Science (2022). The conclusions of this chapter are my own and I am the main author for both the previous publication and the publication in preparation.

Chapter 4 covers the general biocompatibility of the pDA coatings using four model cell types. This data is in preparation for submission in an open-source journal. I did all the experimental work and the conclusions drawn in this chapter are my own. I am the main author of this work.

Chapter 5 covers the ability of the pDA coatings to affect the expression of the AMP dermcidin and to impact the differentiation of pre-adipocytes. This data is in preparation for submission in an open-source journal. I did all the experimental work and the conclusions drawn in this chapter are my own. I am the main author of this work.

Chapter 6 is a summary of all findings and conclusions reached in this dissertation.

Acknowledgements

There are many people I would like to acknowledge for helping me complete this work, but first, I want to thank my advisor - Dr. Rupak Rajachar - and the members of my committee for providing me with the opportunity to earn my doctorate on such a fantastic project. It is not often that a graduate student who works on projects in the biological/ medical realm gets to witness their work be implemented into the field.

Next, I would like to thank my friends who have been there for me through difficulties with experiments and support me in my endeavors outside of academia. To Pegah, I can't express my gratitude for how much you have helped me with the science and acting as someone to help me vent life stressors. To Maureen, the post-experiment and post-meeting discussions got me through so many hard times, but the lavender coffee runs and endless bad whale jokes on every email brightened my day without fail. And to Laura, you were always there to help whenever I needed someone to lean on. You kept life from getting too dull and, without fail, managed to get me to laugh every time we talked.

I also want to thank my husband - Joseph Smies - for endlessly supporting me in my career goals. Completing a Ph.D. while simultaneously maintaining a long-distance relationship was not easy, but Joe, you made it much more manageable. Thank you for being willing to take the long car rides and being there to remind me why I wanted to do this when I felt like quitting. Words will never be enough to convey how much you have helped me - I couldn't have done it without you.

And finally, I would like to thank my parents - I wouldn't be who I am today without you. You stressed education and compassion, and I feel this dissertation encompasses both of those values.

List of Abbreviations

aa	Amino acids
AMP	Antimicrobial Peptide
CT	Coating Time
DCD	Dermcidin
DMEM	Dulbecco's Modified Eagle Medium
EGF	Epidermal Growth Factor
EMEM	Eagle's Minimum Essential Medium
FBS	Fetal Bovine Serum
FOX	Ferrous Oxidative
H_2O_2	Hydrogen Peroxide
HIF	Hypoxic Induction Factor
HLA	Human Leukocyte Antigen
NADPH	Nicotinamide Adenine Dinucleotide Phosphate
NO	Nitric Oxide
PBS	Phosphate Buffered Saline
pDA	Polydopamine
RNS	Reactive Nitrogen Species
ROS	Reactive Oxygen Species
SS	Stainless Steel
TGF	Transforming Growth Factor
TSB	Tryptic Soy Broth
VEGF	Vascular Endothelial Growth Factor

Abstract

Satellite telemetry tags are used to track the migration patterns of large cetaceans. These tags penetrate the dermis and remain embedded in the underlying blubber tissue. As the dermis of cetaceans is host to a diverse microbiome, and it is impossible to clean the skin before implanting the devices, the potential for infection is increased when the tags penetrate through the skin. H_2O_2 is a potential antimicrobial agent that, in addition to showing broad-spectrum efficacy against gram-negative and gram-positive bacteria, can promote wound healing outcomes by promoting proliferative factors and peptides that protect against oxidative stress. However, delivering H_2O_2 in a controlled manner and maintaining a stable solution concentration has previously been difficult. Polydopamine (pDA) is one polymer that can release H_2O_2 in a controlled manner. During polymerization, the catechol on the monomer of dopamine will oxidize and generate H_2O_2. However, not all catechol will be oxidized after polymerization allowing for continued generation after coating deposition. This release profile can be tailored through simple changes in the coating environment such as solution pH, temperature, and coating time. We found, when exposed to a high pH (8.5) and an increased coating temperature (37°C) there was significantly more release compared to other coating conditions tested (40μM vs 80μM). These controlled doses of H_2O_2 generated through additional oxidization reduce bacterial adhesion from common terrestrial bacteria strains (*Escherichia coli* [70% reduction] and *Staphylococcus epidermidis* [25% reduction]) and aquatic strains from the two most populous genera located in the microbiome of healthy cetaceans (*Psychrobacter* [80% reduction] and *Tenacibaculum* [70% reduction]) on the surface of medical-grade stainless steel. H_2O_2 generated by our pDA coatings was also seen to be less toxic against model cell types over a 24 hour period indicating cells are more tolerant to H_2O_2 when delivered in a continuous dose as opposed to bolus doses. These same coatings, when introduced during the differentiation process, are able to promote the differentiation of pre-adipocytes into adipocytes (23% increase) and potentially induce dedifferentiation of adipocytes into their precursor cell types. In a model cell type, the pDA coatings also increase the endogenous expression of the antimicrobial peptide dermcidin (72% increase) without the same significant decrease in cell viability seen after a bolus dose of H_2O_2.

CHAPTER 1

INTRODUCTION

1.1 BACKGROUND AND SIGNIFICANCE

The ability to track the long-term migratory behavior of cetaceans is a major area of development in the marine conservation field. Currently, satellite telemetry tags that penetrate through the dermis and into the underlying tissue are utilized to obtain this data (Mate et al., 2007; Balmer et al., 2014). However, due to the nature of these tags penetrating through the dermis which contains a highly diverse microbiome (Nelson et al., 2015) the chances for infection are increased. The tag can act as a vehicle for bacterial colony adhesion and subsequent biofilm formation which can lead to long-term infection in which the outcomes range from premature tag ejection to death. To prevent infection multiple strategies have been employed, mainly tag sterilization using ethylene oxide and antibiotic surface coatings (Andrews et al., 2019). With continued use, there is an increased possibility that antibiotic-resistant pathogens could evolve and cause harm. Due to this concern, there is an interest in developing methods in which non-antibiotic-based approaches can be deployed to prevent infection. Hydrogen peroxide has previously been widely used as a disinfectant and wound debridement solution (Linley et al., 2012). As a reactive oxygen species, H_2O_2 has the potential to act as a broad-spectrum biocide in high doses (>10mM) while acting to improve wound healing at lower doses (1-10mM) (Zhu et al., 2017). The goal of this work is to develop a non-antibiotic-based surface coating that utilizes H_2O_2 to reduce the chance of biofilm formation on the surface of medical grade stainless steel without hindering the local wound healing mechanisms.

1.2 CETACEAN RESEARCH AND CONSERVATION

Over the last two centuries, cetaceans were hunted to near extinction for food as well as sport and the populations have, more recently, been impacted by ship strikes and fishing gear entanglements. This decrease in population has led to many changes throughout the ocean - most notably ocean acidification and decreases in biodiversity (Trathan and Reid, 2009; Pershing et al., 2010; Guertin, 2016). Recently, some populations of cetaceans have been able to recover due to conservation-related efforts (Best, 1993; Zerbini et al., 2019; Calderan et al., 2020). The most effective conservation efforts for large cetaceans mainly

center around developing policies that create protected areas where populations are less likely to encounter common causes of death for cetaceans: entanglements and ship strikes (Clapham et al., 1999; Van der Hoop et al., 2013; Robbins et al., 2015; Schoeman et al., 2020). To successfully create these protected areas, conservationists and policymakers must first know what paths cetaceans are most likely to use during migration as well as areas to congregate for feeding and breeding. To do this, satellite telemetry tags are attached and the desired patterns are observed (Garrigue C et al., 2010; Modest et al., 2021; Urbán R et al., 2021). These tags, made using medical-grade stainless steel (316L), can be broken down into two separate types: invasive and non-invasive (Mate et al., 2007; Andrews et al., 2019).

Non-invasive tags adhere to the surface of the skin and are primarily attached using suction cups. However, the outer layer of the epidermis is estimated to slough off every 12 hours (~8.5x faster than humans) (Hicks et al., 1985), which may lead to tags detachment within a few hours of deployment. These tags are primarily used to monitor diving behavior due to their short service life (Croll et al., 2001; Madsen et al., 2002; Heide-Jørgensen et al., 2013). Superficial telemetry tags have the benefit of remaining on the surface of the skin which diminishes the chances for complications including infection or necrosis of the attachment site. There have been improvements made to these dermal tags over the past decade (Moore et al., 2011). These improvements include the addition of adhesives or modifying the site at which the tags are placed. While diving data is important and can give researchers a better idea of behavior for healthy populations or reveal the diving behavior for unhealthy individuals, migration patterns prove to be more beneficial in conservation efforts.

Invasive tags penetrate through the skin layer into and sometimes through the underlying tissue (blubber) (**Figure 1.1**) (Szesciorka et al., 2016; Guzman and Capella, 2017). These tags have a longer service life than non-invasive tags and are typically used to monitor migration patterns (Robbins et al., 2013) however they can also be used to observe diving patterns. There are three categories of invasive tags: type A, type B, and type C (Andews et al., 2019). Type A and B tags carry the telemetry device (electronics) externally while having a barbed anchor into the underlying tissue (Type A) or having a bolt pass through the tissue to provide the anchor point - similar to a piercing (Type B). Type C tags are also known as consolidated tags. These tags are similar to type A tags, however, the

electronics are carried inside the tag body. The telemetry device is triggered via a salt-water switch so only a minor portion of the tag is external (**Figure 1.1**)

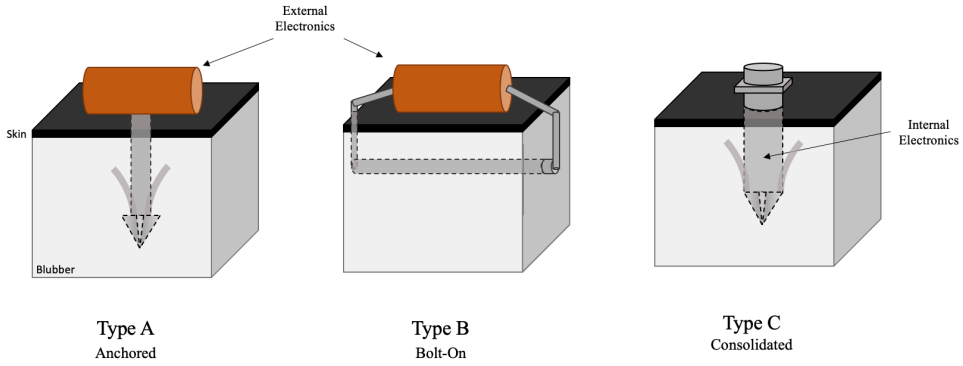

Figure 1.1 | *Types of Invasive Telemetry Tags.* Satellite telemetry tags that penetrate through the skin and into the underlying tissue are considered to be invasive tags. There are three main types: Type A - Anchored, Type B - Bolted on, and Type C - consolidated. Type A and B tags have externally located electronics while Type C tags house the electronics in the tag body.

Due to the invasive nature of tags that penetrate through the dermis and into the underlying tissue, there is a concern for infection as there is a complex microbiome present (Apprill et al., 2014; Nelson et al., 2015; Bierlich et al., 2018). There are few infections known to be caused by an implanted tag, however, one prominent infection that occurred in an orca resulted in the death of the animal (Yates and Ford, 2016). After this incident, there was an increase in the preventative use of antibiotics which - while beneficial in the short term - may lead to the development of antibiotic-resistant pathogens (Moore et al., 2012; Hjelmstedt et al., 2020).

1.3 Antibiotic Surface Coatings

A wide variety of antibiotics have been used on the surface of metallic implants to prevent the formation of biofilms. A few prominent antibiotics used in surface coatings include gentamicin for gram-negative bacteria and vancomycin for gram-positive bacteria. These antibiotics use two different mechanisms to prevent bacterial growth: Gentamicin disrupts protein synthesis through the A-Site on the 50S protein (**Figure 1.2A**) (Hahn and Sarre, 1969) while vancomycin disrupts cell wall synthesis (**Figure 1.2B**) (Watanakunakorn, 1984). These antibiotics have been widely used in surface coatings and have shown to be effective at preventing bacterial adhesion to the surface of implants (Darouiche et al., 1994; Jensen et al., 2019). However, due to the wide use of

these antibiotics, resistances have been observed in clinical applications (Livermore, 2000).

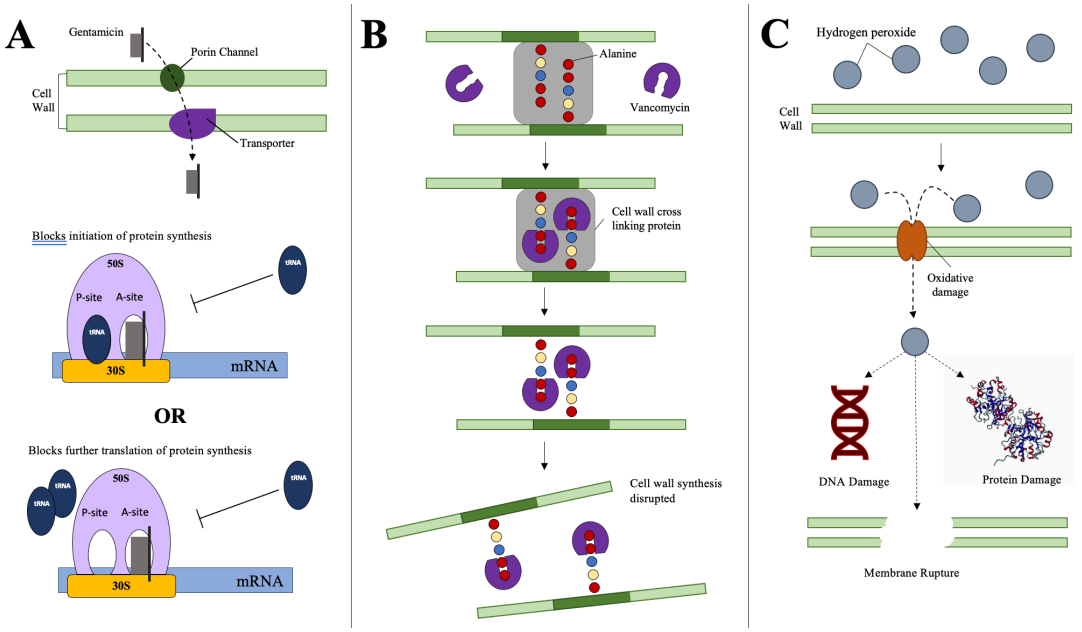

Figure 1.2 | *Mechanism of action for antibiotic activity for (A) Gentamicin, (B) Vancomycin, and (C) Hydrogen Peroxide.* (A) Gentamicin enters gram-negative bacteria through the cell membrane via porin channels and a molecule transporter. Once the gentamicin has entered the bacteria, it acts as an antibiotic through two possible mechanisms by binds to the 30S subunit located on mRNA strands and occupies the A-site in the 50S ribosomal subunit. Through the occupation of the A-site, gentamicin will either block the initiation of protein synthesis or block further translation of protein synthesis. (B) Vancomycin works in gram-positive bacteria and acts to disrupt cell wall synthesis. Vancomycin will bind to the alanine amino acids that act as cross linking vectors and cause the cell wall cross linking protein to detach and therefore disrupt cell wall synthesis. (C) Hydrogen peroxide, which can be effective on both gram-positive and gram-negative bacterial strains acts to inflict oxidative damage on the surface of the cell wall which can lead to bacterial death through 3 outcomes: [1] damaging the cell's DNA, [2] inducing membrane rupture, and [3] damaging proteins within the bacterium.

1.3.1 GENTAMICIN

Gentamicin is a commonly used antibiotic for gram-negative bacteria (Hahn and Sarre, 1969). It acts to prevent bacterial growth through a disruption in protein synthesis. The gentamicin molecule will enter the bacterial cell through a porin channel and will bind to the 30S subunit on mRNA which will prevent proper binding on the A-site of the 50S ribosomal subunit (**Figure 1.2A**) (Beganovic et al., 2018). This will disrupt subsequent protein synthesis and, ultimately, cause cell death. Resistance to gentamicin was first observed in the 1970s (Dowding, 1977). Bacteria evolved a resistance through alterations

in the ribosomal unit as well as through alterations in the porin channels (Shakil et al., 2008).

1.3.2 VANCOMYCIN

The first sign of resistance to vancomycin occurred approximately 30 years ago (~1990) (Zanella et al., 1999). It was thought resistance was not likely to form due to the simple but effective nature of the antibiotic. Vancomycin, instead of targeting a singular protein, target the amino acid alanine to disrupt cell wall synthesis and is only effective in gram-positive bacteria. This target makes it difficult to form a simple resistance mechanism making it a highly effective antibiotic. However, a complex mechanism has been formed in various bacteria that confers resistance to vancomycin (Bugg et al., 1991; Périchon and Courvalin, 2012). The most common mechanism relies on the adjustment of the amino acid group to which vancomycin has a high affinity, d-Ala-d-Ala, to one in which vancomycin has a lower affinity, d-Ala-d-lac or d-Ala-d-Ser (**Figure 1.2B**) (Hong et al., 2004). Due to this resistance, vancomycin is currently being used as a sort of 'last ditch' effort for dealing with infection for gram-positive bacteria as, once the resistance is universal, the antibiotic will be rendered ineffective.

1.4 ANTIMICROBIAL AGENTS

Alternatives to antibiotics are becoming more and more prevalent. A number of groups are exploring the antimicrobial properties of metallic ions, typically incorporated via nanoparticles, for both biological and commercial applications. Others are exploring naturally occurring ROS such as H_2O_2 and reactive nitrogen species (RNS) such as nitric oxide (NO) to act as a bactericide as well as promote wound healing.

1.4.1 METALLIC IONS

Silver ions (Ag^+) have various pathways in which they can inhibit reproduction in bacteria (Kim et al., 2007). Initially, Ag^+ ions will enter into the bacteria cell via their affinity with sulfur proteins (**Figure 1.3A**) (Jung et al., 2008). Next, the ions will either bind to ribosomes - which will denature them - and inhibit protein synthesis or they will bind to respiratory enzymes causing generation of ROS and disruption of ATP production (**Figure 1.3B-C**) (Dakal et al., 2016). The ROS can then act to induce cell membrane disruption (**Figure 1.3D**). The excess of ROS, in addition to the presence of Ag^+, will

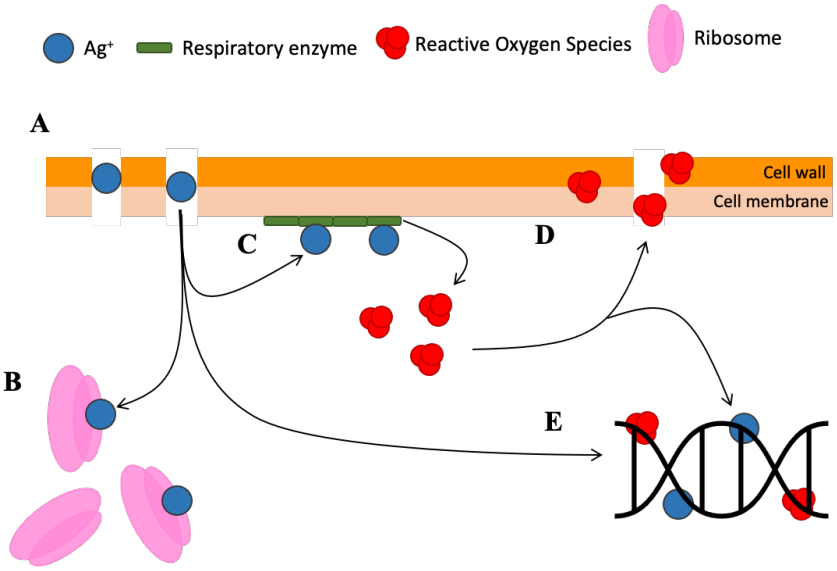

Figure 1.3 | *Mechanism of action for silver metallic ions (Ag^+).* (A) When exposed to the cell wall of a bacterium Ag+ ions will bind to sulfur proteins and penetrate through the cell wall. Once inside the bacterium, Ag+ ions can take a few paths; (B) The ions can bind to and denature ribosomes which will inhibit protein synthesis. (C) Ion can also bind directly to respiratory enzymes which will cause an increased generation of ROS and disruption of ATP production. The increased presence of ROS can further rupture the cell wall as well as disrupt DNA synthesis. Finally, (E) ions can also directly bind to DNA and disrupt further synthesis.

bind to DNA and disrupt further synthesis (**Figure 1.3E**) (Kim et al., 2007). Ag^+ ions are most effective at disrupting the growth of gram-negative bacteria due to the narrower cell wall when compared to gram-positive bacteria (Morones et al., 2005). When incorporated into nanoparticles, an aggregation can occur which will cause cell wall perforation and can disrupt cell wall synthesis by embedding themselves.

The antimicrobial capability of copper ions (Cu^{2+}) is mostly attributed to its support of the Fenton reaction which leads to the production of hydroxy-radicals (Rodriguez-Montelongo et al., 1993; Pham et al., 2013). However, when introduced to bacteria via nanoparticles, copper can penetrate through the cell wall and act to damage proteins and DNA in addition to increasing the concentration of ROS within the bacteria (Usman et al., 2013). The efficacy of copper nanoparticles is highly dependent on their size, smaller particles are associated with an increased ability to penetrate and accumulate within the bacterial cell wall (Chatterjee et al., 2012).

1.4.2 Reactive Oxygen/Nitrogen Species

The main mechanism for the death of bacterial cells using non-antibiotic approaches centers on the accumulation of ROS within the cell which causes oxidative damage to the cell wall and subsequent DNA or protein damage (**Figure 1.2C**). The primary mechanism for bacterial cell death using reactive species centers around the accumulation of H_2O_2.

Hydrogen Peroxide

H_2O_2, although only considered a mild ROS, is a very powerful oxidizer and has been demonstrated to function as an effective broad-spectrum biocide in many industrial and biomedical applications (Linley et al., 2012). It is an environmentally friendly disinfectant as it has biocompatible degradation products (oxygen and water) (Pędziwiatr et al., 2018). H_2O_2 is generated in small doses endogenously during a wide variety of normal metabolic processes such as phagocytosis of invading organisms or in damaged tissue (Yoo and Huttenlocher, 2009; Goudarzi et al., 2018b). It activates many signaling pathways and is continuously suggested as a second messenger that exerts prolonged effects (Appenzeller-Herzog et al., 2016). The biological responses in humans to H_2O_2 are highly dependent on its concentration (**Figure 1.4**). The introduction of a moderately high concentration of H_2O_2 (10^3-10^4μM) is considered to be bacteriostatic, or limiting bacterial growth, and has been shown to accelerate wound healing in humans (**Figure 1.4A**) (Roy et al., 2006; Niethammer et al., 2009; Loo et al., 2012). The concentration that will induce bacteriostatic behavior when released in continuous quantities has been found to be less than that of a one-time dose (**Figure 1.4B**). High concentrations of H_2O_2

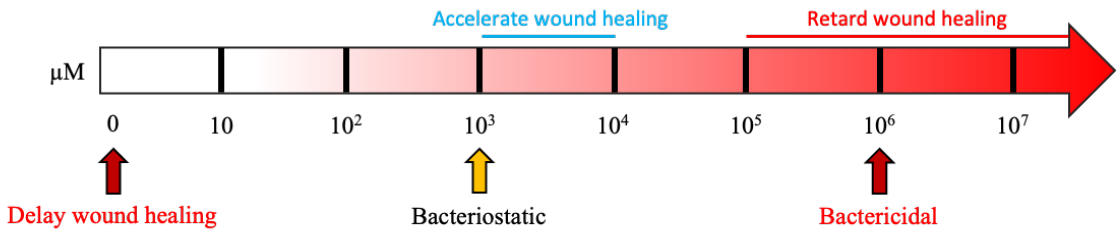

Figure 1.4 | *Biological effects of H_2O_2 delivered in a bolus dose correlated to concentration.* If you remove H_2O_2 from the system completely, it will inhibit wound healing and, if there are high concentrations present, there will be increased cell death which will retard wound healing. There is a 'goldilocks' zone in terms of H_2O_2 concentration in human biological systems (10^3-10^4μM) where there will be accelerated wound healing and bacteriostatic conditions.

(>10^6μM) are considered to be bactericidal, or lethal to bacterial cells, but can retard wound healing (Sen and Roy, 2008a). Complete removal of H_2O_2 by catalase also has been shown to delay wound healing potentially forming a chronic wound environment. It is currently unknown what range of H_2O_2 will promote or accelerate wound healing in cetaceans. Thus, H_2O_2 concentration needs to be carefully tailored depending on the application.

Nitric Oxide (NO)

NO acts similarly to H_2O_2 in that the cellular response is heavily dose-dependent. At low concentrations (<1μM) NO acts as a signaling molecule to recruit macrophages to a wound site as well as protect against oxidative damage induced by the accumulation of H_2O_2 (Wink and Mitchell, 1998; Radi, 2018). At larger concentrations, NO will induce nitrosation, nitration, and oxidation reactions. These reactions will damage the cells by altering the DNA, inhibiting enzyme functions, and inducing lipid peroxidation (Noriko et al., 1993; Toledo Jr and Augusto, 2012).

Due to the very short half-life of NO, it is not responsible for damaging the DNA within a bacterial cell, rather, the reactive nitrogen species formed via autoxidation of NO damages the DNA in three distinct mechanisms: (1) a direct reaction with the DNA structure (Hogg and Kalyanaraman, 1999), (2) increased generation of alkylating agents and hydrogen peroxide, and (3) inhibiting DNA repair. The antimicrobial activity of NO is enhanced by the presence of ROS such as H_2O_2 as well as glutathione (Privett et al., 2012).

1.4.3 DERMCIDIN

Dermcidin can be found in the secretions of eccrine sweat glands and in various types of cancer cells and has recently been found in significant quantities in the blubber of cetaceans (Rieg et al., 2006; Stewart et al., 2007; Kershaw et al., 2018). The two anionic derivatives of dermcidin are DCD-1 (47mer) and DCD-1L (48mer) where the only difference is the presence of the last amino acid, leucine (Burian and Schittek, 2015). There is a cationic dermcidin derivative, SSL-25 (25mer), however, it has not been as well studied. Compared to other antimicrobial peptides (AMPs), dermcidin acts in a unique fashion. DCD-1L is initially unstructured and monomeric (**Figure 1.5A**). Once it ventures close enough to the negatively charged bacterial membrane, both gram-positive

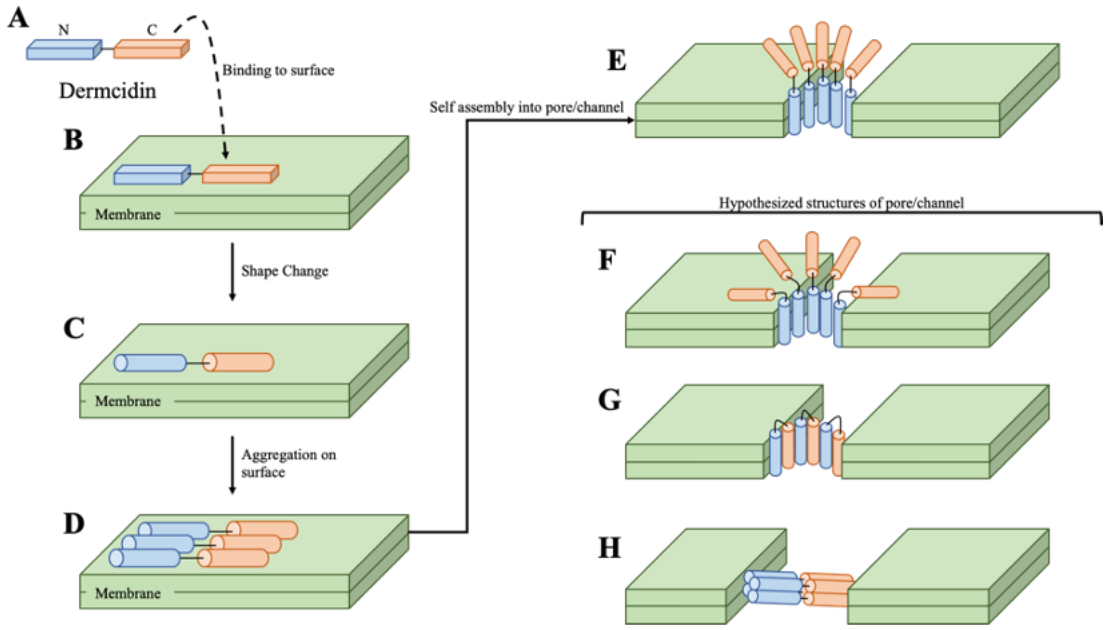

Figure 1.5 | *Dermcidin proposed mechanisms of action*. (A) DCD-1L before attachment, it is an unstructured monomeric unit. (B) Monomeric unit attaches to the bacterial membrane. Depending on the charge of the membrane - which is typically negatively charged - either the cationic N-terminal region or the anionic C-terminal region will bind. (C) When the C-terminal interacts with the membrane there will be a change in the conformation of the peptide, mainly it will elevate from a random coil to an alpha-helical conformation. (D) Next, it will self-assemble into a higher oligomeric state. This will now form an ion channel in the membrane resulting in cell death. There are a few hypothesized models of what this channel looks like structurally. (E) The negative C-terminus is floating above the membrane while the positive N-terminus is holding the ion channel open, (F) The cationic N-terminal will fold back to the anionic C-terminal forming a transmembrane hairpin, or (G) the DCD-1L becomes tilted enough to maintain the channel within the membrane. (Adapted from Burian and Schittek, 2015)

and gram-negative bacteria have negatively charged cell walls, the cationic N-terminal region will attach while the anionic C-terminal region will remain unattached (**Figure 1.5B**) (Senyürek et al., 2009). When the C-terminal interacts with the membrane there will be a change in the conformation of the peptide, mainly it will elevate from a random coil to an alpha-helical conformation (**Figure 1.5C**). Once this new conformation is attained it will self-assemble (**Figure 1.5D**) into a higher oligomeric state. This will now form an ion channel in the membrane resulting in cell death (**Figure 1.5E**). There are a few hypothesized models of what this channel looks like structurally. One group hypothesizes the negative C-terminus is floating above the membrane while the positive N-terminus is holding the ion channel open (**Figure 1.5F**). Another group believes the cationic N-terminal will fold back to the anionic C-terminal forming a transmembrane

hairpin (**Figure 1.5G**). The third model hypothesizes the DCD-1L becomes tilted enough to maintain the channel within the membrane (**Figure 1.5H**).

1.4.4 POLYDOPAMINE

A more recent advance in antimicrobial technology stems from the discovery of polydopamine (pDA). In the 1990s, scientists were observing how marine mussels adhere to various organic and inorganic surfaces via mussel adhesive proteins (Filpula et al., 1990). The features that inspired pDA were primarily 3,4-dihydroxy-L-phenylalinine (DOPA) and lysine/histidine residues. DOPA contributes to the adhesive character primarily via high catechol content (Lee et al., 2007). The adhesive properties of pDA stem from the abundance of catechol present on the monomer (Lee et al., 2007; Beckford and Zou, 2014). Catechol located on DOPA will interact with primary amines and form strong bonds which led to growing interest in catechol-based adhesives. Its was found catechol has the ability to adhere to both organic and inorganic surfaces through interaction with amine groups making it one of the most versatile adhesives available (Saiz-Poseu et al., 2019).

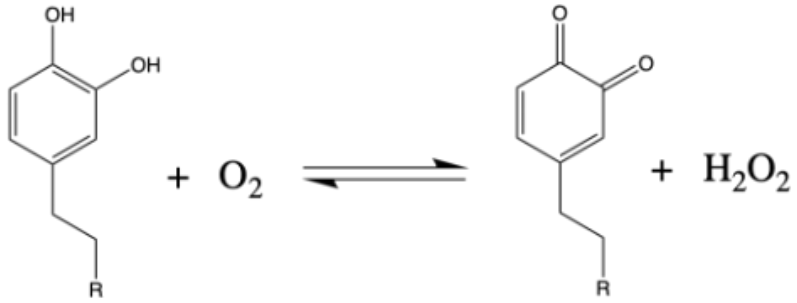

Figure 1.6 | *Mechanism of H_2O_2 release from catechol.* Autoxidation of catechol moiety on a dopamine molecule into semiquinone and quinone in a neutral to basic solution, or when exposed to oxygen, results in the generation of H_2O_2.

Dopamine-HCl is a relatively inexpensive and commercially available reagent that has a high catechol concentration which makes it a good substitute for DOPA in adhesive development and the exploration of catechol chemistry. When dopamine-HCl is oxidized, a dopamine quinone will form which can then self-assemble onto the surface of whatever substrate is chosen and form a polydopamine coating. In addition to being a strong adhesive, during polymerization, catechol releases the ROS H_2O_2 which, as previously discussed, has both antimicrobial and wound healing capabilities (**Figure 1.6**) (Meng et al., 2019; Kord Forooshani et al., 2020). However, all catechol are not necessarily

oxidized during polymerization which can allow for further H_2O_2 generation after coating formation. These coatings have been shown to release low doses of H_2O_2 when exposed to oxygen (Tyo et al., 2019) (**Figure 1.7**).

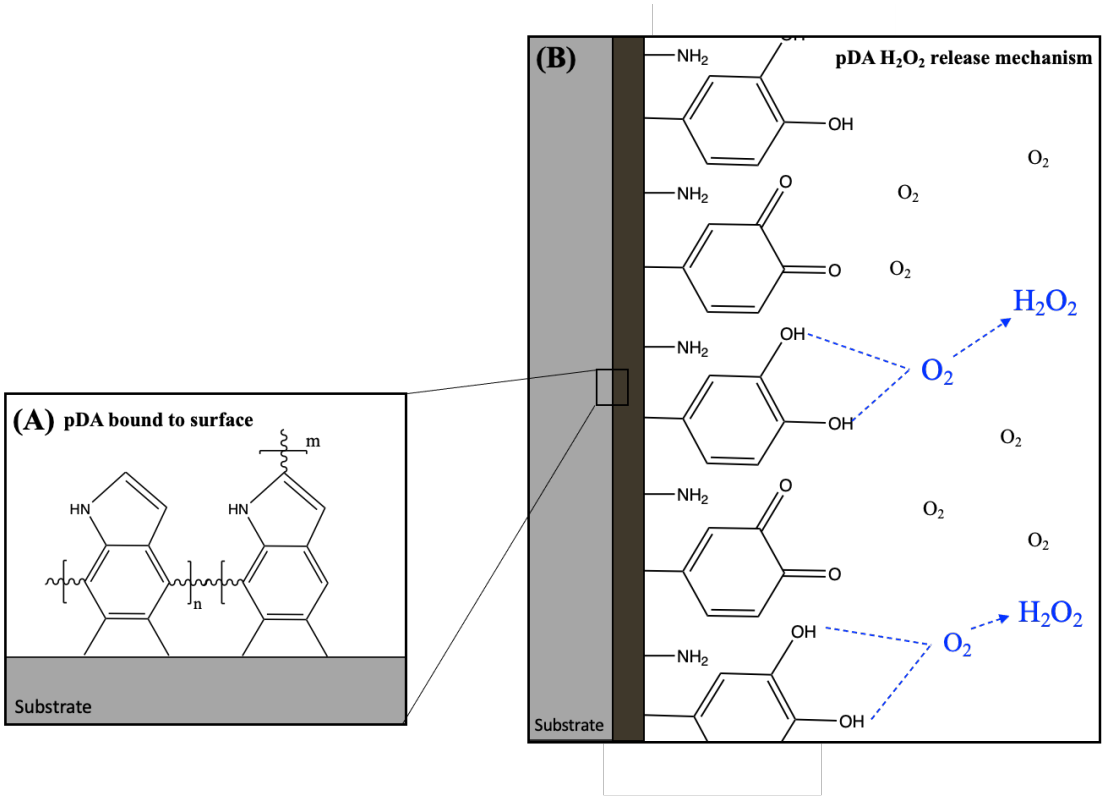

Figure 1.7 | *Schematic representation of pDA polymerization on the surface of a stainless steel substrate and mechanism of H_2O_2 release from pDA surface coatings.* (A) Chemical structure of pDA which binds to the surface of the stainless steel. Additional dopamine molecules can bind vertically to thicken the coating. (B) When exposed to oxygen, the catechol on unoxidized dopamine molecules will oxidize and form the reactive oxygen species hydrogen peroxide.

1.5 Wound Healing

Oxidant homeostasis, or a balance in redox control, plays an important role in rapid dermal healing (Sen and Roy, 2008b). The shift of homeostasis results in oxidative stress or hypoxic stress which can induce the formation of a chronic wound. Wound healing is a dynamic process that can be described with different but overlapping phases including inflammation, proliferation, and tissue remodeling. In humans, the inflammation phase is initiated by infiltration of immune cells, including neutrophils and macrophages, at the wound site. This results in the production of large amounts of ROS (Bae et al., 2009). ROS are essential in the differentiation of M2 macrophages which induce tissue

regeneration and anti-inflammatory responses. When the levels of ROS are then reduced, cellular migration and proliferation are encouraged. ROS are highly reactive chemical species containing oxygen (O_2) and are divided into two different groups: superoxide ($O_2^{\cdot -}$) and hydroxyl radical ($OH^{\cdot}$) and non-radical species such as H_2O_2. The presence of H_2O_2 can induce differentiation of keratinocytes (Lisse et al., 2016) which causes the restoration of the epidermal barrier as well as differentiation of adipose-derived stem cells (Goudarzi et al., 2018a). Topical administration of H_2O_2 has been shown to promote wound healing in an impaired healing animal model (Gao et al., 2021; Rai et al., 2021) while complete removal has been shown to significantly delay the wound healing process (Schreml et al., 2010).

1.6 AIMS/HYPOTHESIS

The purpose of this work is to increase tag retention in the blubber of cetaceans by modifying current tags used in the field to be more biocompatible. Biocompatibility is defined as both reducing infections as well as modulating cellular responses within the tissue that will improve wound healing outcomes, for example, through an increase in adipogenic factors. We hypothesize a conformational surface coating with a tailored release of reactive oxygen species (ROS) can be used to (1) prevent the formation of biofilms on the surface of 316L stainless steel and (2) modulate the cellular behavior of

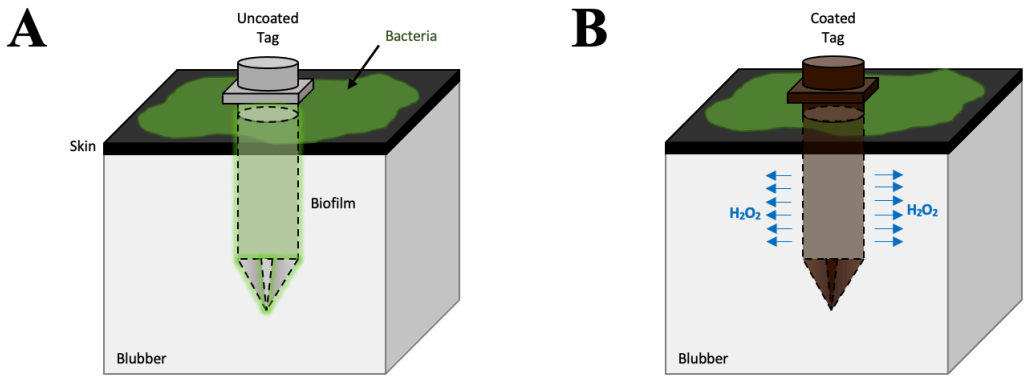

Figure 1.8 | *Schematic representation of the predicted behavior of bacteria on (A) uncoated and (B) polydopamine coated tags.* Stainless steel tags coated with polydopamine will release hydrogen peroxide when allowed to oxidize. This will subsequently prevent bacteria from the microbiome naturally present on the skin from establishing a biofilm on the stainless-steel surface. Hydrogen peroxide will be released via the catechol side chains, they contain hydroxyl groups which, when exposed to oxygen, will turn into double bonded oxygen groups. The hydrogen atoms will bind with the oxygen to form hydrogen peroxide.

model cell types, such as adipocytes and fibroblasts, to potentially increase wound healing outcomes (**Figure 1.8**).

HYPOTHESIS 1 – HYDROGEN PEROXIDE RELEASED FROM CONFORMAL PDA SURFACE COATINGS CAN BE CONTROLLED AND OPTIMIZED FOR SERVICE ENVIRONMENTAL CONDITIONS.

Specific Aim 1: *Design and evaluate the chemical and physical properties of conformational surface coatings that release ROS.* The release profile of H_2O_2 from surface coatings is dependent on the environment in which the coating was created (e.g. temperature, pH, coating time, ion content). The release profile of H_2O_2 from surface coatings is also known to be dependent on the environment in which the coatings are evaluated. Polydopamine surface coatings have recently been found to release ROS when allowed to oxidize. The goal of specific aim 1 is to characterize and evaluate the differences in release profiles from coatings when exposed to various relevant service environments.

HYPOTHESIS 2 – HYDROGEN PEROXIDE RELEASED FROM CONFORMATIONAL PDA SURFACE COATINGS CAN INDUCE BACTERIOSTATIC BEHAVIOR AS WELL AS PREVENT BIOFILM FORMATION FROM MARINE-SPECIFIC BACTERIAL STRAINS.

Specific Aim 2: *Determine the required release profile from a pDA surface coating to prevent biofilm formation on the surface of 316L stainless steel and evaluate its ability to prevent bacterial adhesion of marine-specific bacterial strains*. Bacteria have different mechanisms in which they will respond to ROS. Defense mechanisms include the use of catalase and enzymes to break down H_2O_2 into water and oxygen. The time-dependent adhesion of bacteria on the surface can be categorized as either reversible or permanent. Bacteria that form permanent bonds with the surface will begin to colonize the surface and form biofilms which will increase the chances for infection. Low doses of H_2O_2 have the ability to induce bacteriostatic conditions in which the bacteria will not be able to form permanent bonds to the surface and therefore will not be able to colonize and form biofilms. The goal of aim 2 was to determine the quantity of H_2O_2 required to induce a bacteriostatic condition (i.e. no growth of bacteria) in solution and evaluate the ability of a ROS releasing conformational polydopamine coating to prevent biofilm formation on the surface of 316L stainless steel using relevant bacterial strains.

HYPOTHESIS 3 – THE ADDITION OF A ROS RELEASING SURFACE COATING WILL INCREASE THE EXPRESSION OF NATURALLY OCCURRING ANTIMICROBIAL PEPTIDE, DERMCIDIN, FROM RELEVANT CELL TYPES AND PROMOTE MORE EFFECTIVE WOUND HEALING.

Specific Aim 3: *Evaluate the effect continuous low doses of hydrogen peroxide have on the expression of the AMP dermcidin and its effects on model cell types to promote wound healing outcomes.* The antimicrobial and antifungal peptide Dermcidin has been found in significant quantities in the blubber of cetaceans. Dermcidin has been shown to increase the ability of cells to resist oxidative stress - which can be induced using ROS. This peptide is hypothesized to play an important role in the wound healing mechanism in cetaceans as well as protect cells against oxidative stress which could be induced by diving behavior. The goal of aim 3 is to determine if H_2O_2 will increase the expression of dermcidin and if a continuous release of low doses of H_2O_2 will compromise wound healing mechanisms.

1.7 SUMMARY OF CHAPTERS

Each of these chapters is the basis for manuscripts for publication where each manuscript explores a single aim. Chapter 2 will discuss the creation of the pDA surface coatings as well as their release profiles. Chapter 3 will characterize the antimicrobial character of the pDA surface coating. Chapter 4 will explore the cytotoxic effects prolonged doses of H_2O_2 can have on model cell types compared to bolus doses. Chapter 5 will evaluate the effect prolonged release of H_2O_2 has on dermcidin expression as well as the differentiation behavior of pre-adipocytes.

1.7 REFERENCES

Andews, R.D., Baird, R.W., Calambokidis, J., Goertz, C.E.C., Gulland, F.M.D., Heide-Jørgensen, M.P., et al. (2019). Best practice guidelines for cetacean tagging. *Journal of Cetacean Research and Management* 20**,** 40.

Andrews, R.D., Baird, R.W., Calambokidis, J., Goertz, C.E.C., Gulland, F.M.D., Heide-Jorgensen, M.P., et al. (2019). Best practice guidelines for cetacean tagging. *IWC Journal of Cetacean Research and Management* 20(1)**,** 27-66. doi: 10.47536/jcrm.v20i1.237.

Appenzeller-Herzog, C., Bánhegyi, G., Bogeski, I., Davies, K.J., Delaunay-Moisan, A., Forman, H.J., et al. (2016). Transit of H2O2 across the endoplasmic reticulum membrane is not sluggish. *Free Radical Biology and Medicine* 94**,** 157-160.

Apprill, A., Robbins, J., Eren, A.M., Pack, A.A., Reveillaud, J., Mattila, D., et al. (2014). Humpback Whale Populations Share a Core Skin Bacterial Community: Towards a Health Index for Marine Mammals? *PLOS ONE* 9(3)**,** e90785. doi: 10.1371/journal.pone.0090785.

Bae, Y.S., Lee, J.H., Choi, S.H., Kim, S., Almazan, F., Witztum, J.L., et al. (2009). Macrophages generate reactive oxygen species in response to minimally oxidized low-density lipoprotein: toll-like receptor 4- and spleen tyrosine kinase-dependent activation of NADPH oxidase 2. *Circ Res* 104(2)**,** 210-218, 221p following 218. doi: 10.1161/CIRCRESAHA.108.181040.

Balmer, B.C., Wells, R.S., Howle, L.E., Barleycorn, A.A., McLellan, W.A., Ann Pabst, D., et al. (2014). Advances in cetacean telemetry: A review of single-pin transmitter attachment techniques on small cetaceans and development of a new satellite-linked transmitter design. *Marine Mammal Science* 30(2)**,** 656-673. doi: 10.1111/mms.12072.

Beckford, S., and Zou, M. (2014). Wear resistant PTFE thin film enabled by a polydopamine adhesive layer. *Applied Surface Science* 292**,** 350-356. doi: https://doi.org/10.1016/j.apsusc.2013.11.143.

Beganovic, M., Luther, M.K., Rice, L.B., Arias, C.A., Rybak, M.J., and LaPlante, K.L. (2018). A Review of Combination Antimicrobial Therapy for Enterococcus faecalis

Bloodstream Infections and Infective Endocarditis. *Clin Infect Dis* 67(2)**,** 303-309. doi: 10.1093/cid/ciy064.

Best, P.B. (1993). Increase rates in severely depleted stocks of baleen whales. *ICES Journal of marine Science* 50(2)**,** 169-186.

Bierlich, K.C., Miller, C., DeForce, E., Friedlaender, A.S., Johnston, D.W., and Apprill, A. (2018). Temporal and Regional Variability in the Skin Microbiome of Humpback Whales along the Western Antarctic Peninsula. *Appl Environ Microbiol* 84(5). doi: 10.1128/AEM.02574-17.

Bugg, T.D., Wright, G.D., Dutka-Malen, S., Arthur, M., Courvalin, P., and Walsh, C.T. (1991). Molecular basis for vancomycin resistance in Enterococcus faecium BM4147: biosynthesis of a depsipeptide peptidoglycan precursor by vancomycin resistance proteins VanH and VanA. *Biochemistry* 30(43)**,** 10408-10415.

Burian, M., and Schittek, B. (2015). The secrets of dermcidin action. *Int J Med Microbiol* 305(2)**,** 283-286. doi: 10.1016/j.ijmm.2014.12.012.

Calderan, S.V., Black, A., Branch, T.A., Collins, M.A., Kelly, N., Leaper, R., et al. (2020). South Georgia blue whales five decades after the end of whaling. *Endangered Species Research* 43**,** 359-373.

Chatterjee, A.K., Sarkar, R.K., Chattopadhyay, A.P., Aich, P., Chakraborty, R., and Basu, T. (2012). A simple robust method for synthesis of metallic copper nanoparticles of high antibacterial potency against E. coli. *Nanotechnology* 23(8)**,** 085103. doi: 10.1088/0957-4484/23/8/085103.

Clapham, P.J., Young, S.B., and Brownell, R.L. (1999). Baleen whales: conservation issues and the status of the most endangered populations. *Mammal Review* 29(1)**,** 37-62. doi: 10.1046/j.1365-2907.1999.00035.x.

Croll, D.A., Acevedo-Gutiérrez, A., Tershy, B.R., and Urbán-Ramírez, J. (2001). The diving behavior of blue and fin whales: is dive duration shorter than expected based on oxygen stores? *Comp Biochem Physiol A Mol Integr Physiol* 129(4)**,** 797-809. doi: 10.1016/s1095-6433(01)00348-8.

Dakal, T.C., Kumar, A., Majumdar, R.S., and Yadav, V. (2016). Mechanistic Basis of Antimicrobial Actions of Silver Nanoparticles. *Frontiers in microbiology* 7**,** 1831-1831. doi: 10.3389/fmicb.2016.01831.

Darouiche, R.O., Dhir, A., Miller, A.J., Landon, G.C., Raad, I.I., and Musher, D.M. (1994). Vancomycin Penetration Into Biofilm Covering Infected Prostheses And Effect On Bacteria. *The Journal of Infectious Diseases* 170(3)**,** 720-723. doi: 10.1093/infdis/170.3.720.

Dowding, J.E. (1977). Mechanisms of gentamicin resistance in Staphylococcus aureus. *Antimicrob Agents Chemother* 11(1)**,** 47-50. doi: 10.1128/AAC.11.1.47.

Filpula, D.R., Lee, S.M., Link, R.P., Strausberg, S.L., and Strausberg, R.L. (1990). Structural and functional repetition in a marine mussel adhesive protein. *Biotechnol Prog* 6(3)**,** 171-177. doi: 10.1021/bp00003a001.

Gao, D., Zhang, Y., Bowers, D.T., Liu, W., and Ma, M. (2021). Functional hydrogels for diabetic wound management. *APL bioengineering* 5(3)**,** 031503-031503. doi: 10.1063/5.0046682.

Garrigue C, Zerbini AN, Geyer Y, Heide-Jorgensen MP, Hanoka W, and P, C. (2010). Movements of satellite-monitored humpback whales from New Caledonia. *Journal of Mammology* 91(1)**,** 4.

Goudarzi, F., Mohammadalipour, A., Bahabadi, M., Goodarzi, M.T., Sarveazad, A., and Khodadadi, I. (2018a). Hydrogen peroxide: a potent inducer of differentiation of human adipose-derived stem cells into chondrocytes. *Free Radical Research* 52(7)**,** 763-774. doi: 10.1080/10715762.2018.1466121.

Goudarzi, F., Mohammadalipour, A., Bahabadi, M., Goodarzi, M.T., Sarveazad, A., and Khodadadi, I. (2018b). Hydrogen peroxide: a potent inducer of differentiation of human adipose-derived stem cells into chondrocytes. *Free Radic Res* 52(7)**,** 763-774. doi: 10.1080/10715762.2018.1466121.

Guertin, S. (2016). Endangered and Threatened Wildlife and Plants; Identification of 14 Distinct Population Segments of the Humpback Whale and Revision of Species-Wide Listing. *Federal Register* 81(245)**,** 3.

Guzman, H.M., and Capella, J.J. (2017). Short-term recovery of humpback whales after percutaneous satellite tagging. *The Journal of Wildlife Management* 81(4)**,** 728-733. doi: https://doi.org/10.1002/jwmg.21235.

Hahn, F.E., and Sarre, S.G. (1969). Mechanism of action of gentamicin. *J Infect Dis* 119(4)**,** 364-369. doi: 10.1093/infdis/119.4-5.364.

Heide-Jørgensen, M.P., Laidre, K.L., Nielsen, N.H., Hansen, R.G., and Røstad, A. (2013). Winter and spring diving behavior of bowhead whales relative to prey. *Animal Biotelemetry* 1(1)**,** 15. doi: 10.1186/2050-3385-1-15.

Hicks, B.D., St. Aubin, D.J., Geraci, J.R., and Brown, W.R. (1985). Epidermal Growth in the Bottlenose Dolphin, Tursiops truncatus. *Journal of Investigative Dermatology* 85(1)**,** 60-63. doi: https://doi.org/10.1111/1523-1747.ep12275348.

Hjelmstedt, P., Sundh, H., Brijs, J., Ekström, A., Sundell, K.S., Berg, C., et al. (2020). Effects of prophylactic antibiotic-treatment on post-surgical recovery following intraperitoneal bio-logger implantation in rainbow trout. *Scientific Reports* 10(1)**,** 5583. doi: 10.1038/s41598-020-62558-y.

Hogg, N., and Kalyanaraman, B. (1999). Nitric oxide and lipid peroxidation. *Biochimica et Biophysica Acta (BBA)-Bioenergetics* 1411(2-3)**,** 378-384.

Hong, H.J., Hutchings, M.I., Neu, J.M., Wright, G.D., Paget, M.S., and Buttner, M.J. (2004). Characterization of an inducible vancomycin resistance system in Streptomyces coelicolor reveals a novel gene (vanK) required for drug resistance. *Molecular microbiology* 52(4)**,** 1107-1121.

Jensen, L.K., Bjarnsholt, T., Kragh, K.N., Aalbaek, B., Henriksen, N.L., Blirup, S.A., et al. (2019). In Vivo Gentamicin Susceptibility Test for Prevention of Bacterial Biofilms in Bone Tissue and on Implants. *Antimicrob Agents Chemother* 63(2). doi: 10.1128/AAC.01889-18.

Jung, W.K., Koo, H.C., Kim, K.W., Shin, S., Kim, S.H., and Park, Y.H. (2008). Antibacterial activity and mechanism of action of the silver ion in Staphylococcus aureus and Escherichia coli. *Applied and environmental microbiology* 74(7)**,** 2171-2178. doi: 10.1128/AEM.02001-07.

Kershaw, J.L., Botting, C.H., Brownlow, A., and Hall, A.J. (2018). Not just fat: investigating the proteome of cetacean blubber tissue. *Conserv Physiol* 6(1)**,** coy003. doi: 10.1093/conphys/coy003.

Kim, J.S., Kuk, E., Yu, K.N., Kim, J.-H., Park, S.J., Lee, H.J., et al. (2007). Antimicrobial effects of silver nanoparticles. *Nanomedicine: Nanotechnology, Biology and Medicine* 3(1)**,** 95-101. doi: https://doi.org/10.1016/j.nano.2006.12.001.

Kord Forooshani, P., Pinnaratip, R., Polega, E., Tyo, A.G., Pearson, E., Liu, B., et al. (2020). Hydroxyl Radical Generation through the Fenton-like Reaction of Hematin- and Catechol-Functionalized Microgels. *Chemistry of Materials* 32(19)**,** 8182-8194. doi: 10.1021/acs.chemmater.0c01551.

Lee, H., Dellatore, S.M., Miller, W.M., and Messersmith, P.B. (2007). Mussel-inspired surface chemistry for multifunctional coatings. *Science* 318(5849)**,** 426-430. doi: 10.1126/science.1147241.

Linley, E., Denyer, S.P., McDonnell, G., Simons, C., and Maillard, J.Y. (2012). Use of hydrogen peroxide as a biocide: new consideration of its mechanisms of biocidal action. *J Antimicrob Chemother* 67(7)**,** 1589-1596. doi: 10.1093/jac/dks129.

Lisse, T.S., King, B.L., and Rieger, S. (2016). Comparative transcriptomic profiling of hydrogen peroxide signaling networks in zebrafish and human keratinocytes: Implications toward conservation, migration and wound healing. *Scientific Reports* 6(1)**,** 20328. doi: 10.1038/srep20328.

Livermore, D.M. (2000). Antibiotic resistance in staphylococci. *International Journal of Antimicrobial Agents* 16**,** 3-10. doi: https://doi.org/10.1016/S0924-8579(00)00299-5.

Loo, A.E.K., Wong, Y.T., Ho, R., Wasser, M., Du, T., Ng, W.T., et al. (2012). Effects of hydrogen peroxide on wound healing in mice in relation to oxidative damage. *PloS one* 7(11)**,** e49215.

Madsen, P.T., Payne, R., Kristiansen, N.U., Wahlberg, M., Kerr, I., and Møhl, B. (2002). Sperm whale sound production studied with ultrasound time/depth-recording tags. *Journal of Experimental Biology* 205(13)**,** 1899-1906. doi: 10.1242/jeb.205.13.1899.

Mate, B., Mesecar, R., and Lagerquist, B. (2007). The evolution of satellite-monitored radio tags for large whales: One laboratory's experience. *Deep Sea Research Part II: Topical Studies in Oceanography* 54(3), 224-247. doi: https://doi.org/10.1016/j.dsr2.2006.11.021.

Meng, H., Forooshani, P.K., Joshi, P.U., Osborne, J., Mi, X., Meingast, C., et al. (2019). Biomimetic recyclable microgels for on-demand generation of hydrogen peroxide and antipathogenic application. *Acta Biomater* 83, 109-118. doi: 10.1016/j.actbio.2018.10.037.

Modest, M., Irvine, L., Andrews-Goff, V., Gough, W., Johnston, D., Nowacek, D., et al. (2021). First description of migratory behavior of humpback whales from an Antarctic feeding ground to a tropical calving ground. *Animal Biotelemetry* 9(1), 42. doi: 10.1186/s40317-021-00266-8.

Moore, M., Andrews, R., Austin, T., Bailey, J., Costidis, A., George, C., et al. (2012). Rope trauma, sedation, disentanglement, and monitoring−tag associated lesions in a terminally entangled North Atlantic right whale (Eubalaena glacialis). *Marine Mammal Science* 29(2). doi: 10.1111/j.1748-7692.2012.00591.x.

Moore, M., Shorter, A., Johnson, M., Tyack, P., Hurst, T., and Bocconcelli, A. (2011). "Improving Attachments of Non-Invasive (Type III) Electronic Data Loggers to Cetaceans". Woods Hole Oceanographic Institute).

Morones, J.R., Elechiguerra, J.L., Camacho, A., Holt, K., Kouri, J.B., Ramírez, J.T., et al. (2005). The bactericidal effect of silver nanoparticles. *Nanotechnology* 16(10), 2346-2353. doi: 10.1088/0957-4484/16/10/059.

Nelson, T.M., Apprill, A., Mann, J., Rogers, T.L., and Brown, M.V. (2015). The marine mammal microbiome: current knowledge and future directions. *Microbiology Australia* 36(1), 8-13. doi: https://doi.org/10.1071/MA15004.

Niethammer, P., Grabher, C., Look, A.T., and Mitchison, T.J. (2009). A tissue-scale gradient of hydrogen peroxide mediates rapid wound detection in zebrafish. *Nature* 459(7249), 996-999.

Noriko, N., Naohiro, G., and Etsuo, N. (1993). Dynamics of the oxidation of low density lipoprotein induced by free radicals. *Biochimica et Biophysica Acta (BBA)-Lipids and Lipid Metabolism* 1168(3)**,** 348-357.

Pędziwiatr, P., Mikołajczyk, F., Zawadzki, D., Mikołajczyk, K., and Bedka, A. (2018). Decomposition of hydrogen peroxide - kinetics and review of chosen catalysts. *Acta Innovations* (26)**,** 45-52. doi: 10.32933/ActaInnovations.26.5.

Périchon, B., and Courvalin, P. (2012). Antibiotic Discovery and Development. *Eds Dougherty TJ, Pucci MJ Boston: Springer US* 2012**,** 515-542.

Pershing, A.J., Christensen, L.B., Record, N.R., Sherwood, G.D., and Stetson, P.B. (2010). The Impact of Whaling on the Ocean Carbon Cycle: Why Bigger Was Better. *PLOS ONE* 5(8)**,** e12444. doi: 10.1371/journal.pone.0012444.

Pham, A.N., Xing, G., Miller, C.J., and Waite, T.D. (2013). Fenton-like copper redox chemistry revisited: Hydrogen peroxide and superoxide mediation of copper-catalyzed oxidant production. *Journal of Catalysis* 301**,** 54-64. doi: https://doi.org/10.1016/j.jcat.2013.01.025.

Privett, B.J., Broadnax, A.D., Bauman, S.J., Riccio, D.A., and Schoenfisch, M.H. (2012). Examination of bacterial resistance to exogenous nitric oxide. *Nitric Oxide* 26(3)**,** 169-173. doi: 10.1016/j.niox.2012.02.002.

Radi, R. (2018). Oxygen radicals, nitric oxide, and peroxynitrite: Redox pathways in molecular medicine. *Proceedings of the National Academy of Sciences* 115(23)**,** 5839-5848.

Rai, S., Gupta, T.P., Shaki, O., and Kale, A. (2021). Hydrogen Peroxide: Its Use in an Extensive Acute Wound to Promote Wound Granulation and Infection Control - Is it Better Than Normal Saline? *Int J Low Extrem Wounds***,** 15347346211032555. doi: 10.1177/15347346211032555.

Rieg, S., Seeber, S., Steffen, H., Humeny, A., Kalbacher, H., Stevanovic, S., et al. (2006). Generation of multiple stable dermcidin-derived antimicrobial peptides in sweat of different body sites. *J Invest Dermatol* 126(2)**,** 354-365. doi: 10.1038/sj.jid.5700041.

Robbins, J., Knowlton, A.R., and Landry, S. (2015). Apparent survival of North Atlantic right whales after entanglement in fishing gear. *Biological Conservation* 191**,** 421-427. doi: https://doi.org/10.1016/j.biocon.2015.07.023.

Robbins, J., Zerbini, A.N., Gales, N., Gulland, F.M., Double, M., Clapham, P.J., et al. (2013). Satellite tag effectiveness and impacts on large whales: preliminary results of a case study with Gulf of Maine humpback whales. *Paper SC/65a/SH05 presented to the IWC Scientific Committee*.

Rodriguez-Montelongo, L., de la Cruz-Rodriguez, L.C., Farías, R.N., and Massa, E.M. (1993). Membrane-associated redox cycling of copper mediates hydroperoxide toxicity in Escherichia coli. *Biochimica et Biophysica Acta (BBA) - Bioenergetics* 1144(1)**,** 77-84. doi: https://doi.org/10.1016/0005-2728(93)90033-C.

Roy, S., Khanna, S., Nallu, K., Hunt, T.K., and Sen, C.K. (2006). Dermal wound healing is subject to redox control. *Molecular therapy* 13(1)**,** 211-220.

Saiz-Poseu, J., Mancebo-Aracil, J., Nador, F., Busque, F., and Ruiz-Molina, D. (2019). The Chemistry behind Catechol-Based Adhesion. *Angew Chem Int Ed Engl* 58(3)**,** 696-714. doi: 10.1002/anie.201801063.

Schoeman, R.P., Patterson-Abrolat, C., and Plön, S. (2020). A Global Review of Vessel Collisions With Marine Animals. *Frontiers in Marine Science* 7. doi: 10.3389/fmars.2020.00292.

Schreml, S., Szeimies, R., Prantl, L., Karrer, S., Landthaler, M., and Babilas, P. (2010). Oxygen in acute and chronic wound healing. *British Journal of Dermatology* 163(2)**,** 257-268.

Sen, C.K., and Roy, S. (2008a). Redox signals in wound healing. *Biochimica et Biophysica Acta (BBA)-General Subjects* 1780(11)**,** 1348-1361.

Sen, C.K., and Roy, S. (2008b). Redox signals in wound healing. *Biochimica et Biophysica Acta (BBA) - General Subjects* 1780(11)**,** 1348-1361. doi: https://doi.org/10.1016/j.bbagen.2008.01.006.

Senyürek, I., Paulmann, M., Sinnberg, T., Kalbacher, H., Deeg, M., Gutsmann, T., et al. (2009). Dermcidin-derived peptides show a different mode of action than the cathelicidin LL-37 against Staphylococcus aureus. *Antimicrob Agents Chemother* 53(6)**,** 2499-2509. doi: 10.1128/aac.01679-08.

Shakil, S., Khan, R., Zarrilli, R., and Khan, A.U. (2008). Aminoglycosides versus bacteria – a description of the action, resistance mechanism, and nosocomial battleground. *Journal of Biomedical Science* 15(1)**,** 5-14. doi: 10.1007/s11373-007-9194-y.

Stewart, G.D., Lowrie, A.G., Riddick, A.C., Fearon, K.C., Habib, F.K., and Ross, J.A. (2007). Dermcidin expression confers a survival advantage in prostate cancer cells subjected to oxidative stress or hypoxia. *Prostate* 67(12)**,** 1308-1317. doi: 10.1002/pros.20618.

Szesciorka, A.R., Calambokidis, J., and Harvey, J.T. (2016). Testing tag attachments to increase the attachment duration of archival tags on baleen whales. *Animal Biotelemetry* 4(1). doi: 10.1186/s40317-016-0110-y.

Toledo Jr, J.C., and Augusto, O. (2012). Connecting the chemical and biological properties of nitric oxide. *Chemical research in toxicology* 25(5)**,** 975-989.

Trathan, P., and Reid, K. (2009). Exploitation of the marine ecosystem in the sub-Antarctic: historical impacts and current consequences. *Papers and Proceedings of the Royal Society of Tasmania* 143**,** 9-14.

Tyo, A., Welch, S., Hennenfent, M., Kord Fooroshani, P., Lee, B.P., and Rajachar, R. (2019). Development and Characterization of an Antimicrobial Polydopamine Coating for Conservation of Humpback Whales. *Frontiers in Chemistry* 7(618). doi: 10.3389/fchem.2019.00618.

Urbán R, J., Jiménez-López, E., Guzmán, H.M., and Viloria-Gómora, L. (2021). Migratory Behavior of an Eastern North Pacific Gray Whale From Baja California Sur to Chirikov Basin, Alaska. *Frontiers in Marine Science* 8. doi: 10.3389/fmars.2021.619290.

Usman, M.S., El Zowalaty, M.E., Shameli, K., Zainuddin, N., Salama, M., and Ibrahim, N.A. (2013). Synthesis, characterization, and antimicrobial properties of copper

nanoparticles. *International journal of nanomedicine* 8**,** 4467-4479. doi: 10.2147/IJN.S50837.

Van der Hoop, J.M., Moore, M.J., Barco, S.G., Cole, T.V., Daoust, P.Y., Henry, A.G., et al. (2013). Assessment of management to mitigate anthropogenic effects on large whales. *Conserv Biol* 27(1)**,** 121-133. doi: 10.1111/j.1523-1739.2012.01934.x.

Watanakunakorn, C. (1984). Mode of action and in-vitro activity of vancomycin. *J Antimicrob Chemother* 14 Suppl D**,** 7-18. doi: 10.1093/jac/14.suppl_d.7.

Wink, D.A., and Mitchell, J.B. (1998). Chemical biology of nitric oxide: insights into regulatory, cytotoxic, and cytoprotective mechanisms of nitric oxide. *Free Radical Biology and Medicine* 25(4-5)**,** 434-456.

Yates, C., and Ford, M. (2016). "5-Year Review: Southern Resident Killer Whales (Orcinus orca)". National Marine Fisheries Service).

Yoo, S.K., and Huttenlocher, A. (2009). Innate immunity: wounds burst H2O2 signals to leukocytes. *Curr Biol* 19(14)**,** R553-555. doi: 10.1016/j.cub.2009.06.025.

Zanella, R.C., Valdetaro, F., Lovgren, M., Tyrrel, G.J., Bokermann, S., Almeida, S.C., et al. (1999). First confirmed case of a vancomycin-resistant Enterococcus faecium with vanA phenotype from Brazil: isolation from a meningitis case in Sao Paulo. *Microb Drug Resist* 5(2)**,** 159-162. doi: 10.1089/mdr.1999.5.159.

Zerbini, A.N., Adams, G., Best, J., Clapham, P.J., Jackson, J.A., and Punt, A.E. (2019). Assessing the recovery of an Antarctic predator from historical exploitation. *R Soc Open Sci* 6(10)**,** 190368. doi: 10.1098/rsos.190368.

Zhu, G., Wang, Q., Lu, S., and Niu, Y. (2017). Hydrogen Peroxide: A Potential Wound Therapeutic Target? *Med Princ Pract* 26(4)**,** 301-308. doi: 10.1159/000475501.

CHAPTER 2

COATING SYNTHESIS AND CHARACTERIZATION

The chapter covers the synthesis and characterization of polydopamine coatings on medical-grade stainless steel. The characterization specifically covers the degree of polymerization, as well as the impact coating conditions and service conditions, have on hydrogen peroxide release behavior. The content in this chapter addresses Specific Aim 1.

The material in this chapter was previously published in *Frontiers in Chemistry* [Tyo, A., Welch, S., Hennenfent, M., Kord Fooroshani, P., Lee, B.P., and Rajachar, R. (2019). Development and Characterization of an Antimicrobial Polydopamine Coating for Conservation of Humpback Whales. *Frontiers in Chemistry* 7(618). doi: 10.3389/fchem.2019.00618.] or is in preparation for publication in *Frontiers in Marine Science*. Reprinted with permission (see **Appendix A**)

2.1 BACKGROUND

Polydopamine (pDA), a well-known marine-based adhesive, has been found to be a very versatile substance over the last decade (Ryu et al., 2018). Previously, pDA has been used to create surface coatings that are capable of preventing oxidation, degradation, or bacterial adhesion on the surface of various materials (He et al., 2014; Ding, 2016; Li et al., 2016). The most commonly used method to deposit pDA surface coatings onto a substrate is the dip method (Kord Forooshani et al., 2020; Teng et al., 2021). In this method, the substrate is submerged into a dopamine solution and the dopamine is allowed to polymerize under basic pH conditions (Fredi et al., 2020). The polymerization of dopamine can occur both in the solution through the formation of nanoparticles as well as at the surface of a substrate forming a thin conformal coating (Beckford and Zou, 2014). Agitation of the solution encourages the formation of pDA nanoparticles which also have the ability to non-covalently adhere to the surface of a substrate creating a rougher coating (Ma et al., 2013; Zangmeister et al., 2013). This process can be repeated multiple times to increase the thickness of the coatings. Multiple rounds of pDA coating deposition is not the only way to increase coating thickness; the thickness of pDA surface coatings has also been well documented to vary with alterations in the coating

environment (e.g., solution pH, temperature, solution concentration, presence of oxidizing agents, etc.) (Terrill, 2015). The most common changes in the environment are pH, temperature, and agitation. It has been found that more basic pH values (pH 8-9), agitation, and high temperatures (>30°C) increase coating thickness. Most often, pDA surface coatings are used as a priming layer to adhere other antimicrobial elements to the surface of a substrate such as silver nanoparticles. However, pDA is known to generate H_2O_2 during the polymerization process.

The primary mechanism being deployed through the use of pDA-only surface coatings centers around its ability to release H_2O_2 during oxidation. Dopamine will polymerize when oxidized or exposed to a primary amine/ion capable of forming a bond with a hydroxyl (OH) group. During polymerization, a hydroxy radical (OH•) will form during oxidation into a dopamine quinone and will rapidly oxidize into H_2O_2 (**Figure 2.1**). The dopamine quinone will then undergo an intramolecular cyclization reaction leading to the formation of 5,6-dihydroxyindole. This molecule will then further polymerize which can build the thickness of the coating. However, after the pDA coating is deposited, not all catechol will have been oxidized which allows for more potential release upon further oxidation of the coatings.

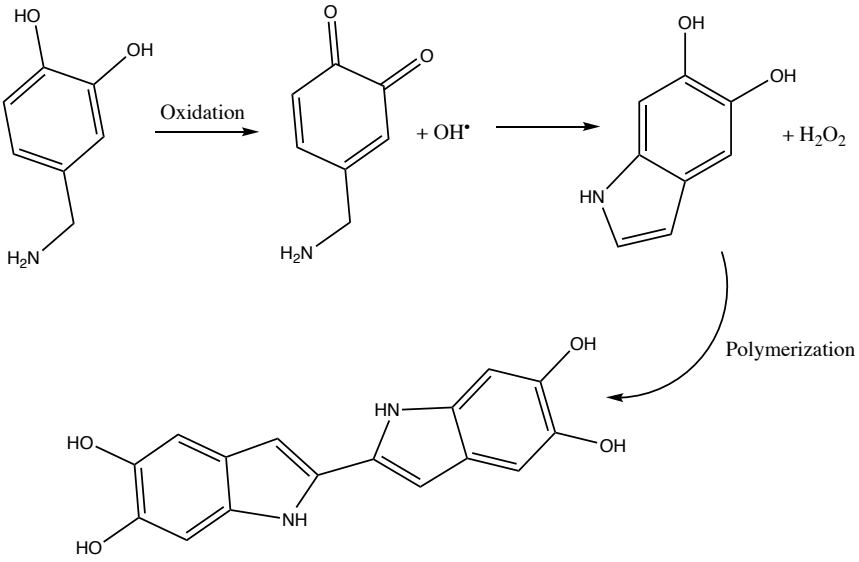

Figure 2.1 | *Oxidation of dopamine into one possible configuration of polydopamine.* After oxidation a dopamine quinone is formed as well as a hydroxy radical. The quinone will then oxidize further and form 5,6-dihydroxyindole and H_2O_2 before polymerization occurs.

2.2 Materials and Methods

2.2.1 pDA Coating Synthesis

316L stainless steel coupons (10mm x 20mm) (McMaster-Carr, Elmhurst IL) were exposed to dopamine-HCl dissolved in a 10mM Tris-HCl buffer (Sigma Aldrich, St. Louis MO) at a concentration of 2 mg/mL and pDA was allowed to polymerize on the surface for 24 hours at room temperature (**Figure 2.2**). After coating, coupons were gently shaken in PBS (pH 7.4, VWR) to remove non-adherent pDA from the surface. Coupons that were not used immediately after coating were air-dried and stored in a nitrogen-rich environment prior to use to avoid oxidation of the coating.

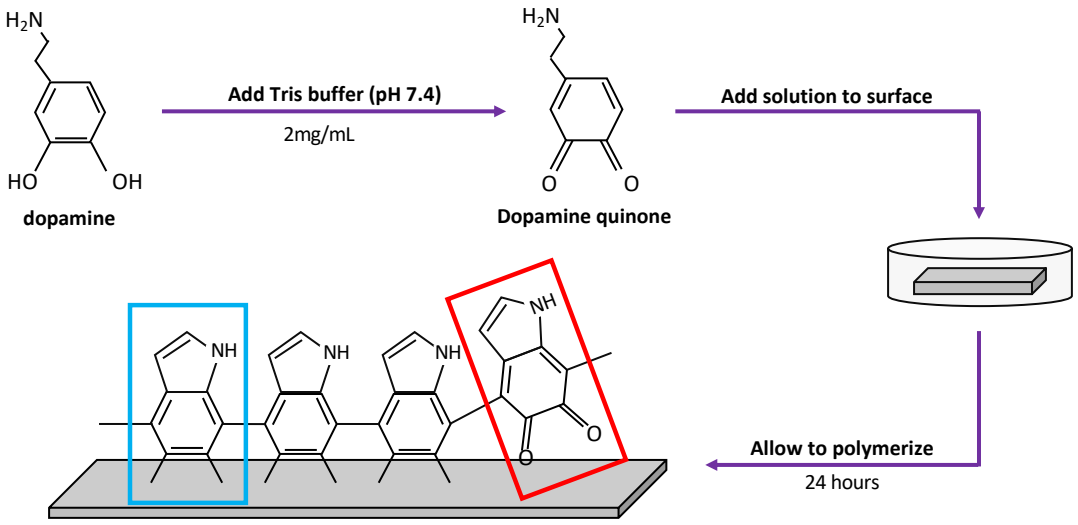

Figure 2.2 | *Process used to coat 316 SS samples with pDA.* To coat 316 SS samples, a pDA solution (2mg/mL) was made using dopamine-HCl and a tris-HCl buffer (pH 7.4). After the tris-HCl buffer is placed onto the dopamine-HCl the dopamine will begin to oxidize immediately, creating a dopamine quinone. The solution is then placed on top of a 316L SS coupon and is allowed to polymerize for 24 hours. Two forms of pDA will form: 5,6-dihydroxyindole (blue box) or 5,6-indolequinone (red box). The type of pDA found in the red box will not adhere to the surface of the metal.

2.2.2 Coating Creation Using Various Coating Conditions

316L stainless steel coupons - standard [Roughness average (Ra)= 0.635µm], brushed (Ra = 0.813µm), and mirrored (Ra = 0.15µm) finishes - were exposed to variations in key coating conditions to evaluate the effect each has on the release of H_2O_2. Two different pH, temperature (T), and coating times (CT) were used to evaluate the effect. It is well known that altering these conditions will affect the thickness of the coating, however, it

was unknown if coating thickness directly relates to release. **Table 2.1** summarizes the various coating conditions used.

Table 2.1 | pDA coating conditions. The highlighted boxes are the two primary coating conditions used in the remainder of this dissertation. Coating condition 1 will be referred to as "Low Release" while condition 7 will be referred to as "High Release"

Coating Condition	***pH***	***Temperature, T*** ***(°C)***	***Coating Time, CT*** ***(Hours)***
1	7.4	21	24
2	7.4	21	48
3	7.4	35	24
4	7.4	35	48
5	8.5	21	24
6	8.5	21	48
7	8.5	35	24
8	8.5	35	48

2.2.3 Thickness, Hydrophobicity, and Degradation

Thickness

Standard [Roughness average (Ra)= 0.635μm], brushed (Ra = 0.813μm), and mirrored (Ra = 0.15μm) finish 316L SS coupons (10mm x 20mm) were coated with pDA as previously described using coating conditions 1 and 7 (see Table 2.1) and were tested immediately after coating to prevent irreversible bonding of N_2 to primary amine groups. Each surface was analyzed using X-ray Photon Spectroscopy (XPS) (PHI 5800, Physical Electronics, Chanhassen MN) with a binding energy of 1235.6 eV for atomic percent composition and thickness of the pDA coating. Atomic percent composition was calculated using survey spectral analysis (187.85 eV pass energy, 0.8 eV/step resolution, and 20 ms/step dwell time) at three random locations for each finish at a nominal diameter of 800μm. The data was then analyzed in Origin® software (OriginLab Corporation, Northampton MA, USA) using a 70:30 Gaussian-Lorenztian peak fit and quantified using the areas under the peaks. The peaks were matched to their element through the binding energies of C1s, N1s, and O1s, which are 284.8, 400, and 532 eV, respectively. An example of the peaks that were integrated on the various surface finishes

can be seen in **Figure 2.3A**. **Equation (2.1)** was then used to calculate atomic percent, where A is the area and S is the sensitivity factor of the element. The sensitivity factors used for Carbon, Nitrogen, and Oxygen are 0.296, 0.477, and 0.711, respectively (Briggs, 1981).

$$Atomic\ \%\ of\ element = \left(\frac{\frac{A}{S}}{\sum_{i=1}^{n} \frac{A_i}{S_i}} \right) x\ 100\% \qquad \textit{(Equation 2.1)}$$

Depth profiles were used to find the pDA coating thickness for each finish at three spots where main elements were tracked through a sputter and survey process at a sputter rate of 5.56 nm/min (2 kV Ar^{+}) and a sampling rate of 0.03Hz. Carbon and iron were tracked and used to obtain thickness measurements. Carbon was used because of its high atomic percent in the pDA coating and low atomic percent in 316L SS. Iron ion (Fe^{+2}) content was monitored to accurately assess where the coating ended and the underlying metal substrate began. Examples of the curves produced from this process on all surface finishes are shown in **Figure 2.3B**. Thickness measurements were obtained by averaging

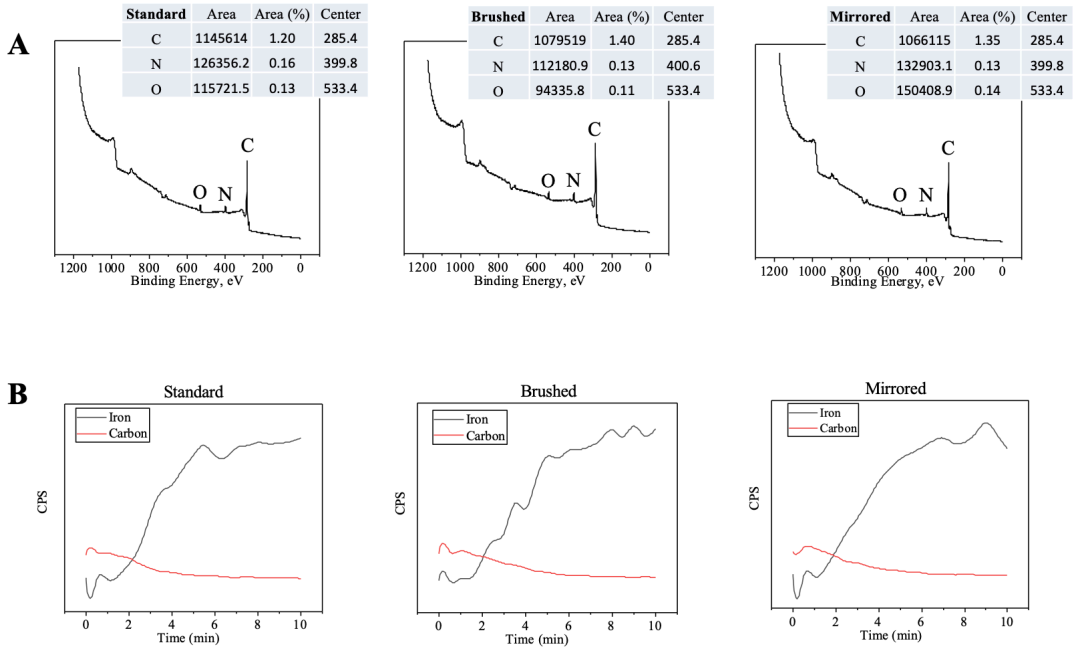

Figure 2.3. | *XPS data used for surface composition characterization.* Stainless steel samples were coated using condition 1 and then were immediately used for XPS analysis. (A) Surface survey on standard, brushed, and mirrored surfaces used for atomic composition with labeled peaks and (B) corresponding depth profiles used for thickness measurements.

the counts per second (CPS) value of the top and bottom plateaus, correlating that value to the time point, and multiplying by the sputter rate.

Hydrophobicity

Contact angle measurements were conducted on all finishes of SS coupons coated under conditions 1 and 7 (see Table 2.1). Coupons were coated and allowed to air dry for 6 hours prior to testing. Coupons had a 5 μL drop of deionized water placed on top of the surface and images were taken to establish the contact angle of the droplet with the surface. Images were processed using ImageJ (NIH, v. 1.51).

Degradation

Degradation of the coating under aqueous conditions was also evaluated using phosphate-buffered saline (PBS) pH 7.4 over one month. Coupons of each surface roughness were coated using conditions 1 and 7 (see Table 2.1) and were allowed to air-dry for 6 hours. The mass of each SS coupon was measured before and after coating. The coupons were then placed into PBS (pH 7.4, Sigma Aldrich, St. Louis MO) at 35°C for one month and the mass of the coupons was recorded every 24 hours and compared to initial measurements.

2.2.4 X-Ray Photon Spectroscopy Evaluation for Degree of Polymerization

Standard finish 316L stainless steel coupons were coated using condition 1 (Low Release) and condition 7 (High Release) (see Table 2.1). Some coupons were coated using the previously mentioned conditions and then were allowed to polymerize at room temperature for 14 days before XPS analysis was conducted while other coupons were analyzed immediately after creation to avoid any irreversible binding of N as well as to avoid unintentional polymerization due to oxidation.

Surface profiles were taken at three spots on each sample where C1s, N1s, and O1s were tracked through a detailed scan using a 70:30 Gaussian-Lorentzian fit. Oxygen was tracked as the side group responsible for the release of H_2O_2, hydroxyl (OH), only releases H_2O_2 when polymerizing (**Figure 2.1**).

2.2.5 H_2O_2 Stability in Solution

The stability of H_2O_2 in various aqueous solutions was evaluated over a 24 hour time period to establish the baseline degradation rate for solutions used to evaluated the release of pDA coatings. DMEM without phenol red, PBS (pH 7.4), and diH_2O were used. A solution with a concentration of 160μM was created in the respective solution and measurements were taken at various time points using a ferrous oxidative (FOX) assay (Sigma Aldrich, St. Louis MO).

2.2.6 Release Characterization

All H_2O_2 release was characterized using a ferrous oxidative (FOX) assay (Sigma Aldrich, St. Louis MO). This assay measures the concentration of H_2O_2 through the oxidation of Fe^{+2} to Fe^{+3} in acidic conditions. During this oxidation, xylenol orange also oxidizes, forming a darker orange/purple color, that can be measured. This colorimetric change was measured through absorbance readings at a wavelength of 560nm using a plate reader. All measurements taken with this assay are considered instantaneous measurements.

2.2.6.1 Varying Coating Conditions

Stainless steel coupons coated were coated with pDA using various coating conditions (see Table 2.1). The coupons were then submerged in a PBS solution (pH 7.4, Sigma Aldrich) or diH_2O at 35°C for 24 hours and the quantity of H_2O_2 was measured.

2.2.6.2 Varying Release Environments

Coupons were coated using coating conditions 1 (Low coated) and 7 (High coated) (see Table 2.1) and the release over 24 hours was evaluated in DMEM without phenol red and saltwater (3.5% NaCl). The release in these two mediums was then compared to PBS (pH 7.4). In addition to evaluating

2.2.6.3 Sterilization and Shelf-Life

Sterilization

Standard surface finish coupons were coated using coating condition 7, rinsed in PBS (pH 7.4, VWR) to remove excess pDA, and were then sterilized using either ethanol or ethylene oxide. After sterilization, the release of H_2O_2 was evaluated and compared to

unsterilized coated coupons. *Ethanol sterilization:* coated coupons were submerged for 5 minutes and then rinsed in PBS (pH 7.4, VWR). The release from the coupons was then evaluated over a 24 hour time period. *Ethylene oxide sterilization:* coated coupons were placed into a sterilization bag and then exposed to ethylene oxide for 12 hours. The bag was then allowed to ventilate for 2-3 hours after sterilization and the release was evaluated over 24 hours.

Shelf Life

The shelf-life of the pDA coatings was evaluated over the course of 30 days after gas sterilization. Samples of standard surface pDA coatings - coated using condition 7 - were created and then stored in various conditions for up to 30 days (**Table 2.2**). The release from the coatings after the storage time (either 14 or 30 days) was then evaluated and the storage method that resulted in the least amount of decrease in release was chosen as the preferred long-term storage solution.

Table 2.2 | pDA coated coupon storage conditions. The highlighted condition resulted in the least amount of release lost over a 1 month period.

Storage Condition	*Temperature (°C)*	*Vacuum Sealed?*	*Backfilled?*
1	4	N	N
2	4	N	Y
3	4	Y	N
4	4	Y	Y
5	21	N	N
6	21	N	Y
7	21	Y	N
8	21	Y	Y

2.3 Results

2.3.1 Release from Varying Coating Conditions

When altering the coating conditions (see **Table 2.1**) it was found that, in general, two separate release profiles could be attained. Most coating conditions saw a release of

<40µM while two conditions saw a release >60µM - conditions 7 and 8 (**Figure 2.4**). It was found that to effectively change the quantity of H_2O_2 generated, both the pH and

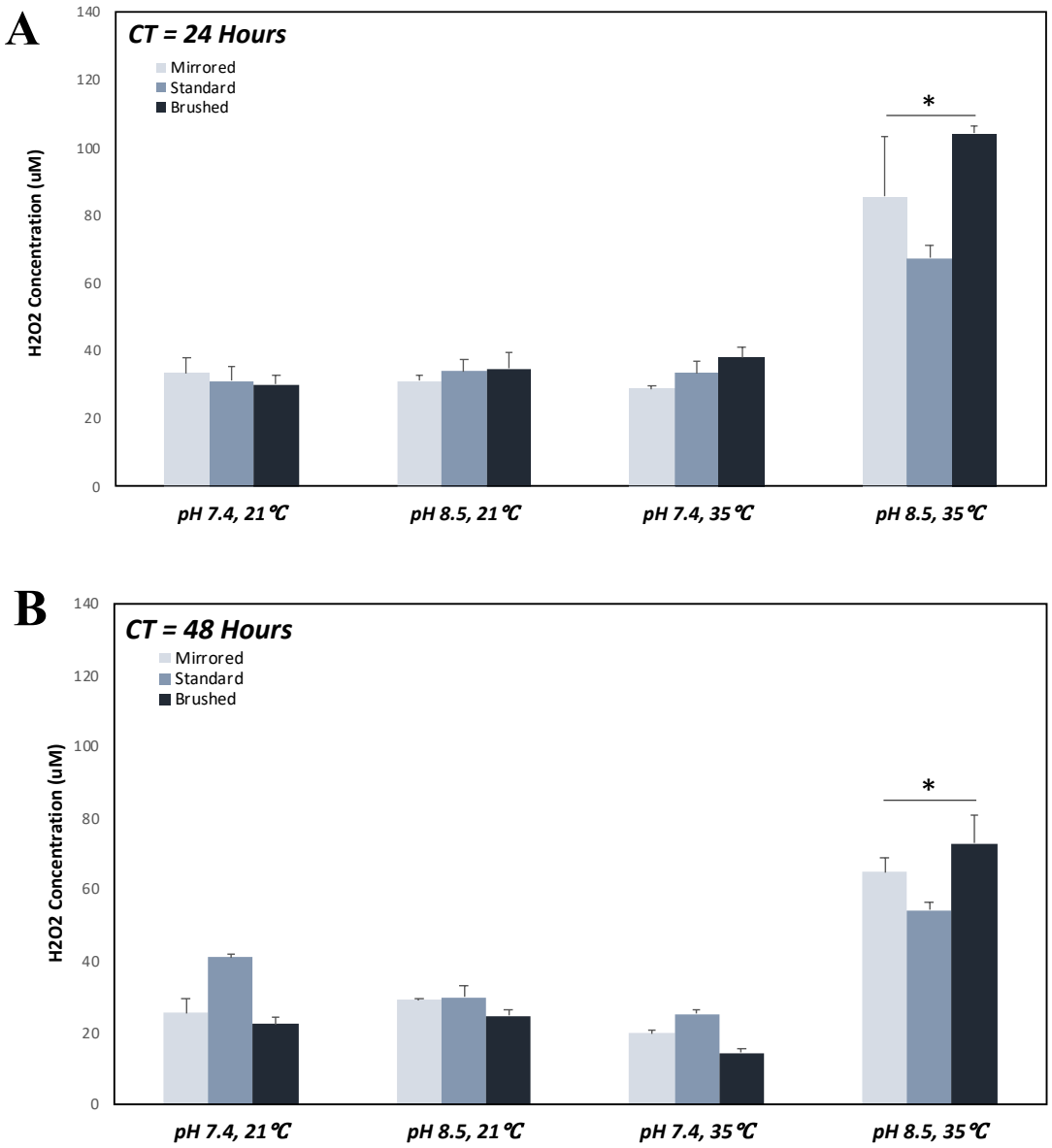

Figure 2.4 | *Hydrogen peroxide release of pDA coatings created under various conditions over a 24-hour period.* Hydrogen peroxide release measured over a 24-hour period on coupons coated for (A) 24 and (B) 48 hours. The highest release was seen on coupons coated with pDA using a pH 8.5 solution at 35°C for 24 hours. When coated for 48 hours there was a smaller increase in release when increasing temperature for pH 8.5 and a slight decrease in release for pH 7.4 with increasing temperature. * indicates a significant difference from all other coating conditions within the surface finish ($p<0.05$). More broken-down results with all significant differences for individual surface finishes can be found in **Appendix B Figure B.1**. [CT = coating time]

temperature had to be elevated. Adjusting either one without the other resulted in no significant change to the release profile. The same release behavior was observed regardless of CT (**Figure 2.4B**). There were various significant differences between coating conditions on each surface finish (**See Appendix B Figure B.1**). Of note, there are more differences between coating conditions for pDA coatings that have a CT of 48 hours.

2.3.2 Thickness, Hydrophobicity, and Degradation

Thickness

There was no significant difference found in the thickness of pDA surface coatings deposited on the varying surface finishes (**Figure 2.5**). All coatings were approximately 15nm thick.

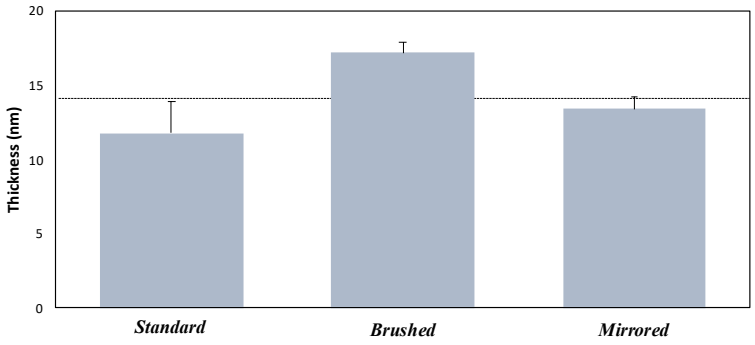

Figure 2.5 | *Thickness measurements of Low Release pDA coatings on various surfaces.* Thickness measurements of the coating on various surface finishes from XPS measurements. The dotted line represents the mean thickness for all measurements. There were no significant differences found between samples.

Hydrophobicity

Coatings were made using conditions 1 and 7 (Low Release and High Release) (see Table 2.1) on standard finished stainless steel. Both pDA surface coatings were hydrophilic (Low Release $\theta = 30^{\circ}$; High Release $\theta = 25^{\circ}$) (**Figure 2.6A**) while the uncoated stainless steel surface had a more hydrophobic contact angle ($\theta = 103^{\circ}$). When the surface roughness was altered to either a brushed or mirrored finish, both the High Release and Low Release pDA surface coatings were not able to be accurately measured for contact angle as complete spreading was observed (**Figure 2.6B**). Overall, the High Release pDA coatings were slightly more hydrophilic than the Low Release pDA coatings (30° vs 20°,

respectively) but the difference was not considered significant (p=0.06). These results were consistent with findings from other groups (Xi et al., 2009; Su et al., 2016).

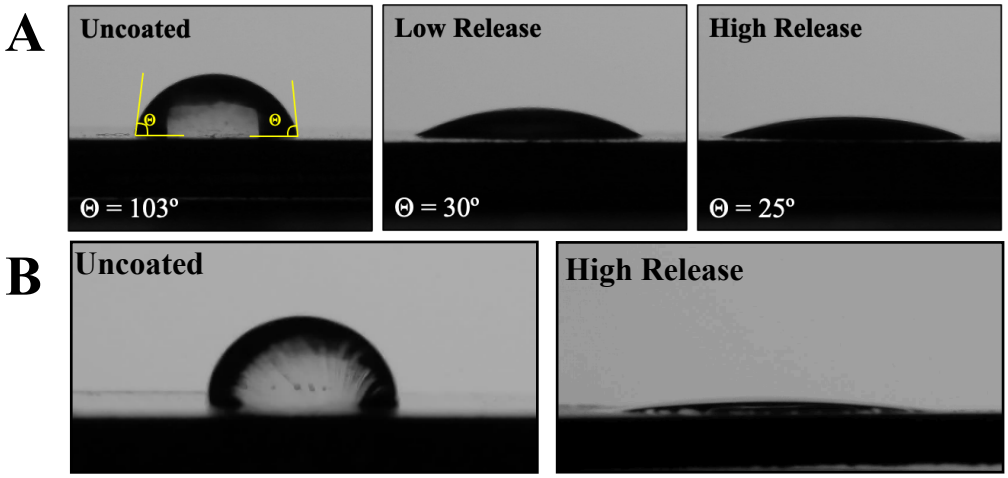

Figure 2.6 | *Contact angle using diH_2O on standard and brushed SS with and without pDA surface coatings.* (A) When a drop of diH_2O was places on the surface of an uncoated piece of SS with a standard surface finish the angle made between the drop and surface was approximately 103º. When the pDA coating was applied, the surface became significantly more hydrophilic ($\theta < 30º$, $p<0.05$). There was no significant difference in hydrophilicity between the pDA coatings. (B) There was no significant difference in contact angle with underlying substrate roughness changed for the uncoated SS surfaces. However, when the pDA surface coatings were applied to either a brushed or mirrored surface there was significantly more spreading ($p<0.05$). The contact angle was not able to be measured as complete spreading was observed on these surfaces.

Degradation

When incubated at 37°C in PBS, there was no evidence of coating degradation over a one-month period.

2.3.3 X-Ray Photon Spectroscopy Evaluation for Degree of Polymerization

After the pDA coatings were synthesized, they were characterized using a broad spectrum XPS scan. The O1 peaks were used to determine the relative quantity of OH side groups which corresponds to the degree of polymerization (Zangmeister et al., 2013). Coatings that had a higher quantity of OH groups indicated a lower degree of polymerization while those with lower quantities of OH groups indicated a higher level of polymerization. It was observed that the pDA coatings that release a larger quantity of H_2O_2 (High Release) had a lower degree of polymerization when compared to the pDA coatings that released a smaller quantity of H_2O_2 (Low Release) (XPS intensity measurements: 60202 vs 33698). (**Figure 2.7A-B**).

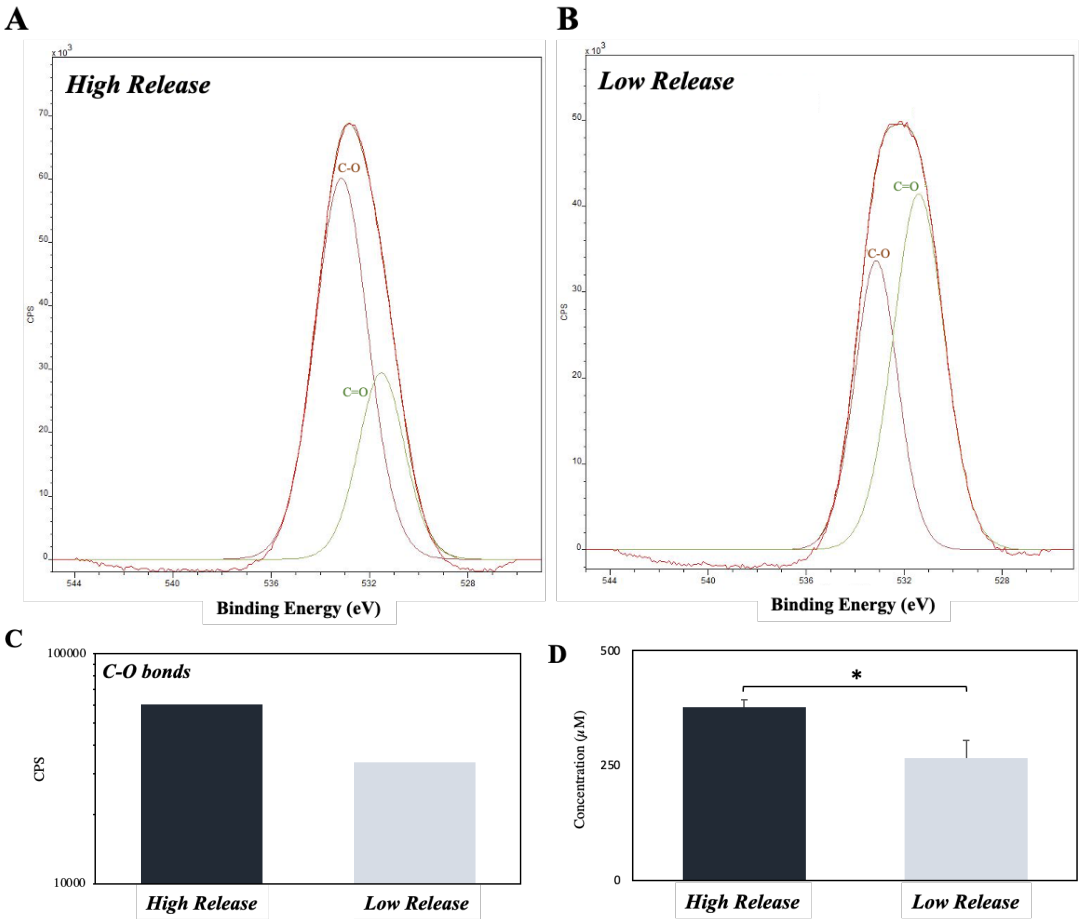

Figure 2.7 | Quantity of C-O bonds on the surface of High Release and Low Release pDA coupons with their corresponding H_2O_2 release. Coupons were coated using the High Release and Low Release coating conditions and were subsequently analyzed for release and quantity of C-O bonds. (a-c) XPS results of O1s. There was a higher concentration of C-O bonds on the high coated coupons when compared to the low coated coupons. (d) Release evaluated from coupons. The higher concentration of C-O bonds appears to correspond with a higher concentration of H_2O_2 in solution after 24 hours. A * indicates a significant difference ($p<0.05$).

2.3.4 H_2O_2 Stability in Solution

The stability of H_2O_2 was evaluated with an initial concentration of 160μM and it was found that >95% of the H_2O_2 was degraded within the first hour in PBS (pH 7.4, Sigma-Aldrich) while only 60% of the initial quantity of H_2O_2 remained in diH_2O (**Figure 2.8B**). After 24 hours there was no H_2O_2 left in the PBS solution and there was approximately 40% left in diH_2O (**Figure 2.8A**).

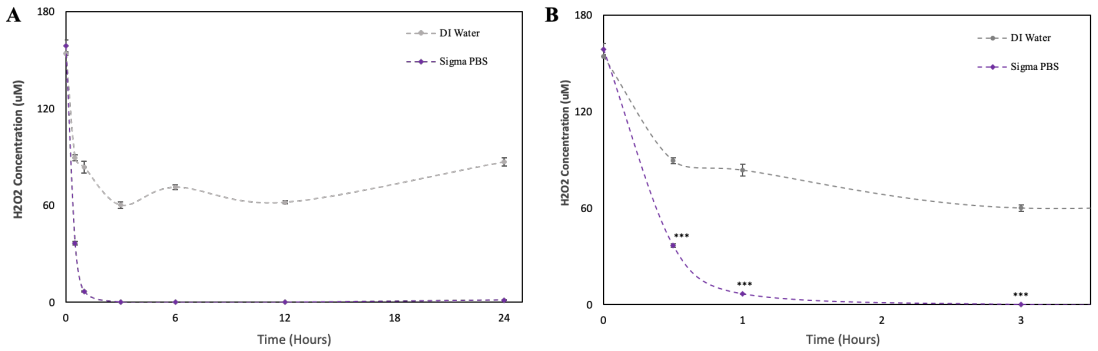

Figure 2.8 | *Stability of Hydrogen Peroxide when incubated in various solutions for up to 24 hours.* An exogenous dose of hydrogen peroxide was allowed to incubate in various solutions and the quantity remaining was evaluated at various timepoints. (A) The quantity of hydrogen peroxide in the various solutions over a 24-hour time period. All hydrogen peroxide was degraded after 3 hours in PBS (Sigma). (B) Quantity of hydrogen peroxide remaining in the solutions up to 3 hours. The quantity of hydrogen peroxide in PBS was significantly reduced almost immediately when compared to DI water (***$p<0.001$).

2.3.5 Sterilization and Shelf-Life

Sterilization

The sterilization method used on satellite telemetry tags is gas sterilization using ethylene oxide. The impact of this sterilization method was determined by testing the release profile of Low Release pDA surface coatings after ethylene oxide sterilization as well as ethanol sterilization and compared to unsterilized pDA coated coupons. With both sterilization methods, there was no significant reduction in release when compared to unsterilized pDA coated coupons (**Figure 2.9**).

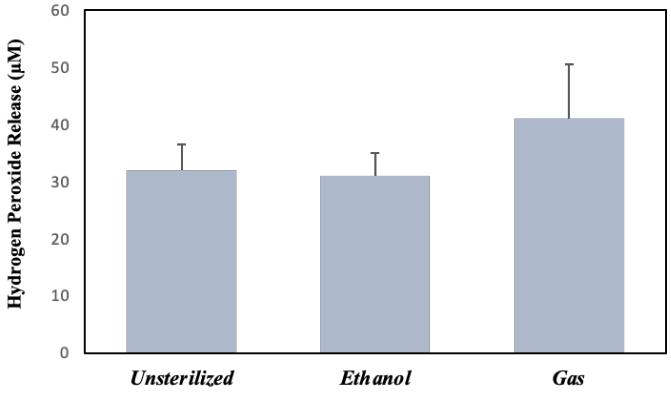

Figure 2.9 | *Sterilization of Low Release pDA coated coupons compared to non-sterilized pDA coated coupons.* Coated coupons were sterilized either using gas or ethanol, and the release of H_2O_2 was evaluated and compared to non-sterilized pDA coated coupons. There were no significant differences found in the release profile with both sterilization techniques.

Shelf-Life

High Release pDA coated stainless steel coupons were stored in various environments to evaluate the ability to store the coated coupons before use. It was found that over a one-month period the H_2O_2 release was significantly reduced regardless of storage method (47µM vs ~30µM) (**Figure 2.10A**). It was found that most of the reduction in release was seen in the first 5 days of storage (approximately (**Figure 2.10B**).

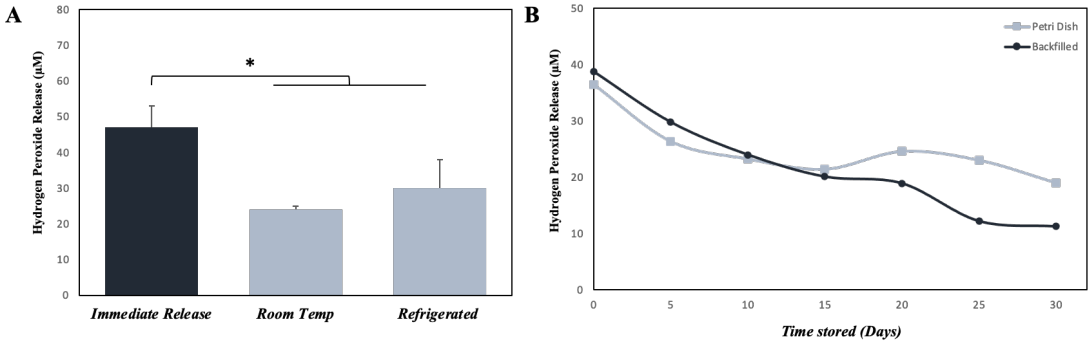

Figure 2.10 | *Shelf-life of High Release pDA coated coupons*. (A) When stored in either room temperature or refrigerated environments, and not in an inert environment, there was a significant reduction in H_2O_2 release when compared to release immediately following coating deposition.(B) Over a one month period the release between High Release pDA coatings was evaluated when stored in an inert environment (N_2 gas) and stored in a petri dish at 4°C was not significantly different. The most release was lost in the first five days (~50% reduction) for both storage methods. A * indicates a significant difference ($p<0.05$)

2.3.6 Release in Various Service Environments

High Release and Low Release pDA coated stainless steel coupons (Ra = 0.625µm) were incubated in three different solutions for 24 hours and the quantity of H_2O_2 was evaluated (**Figure 2.11**). There was significantly more release from the High Release pDA surface coatings in a saltwater solution (3.5% NaCl) when compared to PBS (pH 7.4) (25µM vs 50µM, $p<0.05$). There was no significant difference in release between the PBS and DMEM solutions. The Low Release pDA surface coatings exhibited no change in release over a 24 hour period between the three solutions (~20µM).

2.4 Discussion

With the growing interest in developing robust non-antibiotic approaches, polydopamine surface coatings have the potential to modulate stable marine bacterial colonization to an implant surface with the controlled release of the ROS H_2O_2. Furthermore, since H_2O_2 is

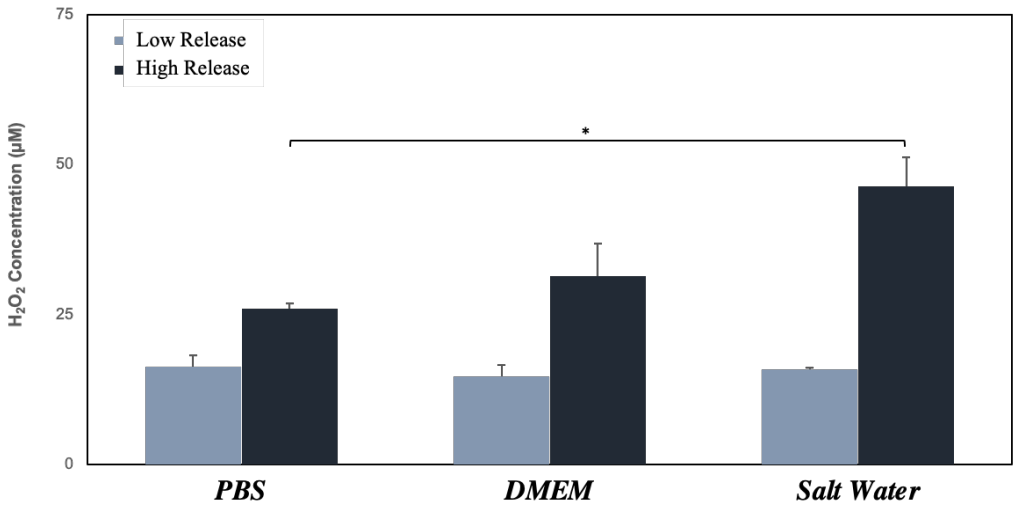

Figure 2.11 | *H_2O_2 generation from Low and High Release pDA coated coupons in various solutions.* The release from pDA coated coupons was evaluated after incubation in PBS, DMEM, or a salt water solution (3.5% NaCl) for 24 hours. There was no significant difference in H_2O_2 generation from the Low Release pDA coatings between the three solutions. There was significantly more release from the High Release pDA coatings in the salt water solution when compared to the PBS solution ($p<0.05$). In all solutions, there was significantly more release from the High Release pDA coatings than the Low Release pDA coatings ($p<0.05$).

also a known effector of stable wound healing (Loo et al., 2012), controlled delivery in a target range could not only facilitate a bacteriostatic behavior conducive to the inherent immune modulation of infection (Rai et al., 2021) but it could also be used to promote stable wound healing.

The pDA surface coatings in this work were established to be conformal on varying surface finishes of 316L stainless steel (SS). The composition and thickness of the coatings remained the same for all finishes (**Figures 2.3 and 2.5**). The coatings did not exhibit any significant differences in chemical composition when the substrate roughness was altered (**Figure 2.3**). This lack of difference in coating characteristics was expected as the substrate roughness has not been found to be a contributing factor to characteristic changes in pDA coatings (Ding, 2016). Previous studies of pDA coatings found the maximum thickness over a 24-hour period that could be established was 50nm at a pH of 8.5 (Lee et al., 2007). Although the thickness of the coatings created under low pH and low temperature had an average thickness of around 14nm (**Figure 2.5**), we saw no significant change in H_2O_2 release when only pH was increased (i.e., coating at a pH of 8.5) (**Figure 2.4**) which indicates thickness as not being a contributing factor to H_2O_2 release. The pDA coatings were also found to increase the hydrophilicity of the stainless

steel surface (**Figure 2.6**). It is well known that the addition of pDA to otherwise hydrophobic surfaces significantly increases the hydrophilicity of the substrate which may contribute to the increased antimicrobial character observed (Xi et al., 2009). Furthermore, the pDA coatings in the current study have a tailored H_2O_2 release profile that can be easily adjusted by altering the pH, time, and temperature during the coating process.

The variation in release of H_2O_2 can be attributed to coating conditions which can alter the chemical arrangement (catechol exposure) of the coatings – therefore altering the H_2O_2 release profiles (Salomaki et al., 2018). Both the temperature and the pH of the coating solution affected release profiles. Previous experiments have concluded that increasing the incubation temperature will increase the rate at which H_2O_2 is generated in a solution with a constant pH due to an increased oxidation state (Wang et al., 2016). In addition, it has been determined that a pH between 8-9 will produce a greater amount of H_2O_2 than a pH between 6-7 on non-metal substrates (Torres et al., 2014). However, there is a lack of literature on the alteration of coating conditions and what effect this may have on H_2O_2 release. It is well known that coating conditions alter the chemical makeup of the coatings, as warmer and more basic conditions allow for more catechol side groups to be available for interaction. However, it is not well studied whether or not these changes contributed to an increased H_2O_2 release on the surface of metal substrates.

We determined the correlation between the difference in release between the Low Release coating condition (pH 7.4 solution at 21°C) and the High Release coating condition (pH 8.5 solution at 35°C) was related to the quantity of available OH groups (**Figure 2.7**) which has been attributed to the degree of polymerization. Due to this correlation, we can conclude the degree of polymerization directly affects the concentration of OH groups which subsequently affects the release profile. It is likely that the conditions in which the coating is created impacts the mechanism in which pDA is formed and therefore the quantity of available catechol after *in situ* polymerization is concluded.

2.5 Conclusion

This chapter explored the effect of various coating conditions (e.g., pH, time, and temperature) on release. There were two general release profiles observed: Low Release (~40μM over 24 hours) and High Release (~80μM over 24 hours). Both types of coatings

were found to be hydrophilic and had similar thicknesses regardless of the substrate surface finish. These coatings can be used to coat medical-grade stainless steel satellite telemetry tags and release low doses of H_2O_2 over a prolonged period of time. These coatings have the potential to mimic the gradient that is naturally present in the wound environment which can prevent bacterial growth as well as promote wound healing outcomes.

2.6 REFERENCES

Beckford, S., and Zou, M. (2014). Wear resistant PTFE thin film enabled by a polydopamine adhesive layer. *Applied Surface Science* 292**,** 350-356. doi: https://doi.org/10.1016/j.apsusc.2013.11.143.

Briggs, D. (1981). Handbook of X-ray Photoelectron Spectroscopy C. D. Wanger, W. M. Riggs, L. E. Davis, J. F. Moulder and G. E.Muilenberg Perkin-Elmer Corp., Physical Electronics Division, Eden Prairie, Minnesota, USA, 1979. 190 pp. $195. *Surface and Interface Analysis* 3(4)**,** v-v. doi: 10.1002/sia.740030412.

Ding, Y.H., Floren, M., and Tan, W. (2016). Mussel-inspired polydopamine for bio-surface functionalization. . *Biosurface and Biotribology* 2(4)**,** 15. doi: 10.1016/j.bsbt.2016.11.001.

Fredi, G., Simon, F., Sychev, D., Melnyk, I., Janke, A., Scheffler, C., et al. (2020). Bioinspired Polydopamine Coating as an Adhesion Enhancer Between Paraffin Microcapsules and an Epoxy Matrix. *ACS Omega* 5(31)**,** 19639-19653. doi: 10.1021/acsomega.0c02271.

He, S., Zhou, P., Wang, L., Xiong, X., Zhang, Y., Deng, Y., et al. (2014). Antibiotic-decorated titanium with enhanced antibacterial activity through adhesive polydopamine for dental/bone implant. *J R Soc Interface* 11(95)**,** 20140169. doi: 10.1098/rsif.2014.0169.

Kord Forooshani, P., Pinnaratip, R., Polega, E., Tyo, A.G., Pearson, E., Liu, B., et al. (2020). Hydroxyl Radical Generation through the Fenton-like Reaction of Hematin- and Catechol-Functionalized Microgels. *Chemistry of Materials* 32(19)**,** 8182-8194. doi: 10.1021/acs.chemmater.0c01551.

Lee, H., Dellatore, S.M., Miller, W.M., and Messersmith, P.B. (2007). Mussel-inspired surface chemistry for multifunctional coatings. *Science* 318(5849)**,** 426-430. doi: 10.1126/science.1147241.

Li, R., Liu, X., Qiu, W., and Zhang, M. (2016). In Vivo Monitoring of H2O2 with Polydopamine and Prussian Blue-coated Microelectrode. *Anal Chem* 88(15)**,** 7769-7776. doi: 10.1021/acs.analchem.6b01765.

Loo, A.E.K., Wong, Y.T., Ho, R., Wasser, M., Du, T., Ng, W.T., et al. (2012). Effects of hydrogen peroxide on wound healing in mice in relation to oxidative damage. *PloS one* 7(11)**,** e49215.

Ma, Y.-r., Zhang, X.-l., Zeng, T., Cao, D., Zhou, Z., Li, W.-h., et al. (2013). Polydopamine-Coated Magnetic Nanoparticles for Enrichment and Direct Detection of Small Molecule Pollutants Coupled with MALDI-TOF-MS. *ACS Applied Materials & Interfaces* 5(3)**,** 1024-1030. doi: 10.1021/am3027025.

Rai, S., Gupta, T.P., Shaki, O., and Kale, A. (2021). Hydrogen Peroxide: Its Use in an Extensive Acute Wound to Promote Wound Granulation and Infection Control - Is it Better Than Normal Saline? *Int J Low Extrem Wounds***,** 15347346211032555. doi: 10.1177/15347346211032555.

Ryu, J.H., Messersmith, P.B., and Lee, H. (2018). Polydopamine Surface Chemistry: A Decade of Discovery. *ACS Applied Materials & Interfaces* 10(9)**,** 7523-7540. doi: 10.1021/acsami.7b19865.

Salomaki, M., Marttila, L., Kivela, H., Ouvinen, T., and Lukkari, J. (2018). Effects of pH and Oxidants on the First Steps of Polydopamine Formation: A Thermodynamic Approach. *J Phys Chem B* 122(24)**,** 6314-6327. doi: 10.1021/acs.jpcb.8b02304.

Su, L., Yu, Y., Zhao, Y., Liang, F., and Zhang, X. (2016). Strong Antibacterial Polydopamine Coatings Prepared by a Shaking-assisted Method. *Scientific Reports* 6(1)**,** 24420. doi: 10.1038/srep24420.

Teng, R., Meng, Y., Zhao, X., Liu, J., Ding, R., Cheng, Y., et al. (2021). Combination of Polydopamine Coating and Plasma Pretreatment to Improve Bond Ability Between PEEK and Primary Teeth. *Frontiers in Bioengineering and Biotechnology* 8. doi: 10.3389/fbioe.2020.630094.

Terrill, H.C. (2015). Optimization of Polydopamine Coatings. University of Akron.

Torres, C.R., Crastechini, E., Feitosa, F.A., Pucci, C.R., and Borges, A.B. (2014). Influence of pH on the effectiveness of hydrogen peroxide whitening. *Operative dentistry* 39(6)**,** E261-E268.

Wang, Z., Wang, K., Zhang, Y., Jiang, Y., Lu, X., Fang, L., et al. (2016). Protein-Affinitive Polydopamine Nanoparticles as an Efficient Surface Modification Strategy for

Versatile Porous Scaffolds Enhancing Tissue Regeneration. *Particle & Particle Systems Characterization* 33(2)**,** 89-100. doi: https://doi.org/10.1002/ppsc.201500187.

Xi, Z.-Y., Xu, Y.-Y., Zhu, L.-P., Wang, Y., and Zhu, B.-K. (2009). A facile method of surface modification for hydrophobic polymer membranes based on the adhesive behavior of poly(DOPA) and poly(dopamine). *Journal of Membrane Science* 327(1)**,** 244-253. doi: https://doi.org/10.1016/j.memsci.2008.11.037.

Zangmeister, R.A., Morris, T.A., and Tarlov, M.J. (2013). Characterization of Polydopamine Thin Films Deposited at Short Times by Autoxidation of Dopamine. *Langmuir* 29(27)**,** 8619-8628. doi: 10.1021/la400587j.

CHAPTER 3

EVALUATION OF ANTIMICROBIAL CHARACTER

The chapter covers the ability of polydopamine coatings to prevent bacterial adhesion and subsequent biofilm formation on medical grade stainless steel. Both terrestrial-based and aquatic-based bacteria species associated with an increased risk of infection were tested.

The material in this chapter was previously published in *Frontiers in Chemistry* [Tyo, A., Welch, S., Hennenfent, M., Kord Fooroshani, P., Lee, B.P., and Rajachar, R. (2019). Development and Characterization of an Antimicrobial Polydopamine Coating for Conservation of Humpback Whales. *Frontiers in Chemistry* 7(618). doi: 10.3389/fchem.2019.00618.] or is in preparation for publication in *Frontiers in Marine Science*. Reprinted with permission (see **Appendix A**).

3.1 BACKGROUND

Monitoring behavioral patterns of marine mammals is a vital component in the ongoing study of general ocean health and the ecology of individual populations. Currently, satellite telemetry tags and biopsy samples are used to monitor migration patterns and animal health status respectively. Telemetry tags and biopsy tips are, most commonly, made from medical grade stainless steel (316L) (Lagerquist et al., 2008; Balmer et al., 2014) or titanium (Andrews et al., 2008). Biopsy tips are used to gather tissue samples which are analyzed to determine the animals' health status and tissue composition. These results can shed light on the current pollutants in the ocean as most marine mammals store pollutants in their blubber tissue (Borobia M et al., 1995). Biopsy samples are also used to run genetic analyses to determine potential population interbreeding through DNA sequencing. Satellite telemetry tags are used to monitor the migration and diving behavior of large marine mammals, most notably cetaceans. Cetacean migration behavior has been monitored using transdermal tags which penetrate through the skin implant into the underlying blubber tissue. While these are useful tools to track movement, they can act as a vehicle for infection. Both these devices, telemetry tags and biopsy tips, penetrate through the exterior dermal layer and into the underlying blubber tissue (Kennedy et al., 2014). Biopsy tips are less likely to cause infection as they are not meant to remain

implanted. However, telemetry tags are used to monitor the migration and behavior patterns of large cetaceans for prolonged periods of time (>2 weeks). The tags can provide a vehicle for bacteria to attach and proliferate, causing biofilm formation and subsequent infection.

The microbiome located on the surface of the skin in cetaceans is complex and vital to the health and well-being of each individual (Nelson et al., 2015; Ross et al., 2019). Cetacean microbiomes change year-round and vary geographically (e.g., they differ in feeding and breeding habitats of migratory whales) (Bierlich et al., 2018). However, there are two main genera of bacteria that make up a majority of the microbiome on cetaceans year-round: *Psychrobacter* and *Tenacibaculum* (Apprill et al., 2014; Bierlich et al., 2018). Conservationists have been studying the impact the microbiome has on the general health and well-being of cetaceans and have found that these bacteria when on the surface of the skin are harmless or even beneficial to individual cetaceans (Nelson et al., 2015). However, if the bacteria were to get into the underlying tissue, the potential for infection is increased. This infection can lead to a rise in morbidity and mortality rates. The mechanism in which bacteria that are present in the microbiome can enter the tissue is most commonly via scratches or bites from rough social interactions or from predators. A less common mechanism can be through the tools conservationists use to study these populations, mainly, metallic implants such as invasive telemetry devices and biopsy tips. When these devices penetrate through the dermis and bass through the microbiome, bacteria can adhere and subsequently colonize the surface of the metallic substrate. Once bacteria colonize the surface of the tag, they can form a biofilm. Once a biofilm is formed it can only be removed through mechanically scrubbing the surface which is not feasible in the implanted devices. This leaves prevention as the only reasonable approach at reducing chances for infection at the tag-tissue interface.

To prevent biofilm formation and subsequent tissue infection, antibiotic-based surface coatings can be used in certain invasive instruments (Mate et al., 2007; IWC, 2020). The primary mechanisms used to prevent bacterial infections include permeabilizing the cell wall and DNA, disrupting protein synthesis, or disrupting cell wall synthesis. These coatings are primarily comprised of the antibiotic's gentamicin or vancomycin. Gentamicin is used against gram-negative bacteria to prevent protein synthesis within the bacteria cells, ultimately, causing cell death (Hahn and Sarre, 1969). Vancomycin can be

used on gram-positive bacteria cells to disrupt cell wall synthesis, causing unwanted pores and subsequent cell death (Watanakunakorn, 1984). These antibiotics, while effective, are subject to resistance formed within a variety of bacterial species (Hong et al., 2004; Shaikh et al., 2015). The most common bacterial species to form a resistance to both Vancomycin and Gentamicin is *Staphylococcus* (Livermore, 2000). This resistance in *Staphylococcus* bacteria can be attributed to antibiotic excess use or misuse. Because of these resistances, there has been growing interest in developing non-antibiotic-based antimicrobial solutions. Recently, the scientific community has discouraged the use of antibiotics in cetaceans in favor of sterilization of instruments or, if necessary, implementation of a non-antibiotic-based antimicrobial system. Some of these antimicrobial solutions include the use of reactive oxygen species (ROS) (Fang, 2011; Vatansever et al., 2013) and other antimicrobial agents such as silver ions (Ag^{+}) (Pal et al., 2007; Jung et al., 2008). These methods interrupt bacterial growth by permeabilizing the cell wall and damaging the cell's DNA (Linley et al., 2012). ROS can be found in the natural wound environment to not only reduce the chances of infection by creating a concentration gradient (Yoo and Huttenlocher, 2009; Zhu et al., 2017) but also to act as a mediator in the wound healing cascade (Ojha et al., 2008; Li et al., 2016). The chances of resistance being formed from the use of ROS are low when compared to the chance with the use of antibiotics due to the necessity of these molecules in cellular signaling pathways. However, due to the inherent instability of many ROS, it is difficult to recreate the natural release profile and subsequent gradient *in vitro* (Madanská et al., 2004).

As infection due to the formation of a biofilm is a concern for the metallic satellite telemetry tags used in cetacean conservation practices, the ability to reduce bacterial adhesion to a metallic substrate without a pronounced chance of resistance being formed is a growing area of interest. H_2O_2 is a promising antimicrobial agent due to its various mechanisms of action, however, the ability to prevent bacterial adhesion on the surface of metallic substrates has not yet been explored. This is primarily due to the difficulty in creating a material that can generate H_2O_2 in a quantity large enough to maintain a stable concentration in solution. In this work, we first address the ability for pDA surface coatings to act as a vehicle for local controlled delivery of H_2O_2 to prevent the adhesion of prevalent bacterial types, both terrestrial and aquatic, associated with infection to the surface of medical-grade stainless steel. Secondly, we evaluate the potential for a

resistance to form in response to previous non-lethal exposure to H_2O_2 from an external source. As H_2O_2 is known to be present in the wound environment, bacteria may be exposed to H_2O_2 multiple times and subsequently form a resistance to the ROS. Ultimately, the goal of this work is to develop a non-antibiotic-based pDA surface coating that can be applied to invasive instruments commonly used to monitor cetacean populations (**Figure 3.1**).

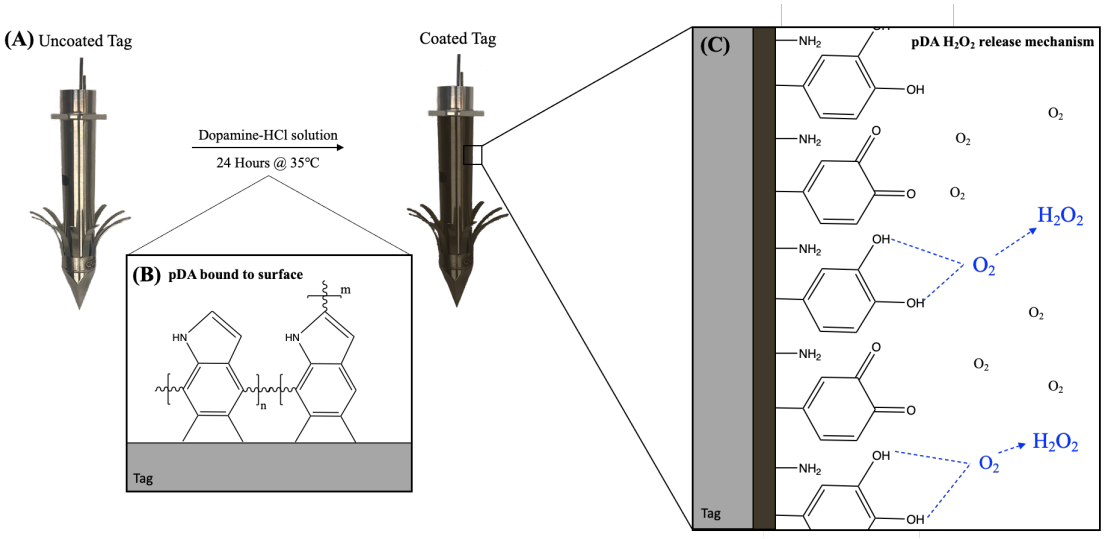

Figure 3.1 | *Schematic representation of deposition of pDA coatings onto the surface of a satellite telemetry tag.* (A) An uncoated tag (left) is placed into a dopamine-HCl solution for 24 hours during which a conformational pDA coating appearing brown in color is formed (right). (B) The chemical structure of pDA which binds to the surface of the stainless steel. Additional dopamine molecules can bind vertically to thicken the coating. (C) When exposed to oxygen, the catechol on unpolymerized dopamine molecules will oxidize and form the reactive oxygen species hydrogen peroxide.

3.2 Materials and Methods

3.2.1 Bacterial Growth Response to Various Doses of Hydrogen Peroxide

The dosing concentration of H_2O_2 required to induce a bacteriostatic response in *Escherichia coli* (*E. coli*) (ATCC BAA-2471), *Staphylococcus epidermidis* (*S. epi*) (ATCC 12228), and *Tenacibaculum Skagerrakense* (*T. skag*) (ATCC BAA-459) was determined prior to the evaluation of bacterial adhesion. The dose required to induce bacteriostatic behavior for 12 hours was determined by incubating cell suspensions ($1.3x10^5$ CFU/cm^2) in their respective growth media determined by the manufacturer with different initial doses of H_2O_2 over at least 24 hours. *E. coli* and *S. epi* were incubated at 37°C in a tryptic soy broth (TSB) solution while *T. skag* and *P. cryo* were incubated at room temperature (21°C) in a marine broth (ATCC, Manassas VA). The

turbidity of the solutions was evaluated at using absorbance readings of optical density (OD) at 600nm (OD_{600}). The absorbance readings were taken using UV-Vis turbidity measurements to determine cell concentration. These concentrations were compared to controls to determine the length of bacteriostatic effects in response to the various doses. The threshold for bacteriostatic behavior was determined to be a turbidity measurement below 0.2.

3.2.2 Bacterial Adhesion to pDA Coated Coupons

Stainless steel coupons, with varying surface roughness, were coated using the Low Release and High Release pDA surface coatings and were incubated in bacterial cell suspensions (10^5 CFU/mL) for one-third of the bacterial growth period. The four bacterium types used were *Psychrobacter cryohalolentis* (*P. cryo*) (ATCC BAA-1226), *T. skag, S. epi*, and *E. coli*. Coupons, coated and uncoated, were incubated in *P. cryo* at room temperature (21°C) for 24 hours, *T. skag* at room temperature for 20 hours, *S. epi* at 37°C for 24 hours, and *E. coli* at 37°C for 6 hours. *P. cryo* and *T. skag* were used as a model for the bacteria present in the microbiome on healthy whale skin. Both belong to the two most abundant genera found on the surface of healthy whale skin. *S. epi* was used to evaluate the reaction of gram-positive bacteria to pDA surface coatings while *E. coli* was used to evaluate the response of more substrate-sensitive pathogens.

After incubating samples in the bacterial suspensions, coupons were removed and rinsed in diH_2O to remove any non-adherent bacteria. Bacteria were then fixed to the surface using a 4% glutaraldehyde solution. Once removed, coupons were serially dehydrated in ethanol before imaging using a field-emission scanning electron microscope (FESEM). Bacteria counts were conducted, and the coated coupons were compared to the uncoated coupons.

3.2.3 Bacterial Adhesion to pDA Coated Coupons After Exposure to H2O2

There is a concern for resistance, or tolerance, to develop after exposure to a non-lethal bolus dose of a ROS. To evaluate this potential, bacterial suspensions (10^5 CFU/mL) were exposed to a 200μM dose of H_2O_2 for 24 hours. After the exposure time, the bacteria were seeded on an agar plate and were grown until individual bacterial colonies were observed: *E. coli* and *S. epi* were grown for 24 hours, *P. cryo* for 72 hours, and *T. skag* for 60 hours. These colonies were then used to create new bacterial suspensions (10^5

CFU/mL) and adhesion was evaluated on coated and uncoated standard finished stainless steel coupons as described in section 2.2.2.

3.3 RESULTS

3.3.1 DOSE-DEPENDENT GROWTH RESPONSE TO H2O2

Turbidity measurements were taken at various timepoints up to 48 hours after being exposed to a single bolus dose of H_2O_2. The quantity of H_2O_2 required to induce a bacteriostatic response for up to 12 hours was determined and used to evaluate how sensitive each bacteria type is to H_2O_2. **Table 3.1** summarizes the doses required to induce bacteriostatic conditions in the four species of bacteria evaluated. S. epi was the most sensitive bacteria, responding with a dose as low as 50µM (**See Appendix C Figure C.1**).

Table 3.1 | The minimum quantity of H_2O_2 required to induce a bacteriostatic response for 12 hours in the bacterium types tested for adhesion to 316L SS coupons.

Bacteria Type	***Minimum One-Time Dose***
E. Coli	100μM
S. Epi	50μM
P. Cryo	100μM
T. Skag	150μM

E. coli and *P. cryo* displayed a bacteriostatic response with the addition of a 100µM dose (**See Appendix C Figures C.2 & C.3**). *T. skag* was the most robust bacteria, requiring a dose of at least 150µM to display bacteriostatic behavior (**See Appendix C Figure C.4**).

3.3.2 BACTERIAL ADHESION TO PDA COATED COUPONS

Overall, the addition of High Release pDA surface coatings was able to reduce gram-negative bacterial adhesion on all tested surfaces (**Figure 3.2**). The gram positive bacteria tested, *S. epi*, saw an increase in adhesion when the High Release pDA surface coating was added. The Low Release pDA surface coatings were variable in their efficacy.

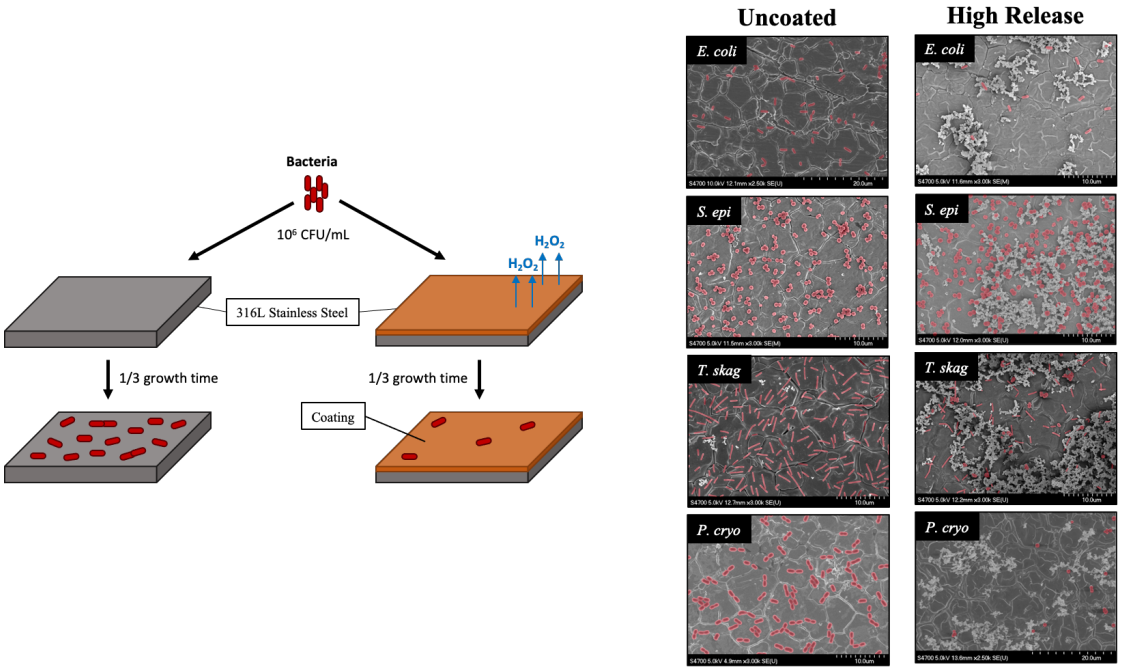

Figure 3.2 | *Schematic of experimental setup (left) and sample FESEM images of bacterial adhesion on 316L stainless steel in response to High Release pDA surface coating (right).* Bacteria were exposed to pDA surface coatings for one-third of their respective growth time. When exposed to a High Release pDA surface coating, gram-negative bacteria (shaded in red) were not able to adhere to the surface of medical grade stainless steel as effectively as they could on an uncoated surface. The gram-positive bacteria tested, *S. epi*, adhered more effectively to a High Release pDA coated surface. Bacteria can be seen on FESEM images and are highlighted in red.

Escherichia Coli

After establishing the minimum one-time dose required to induce bacteriostatic conditions for up to 12 hours in *E. coli* (100µM), pDA coated coupons with varying surface finishes were incubated in a bacterial solution. Previously published results found that the Low Release pDA coatings significantly reduced the adhesion of *E. Coli* on the standard surface finish (70% reduction) while the adhesion was increased on the brushed surface with the addition of the Low Release pDA coating (25% increase) (**Figure 3.3**). There was no statistical difference in adhesion on the mirrored surface with the addition of the Low Release pDA coating. However, when *E. Coli* were exposed to the High Release pDA coating, there was a significant reduction in adhesion observed – at least 60% from each respective uncoated surface control – for all surface finishes ($p<0.05$) (**Figure 3.3**). There was a baseline increase in adhesion observed when the surface roughness was increased (roughly a 3-fold increase) (**Figure 3.3**), however, this result is

consistent with other findings and is a well-known response of *E. coli* (Ortega et al., 2010).

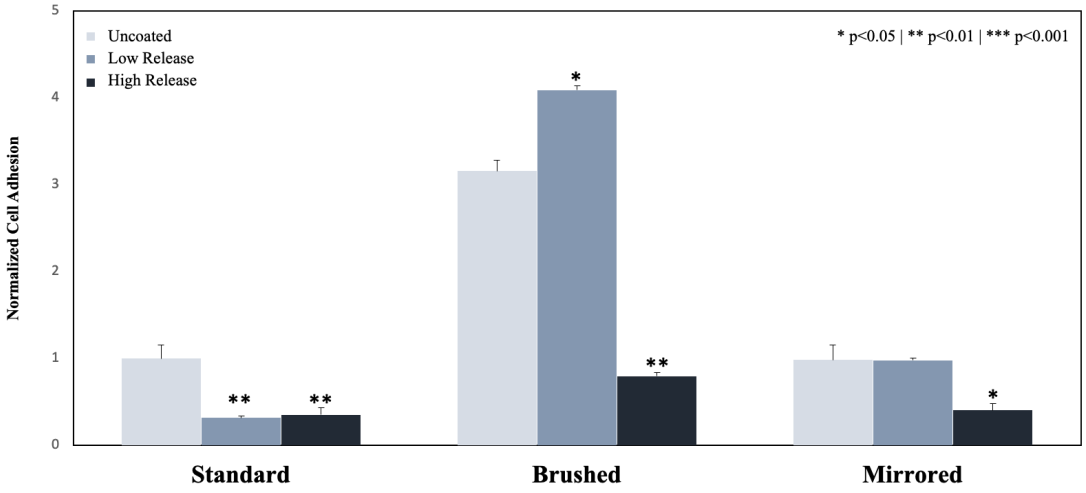

Figure 3.3 | Adhesion of *E. coli* to the surface of 316L SS coupons. Coupons were coated using both the Low Release (pH 7.4, 21°C) and High Release (pH 8.5, 35°C) coating conditions. The coupons were then incubated for 6 hours in a solution of *E. coli* and the adhesion was evaluated. The adhesion of *E. coli* on Low Release coatings was significantly reduced on the standard surface finish. The adhesion was significantly inhibited by the High Release surface coatings on all surface finishes. An asterisk indicates a significant difference from the respective uncoated surface (* $p<0.05$ | ** $p<0.01$). An analysis of any significant differences between surfaces can be found in **Appendix C Figure C.5A**.

Staphylococcus Epidermidis

The adhesion of *S. epi* bacteria to the surface of uncoated and Low Release pDA coatings was not statistically different on the standard and brushed surface finishes. On the mirrored surface finish, adhesion was significantly reduced (60% reduction when compared to an uncoated mirrored surface) ($p<0.05$) (**Figure 3.4**). The adhesion between all surface finishes was not statistically different without the pDA coating, however, when pDA surface coatings were added there was a significant reduction in adhesion observed on the mirrored surface finish when compared to the standard and brushed surface finishes (**See Appendix C Figure C.5B**). The High Release pDA surface coating on the on the standard and brushed surface finishes did not reduce bacterial adhesion, instead, *S. epi* adhesion was increased ($p<0.05$) (**Figure 3.4**). The increase with the addition of the High Release pDA compared to the uncoated surface was not observed for the mirrored surface finish, rather, a decrease was still observed when compared to the uncoated surface (25% reduction) ($p<0.05$) (**Figure 3.4**).

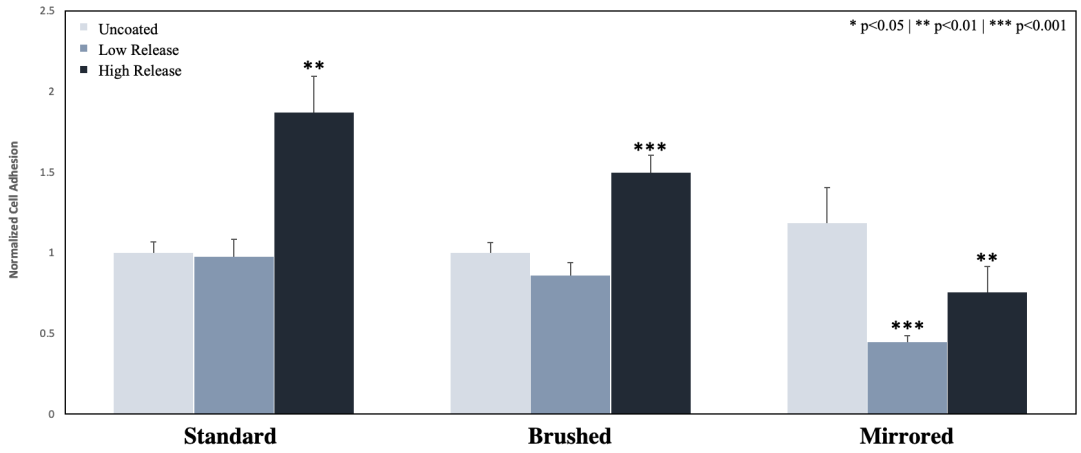

Figure 3.4 | Adhesion of *S. epi* to the surface of 316 SS coupons. Coupons were coated using both the Low Release (pH 7.4, 21°C) and High Release (pH 8.5, 35°C) coating conditions. The coupons were then incubated for 24 hours in a solution of *S. epi* and the adhesion was evaluated. The adhesion of *S. epi* on Low Release coatings was not significantly reduced on standard and brushed surfaces but was significantly inhibited on the mirrored surface. Bacterial adhesion was significantly increased on all High Release coatings when compared to the low coated coupons, however on the mirrored surface the high coated pDA coupons still exhibited significantly less adhesion when compared to the corresponding uncoated coupons. (* $p<0.05$ | ** $p<0.01$ | *** $p<0.001$). An analysis of any significant differences between surfaces can be found in **Appendix C Figure C.5B**.

Psychrobacter Cryohalolentis

Low Release pDA coatings did not reduce the adhesion of *P. cryo* on standard and mirrored surface finishes but did significantly reduce the adhesion on a brushed surface (34% reduction) ($p<0.05$) (**Figure 3.5**). The High Release pDA coatings inhibited bacterial adhesion on all surface finishes when compared to the respective uncoated surface (>30% reduction on all surfaces) (**Figure 3.5**). Bacterial adhesion was reduced by 80% on the standard surface finish, 66% on the brushed surface finish, and 30% on the mirrored surface with the addition of the High Release pDA surface coatings (**Figure 3.5**). Of the tested surface finishes, the mirrored surface finish was the least effective at reducing bacterial adhesion when the High Release pDA coating was added (**See Appendix C Figure C.6A**).

Tenacibaculum Skagerrakense

Stainless steel coupons coated with Low Release and High Release pDA coatings were both observed to significantly decrease the overall bacterial adhesion of *T. Skag* bacteria (**Figure 3.6**). Different from the other tested bacterial species, *T. Skag* undergoes a substantial change in morphology when growing exponentially. When stagnant, the

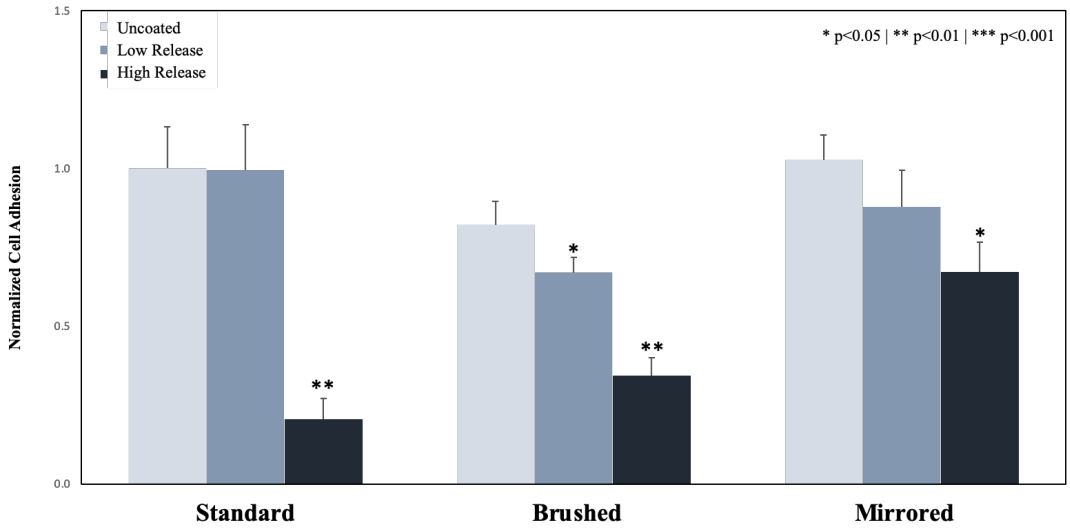

Figure 3.5 | Adhesion of *P. cryo* to the surface of 316 SS coupons. Coupons were coated using both the Low Release (pH 7.4, 21°C) and High Release (pH 8.5, 35°C) coating conditions. The coupons were then incubated for 24 hours in a solution of *P. cryo* and the adhesion was evaluated. The adhesion of P. cryohalolentis on Low Release coatings was not significantly reduced for the standard and mirrored surface types but was significantly reduced on the brushed surface. The adhesion was significantly inhibited on all High Release coatings. A * indicates a significant difference from the respective uncoated surface (* p<0.05 | ** p<0.01). An analysis of any significant differences between surfaces can be found in **Appendix C Figure C.6A**.

bacteria have a round/globular morphology. When growing exponentially, the bacteria morphology changes into a rod-like/spindly shape (**See Appendix C Figure C.7**) (Frette et al., 2004). When comparing the morphology of the adherent bacteria, it was found that the High Release pDA surface coating both decreased the total adherent bacteria (**Figure 3.6**) and increased the proportion of adherent bacteria that were in the stagnant growth phase. All bacteria on the surface of uncoated stainless steel - regardless of surface finish - were in the exponential growth phase.

3.3.3 Bacterial Adhesion to pDA Coated Coupons After Exposure to Hydrogen Peroxide

Escherichia Coli

After exposure to a non-lethal dose of H_2O_2, there was no significant difference observed between the adhesion of *E. Coli* on the surface of High Release pDA coatings when compared to *E. coli* that were not previously exposed to a high dose of H_2O_2 (**Figure 3.7A**). However, there was still a significant decrease in the adhesion of *E. Coli* to the surface of the standard surface finish stainless steel from the uncoated surface to the coated surfaces regardless of previous exposure to H_2O_2.

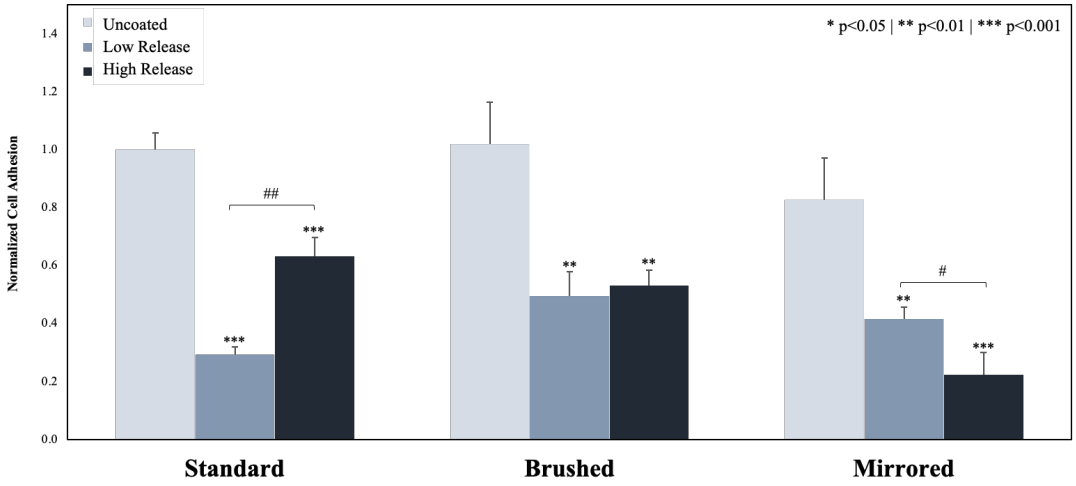

Figure 3.6 | Adhesion of *T. skag* to the surface of 316 SS coupons. Coupons were coated using both the Low Release (pH 7.4, 21°C) and High Release (pH 8.5, 35°C) coating conditions. The coupons were then incubated for 20 hours in a solution of *T. skag* and the adhesion was evaluated. It was found that the addition of pDA surface coatings significantly reduced bacterial adhesion when compared to the uncoated surface. There was a significant difference between the low coated and high coated pDA coatings on the standard and mirrored surface, however, there was no difference in bacterial adhesion on the brushed surface between the coatings. A * indicates a significant difference from the respective uncoated surface (* p<0.05 | ** p<0.01 | *** p<0.01). A # indicates an individual significant difference (# p<0.05 | ## p<0.01). An analysis of any significant differences between surfaces can be found in **Appendix C Figure C.6B**.

Staphylococcus epidermidis

As previously described, on a standard surface finish (control) there was a significant increase in the quantity of *S. epi* adhered to the stainless steel with the addition of a High Release pDA coating (**Figure 3.4**). However, after *S. epi* was exposed to a non-lethal dose of H_2O_2 for 24 hours prior to being exposed to a High Release pDA coating, a significant reduction in adhesion was observed when compared to both the uncoated surface (44% reduction) and the previously unexposed bacteria on a High Release pDA coating (30% reduction) (**Figure 3.7B**).

Psychrobacter cryohalolentis

After *P. cryo* was exposed to a non-lethal dose of H_2O_2 and then exposed to a High Release pDA coated surface, there was a significant reduction in adhesion when compared to both the uncoated surface (90% reduction) and the High Release pDA coating (17% reduction) with previously unexposed bacteria (p<0.01) (**Figure 3.7C**).

Tenacibaculum skagerrakense

After *T. skag* was exposed to the non-lethal dose of H_2O_2 and then exposed to a High Release pDA coating, there was a significant reduction in adhesion when compared to the uncoated surface (40% reduction, $p<0.05$) but was not significantly different from the High Release pDA coating with previously unexposed bacteria (**Figure 3.7D**).

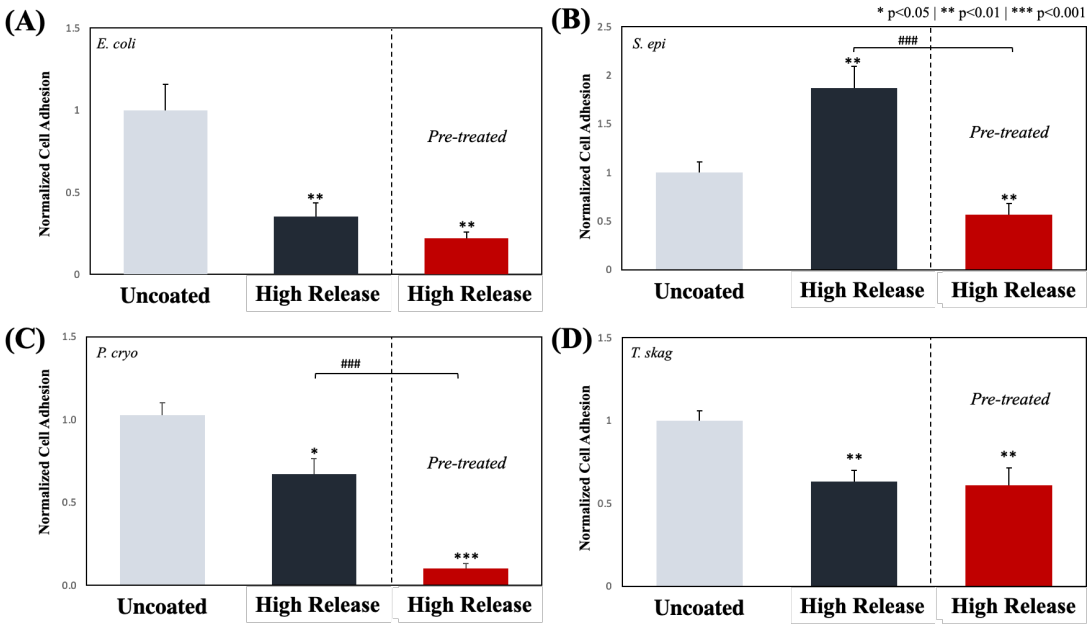

Figure 3.7 | *The effect of pre-treating various bacterium types with 200µM of hydrogen peroxide prior to evaluating adhesion on pDA coated surfaces*. Stainless steel coupons with a standard surface finish with and without the High Release pDA coating were exposed to bacteria that either were never exposed to a non-lethal dose of hydrogen peroxide or were pre-treated with a bolus dose of 200µM for 24 hours before being propagated. On all bacteria tested, no resistance was seen (i.e., there was no increase in adhesion on the pDA coated coupons when pre-treated bacteria was compared to the non-treated bacteria). (A) *E. coli* saw no significant decrease when compared to the non-treated pDA coated coupons, but the adhesion was significantly inhibited compared to the uncoated surface. (B) *S. epi* saw an increase in adhesion from the non-treated bacteria with the addition of the pDA coating however, pre-treated bacteria were less likely to adhere to the pDA coating. (C) *P. cryo* bacteria saw an additional decrease in bacterial adhesion on pDA coated coupons when compared to both the uncoated and coated surface. (D) *T. skag* saw similar results to that of E. coli where there was no resistance seen after treatment but also no additional susceptibility to the pDA coating. A * indicates a significant difference from the uncoated control (*p<0.05 | **p<0.01 | ***p<0.001), while a ### indicates an individual significant difference (p<0.001).

3.4 Discussion

A prevalent concern with implantable devices in cetaceans remains the sterility of the surface prior to and during the deployment and implantation processes. The reasoning for concern surrounds the penetration through the dermal layer which contains a microbiome rich in bacteria. While remaining on the surface of the body, these bacteria can be

beneficial but if allowed to grow internally they can become the cause of localized or systemic infection. This concern has led to the preventative use of antibiotic coatings on the surface of implantable devices (e.g., (Mate et al., 2007)). However, with the increasing use of antibiotics, there comes an increasing concern regarding antibiotic-resistant pathogens within cetacean populations (IWC, 2020). Currently, there are no documented accounts of antibiotic-resistant pathogens developing as a result of antibiotic use on the surface of satellite telemetry tags, however, the potential has driven an interest in non-antibiotic-based approaches to prevent infection. Polydopamine surface coatings can act in place of antibiotic coatings to prevent bacterial adhesion and colonization while minimizing the chances of resistance being formed. During polymerization, pDA surface coatings release micro-doses of H_2O_2 which are comparable to the doses released by epithelial cells after injury (Zhu et al., 2017; Tyo et al., 2019).

Prior to testing bacterial adhesion with pDA surface coatings, bacteria were evaluated for their bacteriostatic threshold. It was found that all bacterium types tested remained in a bacteriostatic condition for at least 12 hours when exposed to a dose of H_2O_2 greater than 150μM. A summary of the minimum exogenous dose required to induce bacteriostatic conditions for 12 hours as well as the reduction in adhesion when exposed to the High Release coating can be found in **Table 3.2**.

It is well known that bacteria respond to antibiotics such as Vancomycin in a concentration-dependent fashion (Marella et al., 2020). The dose can be delivered either in a bolus dose (also known as an immediate release) or through a more extended-release. The extended release has been shown to increase the efficacy of antibiotics as well as reduce the chances for resistance formation within bacterial populations (Adams et al., 2009). Because the half-life of H_2O_2 in solution is less than 2 hours, maintaining a stable solution concentration to test the response of bacteria is difficult. Our pDA coatings provided a vehicle in which a stable solution concentration could be obtained to observe the effect on both the concentration of bacteria in solution as well as the effect on bacterial adhesion. As previously discussed, the dose required to induce a bacteriostatic condition in the four tested species was less than 200μM (**Table 3.2**). When bacteria were exposed to medical-grade stainless steel without the presence of H_2O_2, they were observed to have little problem adhering to the surface over a 24 hour period and, given more time, would have formed a biofilm on the surface. When the same bacteria were

exposed to pDA coated stainless steel, they were not able to form the same stable bonds – with one notable exception: *S. epi* (**Figure 3.2**). Gram-positive bacteria are more likely to have the ability to produce an enzyme that can degrade ROS, essentially, creating a food source for further proliferation. The addition of the High Release pDA surface coating may have provided enough H_2O_2 to trigger the production of enzymes from *S. epi* which will improve survival outcomes.

Table 3.2 | Summary of bacterial responses to one-time bolus doses of hydrogen peroxide and High Release pDA surface coatings. The minimum one-time dose was calculated as the minimum dose required to induce a bacteriostatic response (turbidity measurement < 0.2) for 12 hours. The change in adhesion value is representative of the adhesion to the High Release pDA surface coatings for each bacteria type relative to the uncoated stainless-steel control.

Bacteria Type	***Minimum One-Time Dose***	***Change in Adhesion***
E. coli	100μM	-65%
P. Cryohalolentis	100μM	-80%
T. Skagerrakense	100μM*	-37%
S. Epidermidis	50μM	+86%

*The baseline bacterial growth at 12 hours was not above 0.2. Because of this, the tine threshold used to evaluate bacteriostatic conditions was 18 hours.

The Low Release pDA surface coating proved to be effective at preventing bacterial adhesion to stainless steel with a standard surface finish on half the tested strains (*E. coli* and *T. skag*) while the High Release coating was able to reduce adhesion on all gram-negative bacterial strains for the three tested surface finishes. The Low Release pDA coating only reduced bacterial adhesion with *E. coli* on a standard surface finish (**Figure 3.4**) and was able to consistently reduce adhesion, regardless of surface finish, with *T. skag* (**Figure 3.6**). The two aquatic bacterial strains exhibited sensitivity to the High Release pDA surface coating regardless of surface finish. These gram-negative bacteria strains are more likely to be susceptible to ROS as they do not inherently possess a mechanism to degrade H_2O_2 into its byproducts. *Staphylococcus* bacteria have the less common ability to degrade H_2O_2 into its byproducts - water and oxygen - and use them as a source of nutrients to increase growth (Ryan and Kleinberg, 1995; Painter et al., 2015). We see this behavior when *S. epi* was exposed to our High Release pDA coatings regardless of surface finish. Once the effectiveness of our High Release pDA surface coatings to reduce bacterial adhesion was established, the potential for a resistance to be

formed or for efficacy against bacterial adhesion to decline after prior exposure needed to be established. Most works examining resistance use bolus doses of H_2O_2 which induce a 90% reduction in viability. Interestingly, *S. epi* seemed to become more susceptible to pDA coatings after prior exposure to H_2O_2 (200µM) (**Figure 3.7**) while the other bacteria species tested showed no significant change in adhesion between pre-treated and untreated bacteria. It has been observed that extracellular DNA contributes to an increase in bacterial adhesion and subsequent biofilm formation (Pakkulnan et al., 2019). As H_2O_2 can damage DNA, both intracellular and extracellular, it is possible that any extracellular DNA deposited on the surface of the stainless steel which would have acted to improve bacterial adhesion is unable to due to the presence of the pDA surface coatings.

Currently, pDA coatings are primarily used to improve surface adhesive character, either by priming the surface to better bind to a secondary substrate or acting synergistically with a secondary adhesive (Beckford and Zou, 2014; He et al., 2014; Tran et al., 2018), or are used detect the presence of various molecules (Ma et al., 2013; Lin et al., 2014; Xu et al., 2019). However, this work indicates pDA surface coatings can be an effective way to reduce bacterial adhesion and subsequently reduce the chance of biofilm formation and infection on medical-grade stainless steel. As infection is a concern with the use of implantable devices, not just for cetaceans but for all marine animals, these coatings could be applied to a range of tools used in marine conservation. As pDA has the ability to adhere to multiple types of surfaces (i.e., metal, polymer, ceramics, etc.), it could potentially be used to impart tools used in marine conservation with antimicrobial properties. Although, the coating protocol may need to be optimized for the the specific surface type used in varying applications.

3.5 CONCLUSION

Stainless steel coated with pDA has a demonstrated ability to reduce bacterial adhesion of *E. coli*, *T. skag*, and *P. cryo* regardless of the underlying surface roughness. There was also no evidence of a resistance being formed after exposure to a non-lethal dose of H_2O_2. On the contrary, there was an increased susceptibility to the pDA surface coating after initial exposure for *S. epi.* The coating, which has a tailorable release profile through the alteration of coating conditions, has the potential to reduce bacterial adhesion and therefore prevent biofilm formation which could lead to subsequent infection. In addition

to being able to prevent bacterial adhesion, the quantities of H_2O_2 released are within the therapeutic range and have the potential to aid in wound healing mechanisms. The next chapter will evaluate the ability for pDA surface coatings to act as a wound healing aid via direct cellular contact or through the prolonged release of micro-doses of H_2O_2.

3.6 REFERENCES

Adams, S.B., Jr., Shamji, M.F., Nettles, D.L., Hwang, P., and Setton, L.A. (2009). Sustained release of antibiotics from injectable and thermally responsive polypeptide depots. *Journal of biomedical materials research. Part B, Applied biomaterials* 90(1)**,** 67-74. doi: 10.1002/jbm.b.31254.

Apprill, A., Robbins, J., Eren, A.M., Pack, A.A., Reveillaud, J., Mattila, D., et al. (2014). Humpback Whale Populations Share a Core Skin Bacterial Community: Towards a Health Index for Marine Mammals? *PLOS ONE* 9(3)**,** e90785. doi: 10.1371/journal.pone.0090785.

Balmer, B.C., Wells, R.S., Howle, L.E., Barleycorn, A.A., McLellan, W.A., Ann Pabst, D., et al. (2014). Advances in cetacean telemetry: A review of single-pin transmitter attachment techniques on small cetaceans and development of a new satellite-linked transmitter design. *Marine Mammal Science* 30(2)**,** 656-673. doi: 10.1111/mms.12072.

Beckford, S., and Zou, M. (2014). Wear resistant PTFE thin film enabled by a polydopamine adhesive layer. *Applied Surface Science* 292**,** 350-356. doi: https://doi.org/10.1016/j.apsusc.2013.11.143.

Bierlich, K.C., Miller, C., DeForce, E., Friedlaender, A.S., Johnston, D.W., and Apprill, A. (2018). Temporal and Regional Variability in the Skin Microbiome of Humpback Whales along the Western Antarctic Peninsula. *Appl Environ Microbiol* 84(5). doi: 10.1128/AEM.02574-17.

Borobia M, J., G.P., Simard Y, N., G.J., and P., B. (1995). Blubber fatty acids of finback and humpback whales from the Gulf of St. Lawrence. *Marine Biology* 122(3)**,** 12.

Fang, F.C. (2011). Antimicrobial actions of reactive oxygen species. *mBio* 2(5). doi: 10.1128/mBio.00141-11.

Frette, L., Jorgensen, N.O.G., Irming, H., and Kroer, N. (2004). Tenacibaculum skagerrakense sp. nov., a marine bacterium isolated from the pelagic zone in Skagerrak, Denmark. *Int J Syst Evol Microbiol* 54(Pt 2)**,** 519-524. doi: 10.1099/ijs.0.02398-0.

Hahn, F.E., and Sarre, S.G. (1969). Mechanism of action of gentamicin. *J Infect Dis* 119(4)**,** 364-369. doi: 10.1093/infdis/119.4-5.364.

He, S., Zhou, P., Wang, L., Xiong, X., Zhang, Y., Deng, Y., et al. (2014). Antibiotic-decorated titanium with enhanced antibacterial activity through adhesive polydopamine for dental/bone implant. *J R Soc Interface* 11(95)**,** 20140169. doi: 10.1098/rsif.2014.0169.

Hong, H.J., Hutchings, M.I., Neu, J.M., Wright, G.D., Paget, M.S., and Buttner, M.J. (2004). Characterization of an inducible vancomycin resistance system in Streptomyces coelicolor reveals a novel gene (vanK) required for drug resistance. *Molecular microbiology* 52(4)**,** 1107-1121.

IWC (2020). Report of the Joint US Office of Naval Research, International Whaling Commission and US National Oceanic and Atmospheric Administration Workshop on Cetacean Tag Development, Tag Follow-up and Tagging Best Practices.

Jung, W.K., Koo, H.C., Kim, K.W., Shin, S., Kim, S.H., and Park, Y.H. (2008). Antibacterial activity and mechanism of action of the silver ion in Staphylococcus aureus and Escherichia coli. *Applied and environmental microbiology* 74(7)**,** 2171-2178. doi: 10.1128/AEM.02001-07.

Kennedy, A.S., Zerbini, A.N., Vásquez, O.V., Gandilhon, N., Clapham, P.J., and Adam, O. (2014). Local and migratory movements of humpback whales (Megaptera novaeangliae) satellite-tracked in the North Atlantic Ocean. *Canadian Journal of Zoology* 92(1)**,** 9-18. doi: 10.1139/cjz-2013-0161.

Lagerquist, B.A., Mate, B.R., Ortega-Ortiz, J.G., Winsor, M., and Urbán-Ramirez, J. (2008). Migratory movements and surfacing rates of humpback whales (Megaptera novaeangliae) satellite tagged at Socorro Island, Mexico. *Marine Mammal Science* 24(4)**,** ???-??? doi: 10.1111/j.1748-7692.2008.00217.x.

Li, R., Liu, X., Qiu, W., and Zhang, M. (2016). In Vivo Monitoring of H2O2 with Polydopamine and Prussian Blue-coated Microelectrode. *Anal Chem* 88(15)**,** 7769-7776. doi: 10.1021/acs.analchem.6b01765.

Lin, L.-S., Cong, Z.-X., Cao, J.-B., Ke, K.-M., Peng, Q.-L., Gao, J., et al. (2014). Multifunctional Fe3O4@Polydopamine Core–Shell Nanocomposites for Intracellular mRNA Detection and Imaging-Guided Photothermal Therapy. *ACS Nano* 8(4)**,** 3876-3883. doi: 10.1021/nn500722y.

Livermore, D.M. (2000). Antibiotic resistance in staphylococci. *International Journal of Antimicrobial Agents* 16**,** 3-10. doi: https://doi.org/10.1016/S0924-8579(00)00299-5.

Ma, Y.-r., Zhang, X.-l., Zeng, T., Cao, D., Zhou, Z., Li, W.-h., et al. (2013). Polydopamine-Coated Magnetic Nanoparticles for Enrichment and Direct Detection of Small Molecule Pollutants Coupled with MALDI-TOF-MS. *ACS Applied Materials & Interfaces* 5(3)**,** 1024-1030. doi: 10.1021/am3027025.

Madanská, J., Vitková, Z., and Capková, Z. (2004). [Examination of the stability of hydrogen peroxide solutions]. *Ceska Slov Farm* 53(5)**,** 261-263.

Marella, P., Roberts, J., Hay, K., and Shekar, K. (2020). Effectiveness of Vancomycin Dosing Guided by Therapeutic Drug Monitoring in Adult Patients Receiving Extracorporeal Membrane Oxygenation. *Antimicrobial Agents and Chemotherapy* 64(9)**,** e01179-01120. doi: doi:10.1128/AAC.01179-20.

Mate, B., Mesecar, R., and Lagerquist, B. (2007). The evolution of satellite-monitored radio tags for large whales: One laboratory's experience. *Deep Sea Research Part II: Topical Studies in Oceanography* 54(3)**,** 224-247. doi: https://doi.org/10.1016/j.dsr2.2006.11.021.

Nelson, T.M., Apprill, A., Mann, J., Rogers, T.L., and Brown, M.V. (2015). The marine mammal microbiome: current knowledge and future directions. *Microbiology Australia* 36(1)**,** 8-13. doi: https://doi.org/10.1071/MA15004.

Ojha, N., Roy, S., He, G., Biswas, S., Velayutham, M., Khanna, S., et al. (2008). Assessment of wound-site redox environment and the significance of Rac2 in cutaneous healing. *Free Radical Biology and Medicine* 44(4)**,** 682-691. doi: https://doi.org/10.1016/j.freeradbiomed.2007.10.056.

Ortega, M.P., Hagiwara, T., Watanabe, H., and Sakiyama, T. (2010). Adhesion behavior and removability of Escherichia coli on stainless steel surface. *Food Control* 21(4)**,** 573-578. doi: https://doi.org/10.1016/j.foodcont.2009.08.010.

Painter, K.L., Strange, E., Parkhill, J., Bamford, K.B., Armstrong-James, D., and Edwards, A.M. (2015). Staphylococcus aureus adapts to oxidative stress by producing H2O2-resistant small-colony variants via the SOS response. *Infection and immunity* 83(5)**,** 1830-1844. doi: 10.1128/IAI.03016-14.

Pakkulnan, R., Anutrakunchai, C., Kanthawong, S., Taweechaisupapong, S., Chareonsudjai, P., and Chareonsudjai, S. (2019). Extracellular DNA facilitates bacterial adhesion during Burkholderia pseudomallei biofilm formation. *PLoS One* 14(3), e0213288. doi: 10.1371/journal.pone.0213288.

Pal, S., Tak, Y.K., and Song, J.M. (2007). Does the antibacterial activity of silver nanoparticles depend on the shape of the nanoparticle? A study of the Gram-negative bacterium Escherichia coli. *Applied and environmental microbiology* 73(6), 1712-1720. doi: 10.1128/AEM.02218-06.

Ross, A.A., Rodrigues Hoffmann, A., and Neufeld, J.D. (2019). The skin microbiome of vertebrates. *Microbiome* 7(1), 79. doi: 10.1186/s40168-019-0694-6.

Ryan, C.S., and Kleinberg, I. (1995). Bacteria in human mouths involved in the production and utilization of hydrogen peroxide. *Archives of Oral Biology* 40(8), 753-763. doi: https://doi.org/10.1016/0003-9969(95)00029-O.

Shaikh, S., Fatima, J., Shakil, S., Rizvi, S.M., and Kamal, M.A. (2015). Antibiotic resistance and extended spectrum beta-lactamases: Types, epidemiology and treatment. *Saudi J Biol Sci* 22(1), 90-101. doi: 10.1016/j.sjbs.2014.08.002.

Tran, N.T., Flanagan, D.P., Orlicki, J.A., Lenhart, J.L., Proctor, K.L., and Knorr, D.B. (2018). Polydopamine and Polydopamine–Silane Hybrid Surface Treatments in Structural Adhesive Applications. *Langmuir* 34(4), 1274-1286. doi: 10.1021/acs.langmuir.7b03178.

Tyo, A., Welch, S., Hennenfent, M., Kord Fooroshani, P., Lee, B.P., and Rajachar, R. (2019). Development and Characterization of an Antimicrobial Polydopamine Coating for Conservation of Humpback Whales. *Frontiers in Chemistry* 7(618). doi: 10.3389/fchem.2019.00618.

Vatansever, F., de Melo, W.C., Avci, P., Vecchio, D., Sadasivam, M., Gupta, A., et al. (2013). Antimicrobial strategies centered around reactive oxygen species--bactericidal antibiotics, photodynamic therapy, and beyond. *FEMS Microbiol Rev* 37(6), 955-989. doi: 10.1111/1574-6976.12026.

Watanakunakorn, C. (1984). Mode of action and in-vitro activity of vancomycin. *J Antimicrob Chemother* 14 Suppl D, 7-18. doi: 10.1093/jac/14.suppl_d.7.

Xu, S., Zhang, G., Fang, B., Xiong, Q., Duan, H., and Lai, W. (2019). Lateral Flow Immunoassay Based on Polydopamine-Coated Gold Nanoparticles for the Sensitive Detection of Zearalenone in Maize. *ACS Applied Materials & Interfaces* 11(34)**,** 31283-31290. doi: 10.1021/acsami.9b08789.

Yoo, S.K., and Huttenlocher, A. (2009). Innate immunity: wounds burst H2O2 signals to leukocytes. *Curr Biol* 19(14)**,** R553-555. doi: 10.1016/j.cub.2009.06.025.

Zhu, G., Wang, Q., Lu, S., and Niu, Y. (2017). Hydrogen Peroxide: A Potential Wound Therapeutic Target? *Med Princ Pract* 26(4)**,** 301-308. doi: 10.1159/000475501.

Chapter 4

Evaluation of Bolus Versus Chronic Exposure to H_2O_2 on Cell Viability

The chapter explores the effect of H_2O_2 released from polydopamine coatings and exogenously delivered in discrete doses on the viability of various relevant model cell types. The cell types evaluated are L929 fibroblasts, adult human epidermal keratinocytes (HeKa), malignant melanoma (MeWo) fibroblasts, and pre-adipocytes (3T3-L1).

The material in this chapter is currently part of a manuscript in preparation for submission in the Fall of 2022.

4.1 Background

Satellite telemetry tags are used to monitor the migration patterns of large cetaceans. Because they are implanted into the blubber, they are a source of injury and increase the potential for infection. The previous chapter explored the ability of a pDA surface coating to inhibit the adhesion and subsequent biofilm formation on the surface of the tags. It is thought that the reduction in infection can improve the retention of the tags. Other mechanisms to increase retention surround mechanically altering the tag body to include additional retention elements such as stainless steel petals and barbs. These mechanisms, while effective at increasing retention time, cause increased quantities of tissue damage. A different school of thought on how to increase the retention of tags is through the promotion of stable, integrative wound healing mechanisms. It is possible that pDA coatings can improve the retention of the tag through the promotion of local wound healing mechanisms without the addition of mechanical retention elements which may increase local tissue damage.

However, the dermal wound healing cascade is still not well understood in cetaceans. Their extraordinary healing capabilities have interested many; however, there is a high level of difficulty in monitoring individuals and ethical concerns around obtaining samples of wounds in various stages of healing from live animals. To date, there have only been three studies that have examined the macroscopic and histological properties of dermal wound healing (two examined superficial wound healing (Bruce-Allen and

Geraci, 1985; Geraci and Bruce-Allen, 1987) while one examined full-thickness shark bite wounds (Su et al., 2022)). The most notable differences in wound healing between humans and cetaceans were the lack of blood clots and subsequent scab formation in cetaceans and the complete restoration of rete ridges and dermal papillae after a full-thickness wound (Su et al., 2022). Instead of a blood clot, a layer of degenerative cells and vesicles covered wounds. It is believed that rete ridges help prevent delamination of the epidermis from the dermis during high-speed swimming (Giacometti, 1967). At the same time, the dermal papillae increase the ratio of germinative to superficial cells (Reeb et al., 2007). This increased ratio is thought to increase the proliferative capacity of cetacean skin. The most notable structural difference between human and cetacean skin is the absence of the stratum granulosum and stratum lucidum in cetaceans (Cozzi et al., 2017). Other than structural differences potentially leading to improved healing outcomes, there has not been a study into cellular mechanisms that might contribute to cetaceans' extraordinary capabilities.

In humans, cutaneous wound healing occurs in three overlapping phases: inflammation, proliferation/migration, and remodeling. In the inflammation phase (injury to 48 hours after injury), platelets are activated, releasing platelet-derived growth factor and TGF-β1 (Mannaioni et al., 1997). These factors attract additional platelets, neutrophils, and fibroblasts (Camussi et al., 2010). Thrombin in the wound site will activate fibrinogen released from cells locally to form a fibrin network that traps erythrocytes forming a blood clot (Wolberg and Campbell, 2008). Once hemostasis is achieved, the wound environment becomes slightly hypoxic and basic (Leveen et al., 1973; Ruthenborg et al., 2014). These conditions are conducive to activating various growth factors such as VEGFs (Krock et al., 2011) and HIFs (Hong et al., 2014). Monocytes attracted to the wound site via fibrin degradation products (Robson et al., 1994; Jennewein et al., 2011) and TGF-β1 will replace the neutrophils present during the initial coagulation phase (Wahl et al., 1987; Turley et al., 1996). Monocytes then transform into macrophages to kill bacteria locally and clean up any remaining tissue debris. Macrophages will also release growth factors and ROS via a respiratory burst (Forman and Torres, 2001; Tan et al., 2016). The main ROS generated is superoxide (O_2^-) which will almost instantaneously oxidize into H_2O_2 (Hayyan et al., 2016). However, if a basic

environment is maintained, the wound will not progress past the inflammatory phase and a chronic wound can form (Gethin, 2007).

The proliferation/migration phase begins as macrophages finish cleaning the environment (around 24-48 hours after initial injury). During this phase, keratinocytes will undergo a proliferation burst and migrate to the wound (Balasubramanian and Eckert, 2007; Guo et al., 2020). Epidermal growth factor (EGF) activation will stimulate the proliferation of keratinocytes which have also been shown to enhance the activity of immune cells through the expression of HLA (Chen et al., 1993; Gibbs et al., 2000). Suppose a hypoxic environment was maintained during this phase; in that case, the low oxygen content could increase fibroblasts' activation, replication, and longevity and increase the activation of various growth factors. It has been found that during this phase, there is also a significant increase in the local concentration of H_2O_2 (Niethammer et al., 2009) - generated from either macrophages (Bae et al., 2009) or fibroblasts through the NADPH pathway (Buck et al., 2019). In a murine wound model, this concentration has been evaluated to peak at a concentration of 300μM two days after the initial injury (Roy et al., 2006; Niethammer et al., 2009). H_2O_2 in these concentrations can act as a downstream signaling molecule used to improve wound healing outcomes and act as a deterrent to bacterial adhesion.

H_2O_2 has historically been commonly used as a wound debridement solution due to its effectiveness as an antimicrobial agent, with a low chance of resistance being formed by microbes (Linley et al., 2012; Goudarzi et al., 2018b). The H_2O_2 within the wound environment is naturally present as a concentration gradient which, while acting as a downstream signaling molecule, can act as a barrier against bacterial adhesion (**Figure 4.1**). This makes H_2O_2 a promising molecule to prevent infection at the wound site. However, H_2O_2 is inherently unstable in solution, making it challenging to engineer a mechanism in which a stable concentration can be generated (Pędziwiatr et al., 2018). It is currently unknown what range of H_2O_2 will promote or accelerate wound healing in cetaceans. Thus, H_2O_2 concentration needs to be carefully tailored depending on the application. The addition of H_2O_2 exogenously has been shown to induce the expression of VEGF in keratinocytes (Roy et al., 2006). VEGF is a known growth factor that can induce angiogenesis in the wound site. The formation of new and stable blood vessels is essential for supporting the metabolic needs of newly formed tissue. The migration of

keratinocytes to the injured dermis starts the re-epithelization process, which contributes to repairing the epidermal barrier to prevent infection and dehydration.

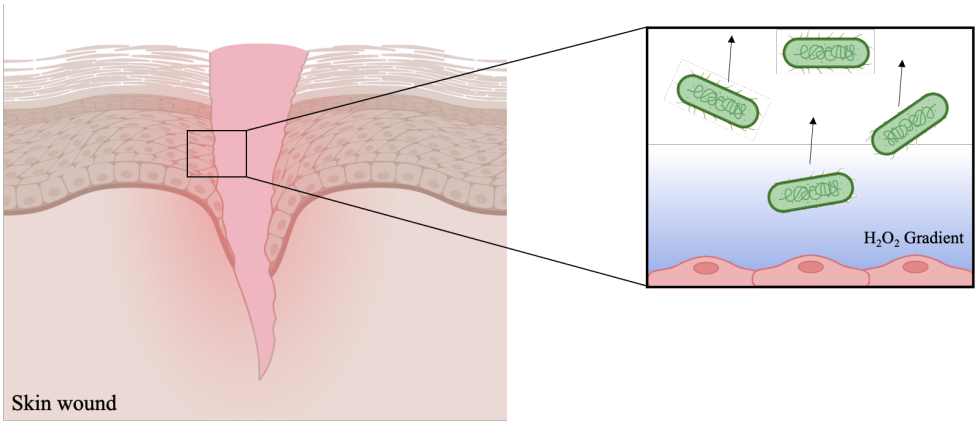

Figure 4.1 | *Schematic representation of hydrogen peroxide gradient generated by epithelial cells after injury.* Epithelial cells will generate H_2O_2 in response to an injury which is part of the oxidative host defense response. This is typically achieved through DUOX expression after injury. The gradient produced will effectively repel most bacteria to reduce overall chances of infection. (Image created using BioRender.com)

H_2O_2 has previously been administered to wounds in bolus doses which degrade within the first few hours of application. To make these doses effective at killing any local bacteria which may have entered the wound site, they have to be higher than at least 1mM (Juven B and M.D., 1996; Linley et al., 2012). This dose can be toxic to the surrounding immune cells and wound effector cell types. As these cells die, the wound healing process may become stunted or even change from regenerating native tissue to a process that is more likely to produce scar tissue. Polydopamine can mimic the H_2O_2 produced locally in the wound environment and generate stable concentrations comparable to the quantity released from cells after injury. This chapter is going to explore the impact pDA surface coatings that have previously been established to prevent bacterial adhesion to the surface of medical grade stainless steel have on model cell types that are highly involved in dermal wound healing. The viability, morphology, and proliferative behavior will be evaluated for four cell types: L929 fibroblasts, adult human epidermal keratinocytes, malignant melanoma fibroblasts, and pre-adipocytes. The malignant melanoma cell line was chosen for its ability to express dermcidin in response to oxidative stress which is explored further in chapter 5.

4.2 Materials and Methods

L929 Fibroblasts (ATCC CCL-1) were cultured using DMEM (Sigma Aldrich, St. Louis MO) supplemented with 10% FBS (Sigma Aldrich, St. Louis MO). The seeding density used unless otherwise indicated was $5x10^4$ cells/cm^2.

Adult Human Epidermal Keratinocytes (HeKa) (ATCC PCS-200-011) were cultured using medium 154 (Thermo Fisher, Waltham MA) supplemented using a human keratinocyte growth supplement (HKGS) kit (Thermo Fisher, Waltham MA). The seeding density used unless otherwise indicated was $4x10^4$ cells/cm^2.

Malignant Melanoma (MeWo) (ATCC HTB-65) were cultured using EMEM (ATCC 30-2003) supplemented with 10% FBS (Sigma Aldrich, St. Louis MO). The seeding density used unless otherwise indicated was $4x10^4$ cells/cm^2. This cell line was chosen as it is known to release the antimicrobial peptide dermcidin in response to oxidative stress. In this chapter, the viability in response to a bolus dose as well as to direct contact from pDA surface coatings is established. Their behavior in response to an indirect dose of H_2O_2 from pDA coatings is explored in chapter 5.

Pre-adipocytes (3T3-L1) (ATCC CL-173) pre-adipocytes were cultured using DMEM supplemented with 15% Fetal Calf Serum (ATCC 30-2030). The seeding density used unless otherwise indicated was $3x10^3$ cells/cm^2.

4.2.1 H_2O_2 Release from pDA Surface Coatings in Cell Culture Media

Low Release and High Release pDA coated coupons were prepared using 1cm^2 stainless steel coupons with a standard surface finish (see Chapter 2 for coating protocol). The coupons were air dried and then submerged into either DMEM or DMEM + 10% FBS without phenol red indicator. The coupons were placed in an incubator at 37°C and 5% CO_2 and a FOX assay was performed at different time points (1.5, 3, 6, 12, and 24 hours) to determined the concentration of H_2O_2 in solution.

4.2.2 Cell Viability in Response to to Bolus Doses of H_2O_2

Cells were seeded onto the bottom of a 12-well plate and were allowed to adhere for 24 hours. Once attached, cells were exposed to various doses of exogenous H_2O_2 (0µM, 50µM, 100µM, and 200µM) for 24 hours. Next, cells were stained using a live (calcein-AM) stain and a dead (ethidium bromide) stain.

4.2.3 Cell Viability in Response to Sustained Release of H_2O_2 from pDA Surface Coatings

Cells were seeded onto the bottom of a 12-well plate and were allowed to adhere for 24 hours. Once attached, cells were exposed to round pDA coated coupons (0.031cm^2) for 24 hours. Coupons were coated using the Low Release and High Release coating conditions (see Chapter 2 for coating protocol) and then sterilized using ethylene oxide. Next, cells were stained using a live (Calcein-AM) stain and a dead (Ethidium Bromide) stain.

L929 fibroblasts and HeKa cells' proliferative state was evaluated using a Ki67 stain after being exposed to pDA coated coupons coated with the Low Release and High Release coatings. The cells were exposed to the H_2O_2 releasing coupons for 24 hours before evaluating proliferation.

4.2.4 Cell Adhesion to the Surface of Medical Grade Stainless Steel

Stainless steel coupons (10mm x 20mm) with varying surface roughness [standard (Ra= 0.635µm), brushed (Ra = 0.813µm), and mirrored (Ra = 0.15µm)] were used. Coupons were then rinsed in PBS and gas sterilized for 12 hours using ethylene oxide. In a 6-well tissue culture treated plate, cells were seeded uniformly on the surface of uncoated stainless steel coupons with a brushed, standard, and mirrored surface finish. The cells were allowed to attach to the surface for 2 hours at 37°C and 5% CO_2 before adding an additional 5mL of media. The plates were then placed back into the incubator for 24 hours. After 24 hours, cells were stained using a live-dead stain (Calcein-AM and Ethidium Bromide, respectively) before being imaged. An Olympus inverted microscope was used for all imaging of stainless steel coupons. The effect of surface roughness on adhesion was not evaluated for MeWo cells as these cells are not present in the wound environment and were only used as a model for endogenous dermcidin expression in response to oxidative stress.

4.2.5 Cell Adhesion to Medical Grade Stainless Steel with pDA Surface Coatings

Standard finished stainless steel coupons were coated with the Low Release or High Release pDA surface coatings (see Chapter 2 for coating method). In a 6-well tissue culture treated plate, cells were seeded uniformly on the surface of uncoated stainless steel coupons with a brushed, standard, and mirrored surface finish. The cells were allowed to attach to the surface for 2 hours at 37°C and 5% CO_2 before adding an

additional 5mL of media. The plates were then placed back into the incubator for 24 hours. After 24 hours, cells were stained using a live-dead stain (Calcein-AM and Ethidium Bromide, respectively) before being imaged. An Olympus inverted microscope was used for all imaging of stainless steel coupons.

4.3 RESULTS

4.3.1 H_2O_2 RELEASE FROM pDA SURFACE COATINGS IN CELL CULTURE MEDIA

The release from pDA surface coatings was markedly different between DMEM without FBS and DMEM supplemented with FBS. There was significantly more release from both the Low Release and High Release pDA coatings when media was supplemented with FBS (**Figure 4.2**). In DMEM there was no significant difference in the release between Low Release and High Release pDA coatings after 24 hours, however, in the supplemented media there were significant differences in the release quantity after 3 hours (**Figure 4.2B**).

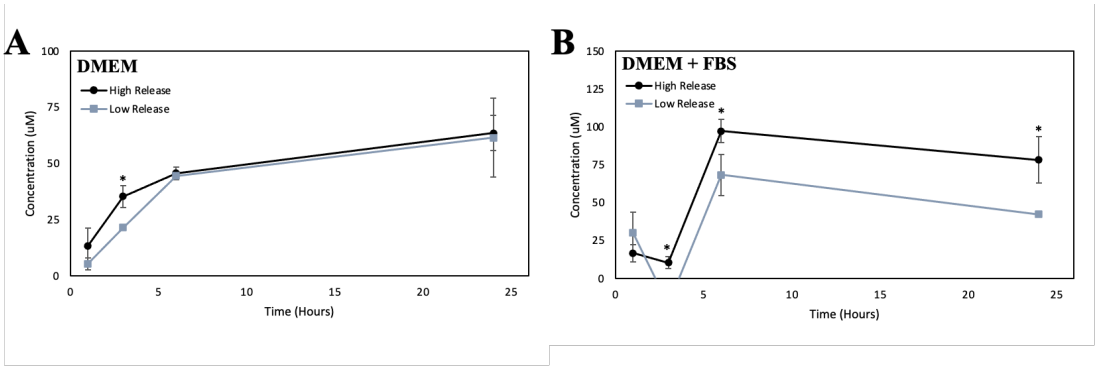

Figure 4.2 | *Release from High Release and Low Release pDA surface coatings in DMEM with and without FBS.* (A) The release from the pDA coatings was not significantly different after 24 hours in DMEM. (B) When added to DMEM with FBS, the release between the two pDA coatings was significantly different and there was significantly more release when compared to DMEM without FBS after 6 hours ($p<0.01$). A * is used to indicate a significant difference between High Release and Low Release pDA coatings. (*$p<0.05$ | **$p<0.01$ | ***$p<0.001$).

4.3.2 CELL VIABILITY IN RESPONSE TO BOLUS DOSES OF H_2O_2

The 100µM dose of H_2O_2 exhibited a significant increase in toxicity for HeKa and MeWo cell lines, while a 200µM dose exhibited no reduction in viability for L929 and 3T3-L1 cell lines. There were no dead cells observed on well plates containing 3T3-L1 pre-adipocytes.

L929 Fibroblasts

After exposure to three different doses of H_2O_2, a live dead stain was performed. The resulting images were used to determine the viability of cells after exposure and their morphology (**Figure 4.3A**). The viability of L929 fibroblasts was not reduced when a dose of up to 200µM was introduced (>95%) (**Figure 4.3B**). However, when looking at the morphology of the cells, there were significantly more cells that exhibited a spread morphology (aspect ratio <0.75). Approximately 50% of cells were considered to have a spread morphology without exposure to H_2O_2, and that value increased to 65% when exposed to 200µM of H_2O_2 (**Figure 4.3C**).

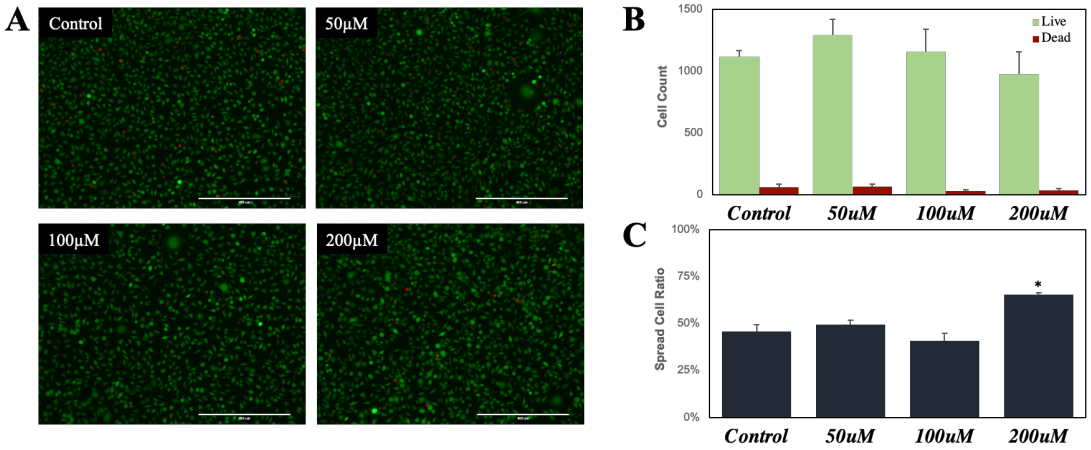

Figure 4.3 | *L929 Fibroblast Responses to bolus doses of Hydrogen Peroxide.* Fibroblasts were seeded (10^5 cells/ well) and allowed to attach overnight before being exposed to various doses of hydrogen peroxide. (A) A live/ dead assay was then performed and (B) cell counts were conducted for each group as well as (C) morphological analysis of the live cells. It was found that after exposure to hydrogen peroxide of any tested amount, there was not a significant decrease in the quantity of live cells. However, after a dose of 200µM, there was a significant increase in the quantity of spread live cells when compared to all other doses ($p<0.05$). [Scale bar = 400µm]

HeKa

Keratinocyte viability was significantly impacted when any quantity of H_2O_2 was introduced (**Figure 4.4**). A dose of 50µM also induced a significant change in morphology for the cell type. Cells appeared highly spread out, almost forming a solid layer across the bottom of the well (**Figure 4.4A**). This was confirmed when evaluating the area covered by live cells (**Figure 4.4C**). There was significant spreading when a low dose of H_2O_2 was administered exogenously to the cells. Doses above 100µM saw more dead cells than live cells adhered to the bottom of the well.

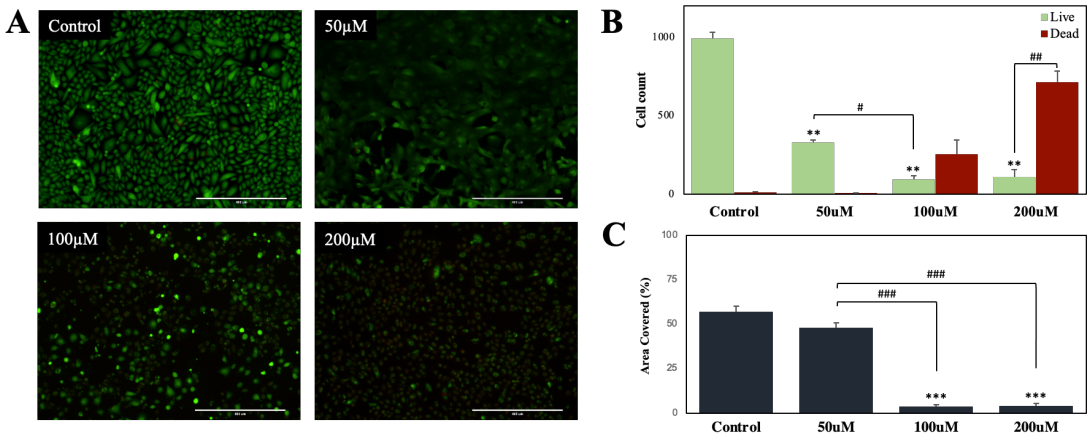

Figure 4.4 | *Keratinocyte Responses to bolus doses of Hydrogen Peroxide.* Keratinocytes were seeded (10^5 cells/ well) and allowed to attach overnight before being exposed to various doses of hydrogen peroxide. (A) A live/ dead assay was then performed and (B) cell counts were calculated for each group. (C) An analysis of area of the bottom of the well covered by live cells for each treatment was also performed to quantify morphological characteristics in place of using an aspect ratio. It was found that after exposure to hydrogen peroxide of any tested amount, there was a significant decrease in the quantity of live cells ($p<0.01$). However, after a dose of 100uM, there was a significant increase in the quantity of dead cells and the morphology of the cells was worsened (more rounded). A * indicates a significant difference compared to the control (**$p<0.01$ | ***$p<0.001$). A # is used to indicate an individual significant difference ($^{\#}$ $p<0.05$ | $^{\#\#}$ $p<0.01$ | $^{\#\#\#}$ $p<0.001$). [Scale bar = 400um]

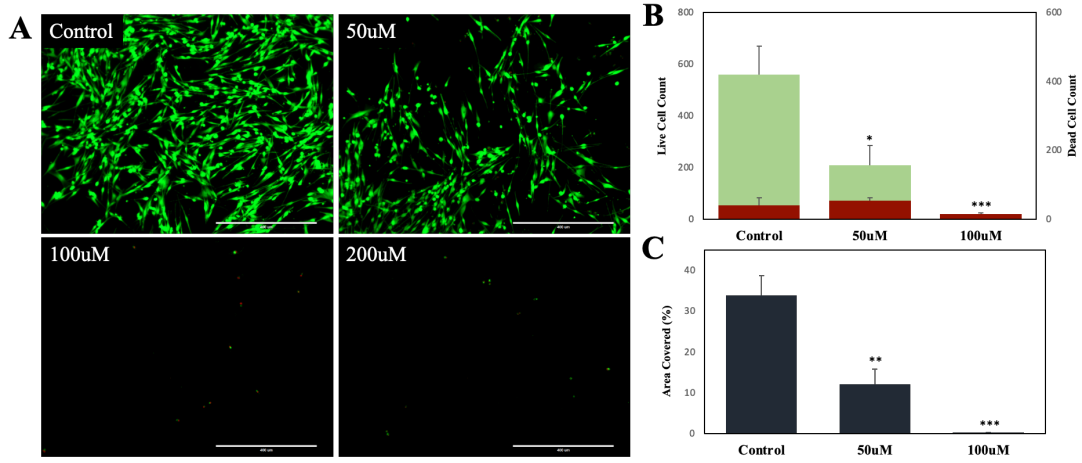

Figure 4.5 | *MeWo Responses to bolus doses of Hydrogen Peroxide.* MeWo cells were seeded and allowed to attach overnight before being exposed to various doses of H_2O_2. (A) A live/dead assay was then performed and (B) cell counts and the (C) area the cells covered were evaluated. It was found that after exposure to hydrogen peroxide of any tested amount there was a decrease in the number of cells. On the controls, MeWo cells were confluent and spread out while, after exposure, a more rounded phenotype was observed. Doses higher than 50µM were observed to significantly reduce cellular adhesion. There was no significant change in the quantity of dead cells regardless of the tested dose. A * indicates a significant difference from the control (*$p<0.05$ | **$p<0.01$ | **$p<0.001$) [Scale bar = 400µm]

MeWo

Malignant melanoma fibroblasts had the most considerable sensitivity to exogenously delivered H_2O_2 (**Figure 4.5**). After a dose of 50µM, there was around a 40% reduction in the number of live cells on the surface of the well plate. The same reduction was also observed for the area these cells covered. As the reduction was the same for both quantity of cells and area covered, the cells' morphology was not significantly altered - those that did attach exhibited a spread morphology similar to the controls (**Figure 4.5A**).

3T3-L1

Pre-adipocytes were exposed to three different doses of H_2O_2, and a live/dead stain was used to evaluate cell counts and morphology (**Figure 4.6A**). When pre-adipocytes were exposed to various quantities of H_2O_2, there was no significant change in the number of adherent cells (**Figure 4.6**). The morphology of the cells was observed to change with an increasing concentration; the cells became more spread, which is reflected by the area covered by live cells (**Figure 4.6C**). Overall, as the dose of H_2O_2 increased, the environment was more conducive to cell growth.

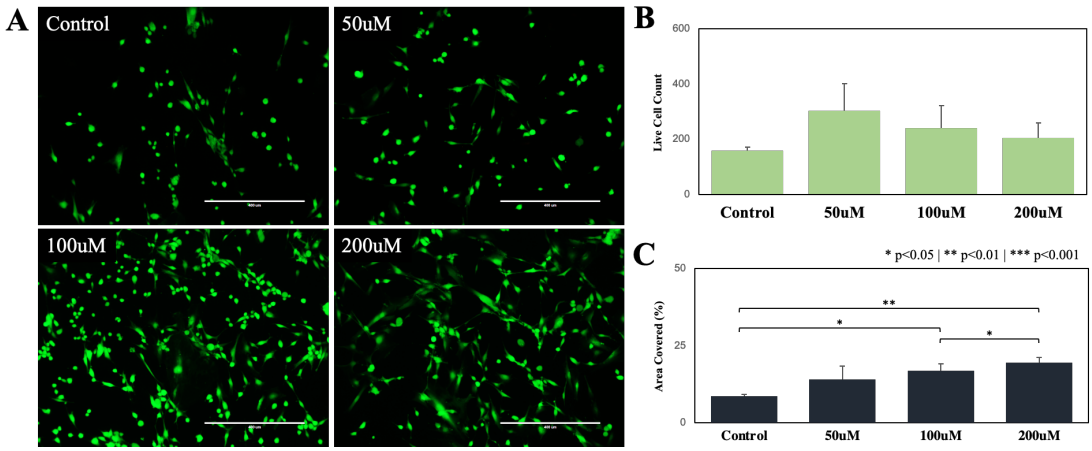

Figure 4.6 | *3T3-L1 Responses to Exogenous Doses of Hydrogen Peroxide.* Pre-adipocytes were seeded then allowed to attach overnight prior to exposure to various doses of H_2O_2. (A) A live/dead assay was performed and (B) cell counts and (C) the area the live cells covered were then calculated. It was found that after exposure there was no significant difference in the quantity of live cells on the surface of the well compared to the control. However, with increasing doses of H_2O_2 the cells spread out to cover more of the bottom of the well. A dose of 50µM did not significantly increase the area covered, but doses of 100 and 200µM covered more than 20% ($p<0.05$). A * indicates a significant difference (*$p<0.05$ | **$p<0.01$ | ***$p<0.001$). [Scale Bar = 400µm]

4.3.3 Cell Viability in Response to Sustained Release of H_2O_2 from pDA Surface Coatings

The tolerance to a number of H_2O_2 when slowly increased and held at a stable concentration was higher for each cell type tested. Cells could cumulatively withstand a greater quantity of H_2O_2 when the solution concentration was not altered quickly - as it would be with an exogenously delivered bolus dose.

L929 Fibroblasts

The overall viability of fibroblasts was not lowered to the point of cytotoxicity when exposed to clean medical grade stainless steel or the H_2O_2 release from the Low Release and High Release pDA coatings. However, there was a significant reduction in the number of cells on the bottom of the well when exposed to uncoated stainless steel (SS) and High Release pDA surface coatings (**Figure 4.7B**). Low Release pDA surface coatings did not reduce the quantity of adhered cells on the bottom of the well plate, and an increase in the proportion of cells that exhibited a spread morphology was observed (**Figure 4.7C**).

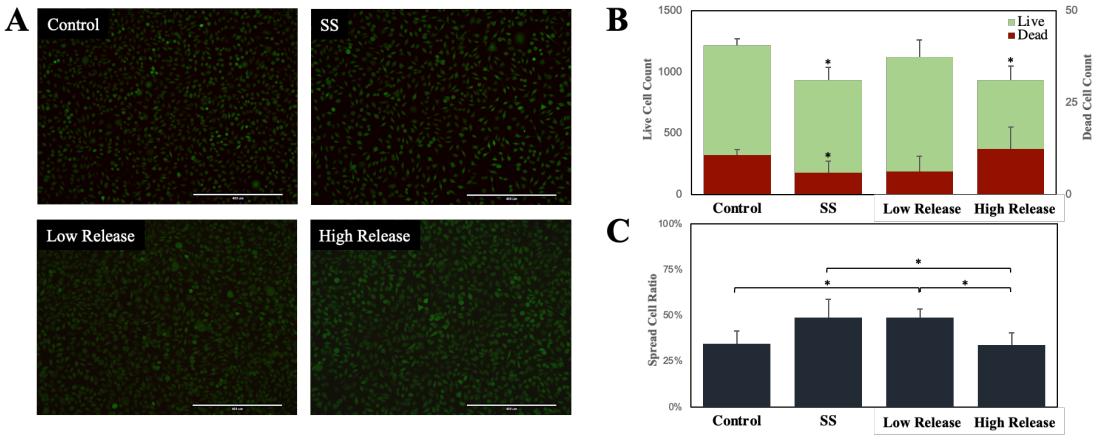

Figure 4.7 | *L929 Fibroblast Responses to indirect exposure from Low Release and High Release pDA coated coupons.* Fibroblasts were seeded (10^5 cells/well) and allowed to attach overnight before being exposed to medical grade stainless steel coupons with and without pDA coatings. (A) A live/dead assay was then performed and (B) cell counts were conducted for each group as well as (C) morphological analysis of the live cells. It was found that after exposure to stainless steel, there was a significant decrease in the quantity of live cells as well as dead cells. There was also a significant decrease in the quantity of live cells on beneath the High Release coupons. Morphologically, there was a significant increase in the quantity of spread live cells (aspect ratio <0.74) on the Low Release coupons when compared to the controls ($p<0.05$). There was a significant reduction in spreading from the stainless-steel control and the Low Release coupons in response to the High Release coupons ($p<0.05$). [Scale bar = 400µm]

The proliferative behavior of L929 fibroblasts was also not considered significantly altered after being exposed to either stainless steel or pDA surface coatings (**Figure 4.8**). Approximately 2-3% of cells expressed the active proliferation marker Ki67 no matter the concentration of H_2O_2 in solution.

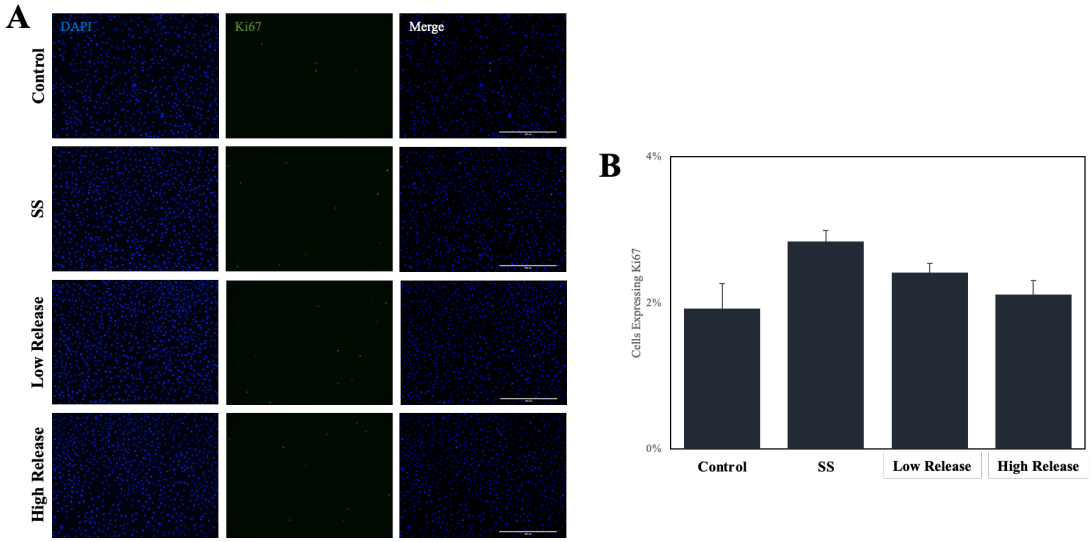

Figure 4.8 | *Fibroblast Ki67 Expression in Responses to indirect exposure from Low Release and High Release pDA coated coupons.*. Fibroblasts were seeded (10^5 cells/well) and allowed to attach overnight before being exposed to uncoated, Low Release, and High Release stainless steel. (A) A Ki67 assay was then performed and (B) the percentage of cells expressing the proliferative marker Ki67 was determined for each group. There was no significant difference between the control group and the treatments. [Scale bar = 400um]

HeKa

The viability of HeKa keratinocytes was not reduced after exposure to either the Low Release or High Release pDA coatings (**Figure 4.9B**). All cells appeared spread; however, some cells appeared to have a more spindly morphology when exposed to the pDA surface coatings (**Figure 4.9A**). This did not correspond with an increase in the area covered; there was no significant difference in the area covered by cells between any of the treatments (**Figure 4.9C**).

The proliferative characteristics of keratinocytes exposed to the pDA coatings were not significantly different from the control group (**Figure 4.10B**). However, between the pDA surface coatings, there were significantly more cells in some stage of proliferation after exposure to the High Release coatings than the Low Release coatings (94% vs. 87%) (**Figure 4.10B**).

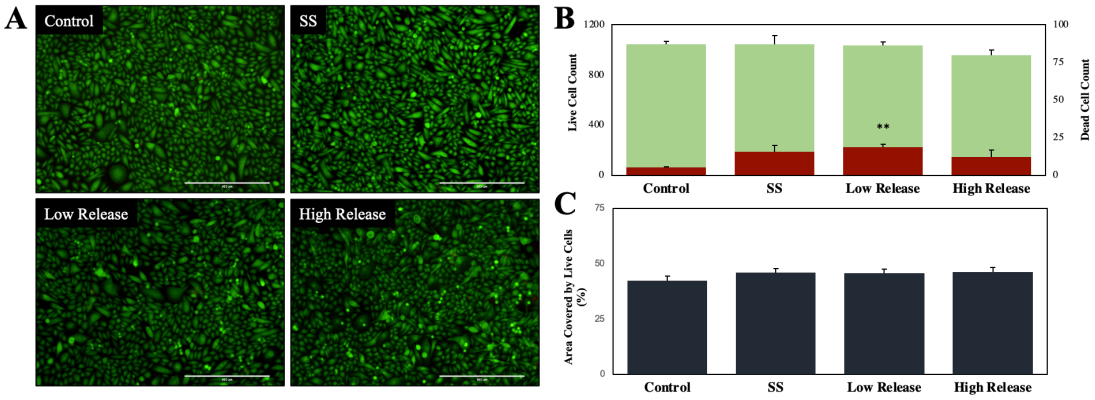

Figure 4.9 | *Keratinocyte Responses to indirect exposure from Low Release and High Release pDA coated coupons.* Keratinocytes were seeded (10^5 cells/well) and allowed to attach overnight before being exposed to uncoated, Low Release, and High Release stainless-steel coupons. (A) A live/dead assay was then performed and (B) cell counts were calculated for each group. There were no significant differences in the number of live cells found between any of the samples. There was a significant increase in the quantity of dead cells on Low Release coupons when compared to uncoated coupons ($p<0.01$). A * indicates a significant difference from control. (*$p<0.05$ | **$p<0.01$) [Scale bar = 400um]

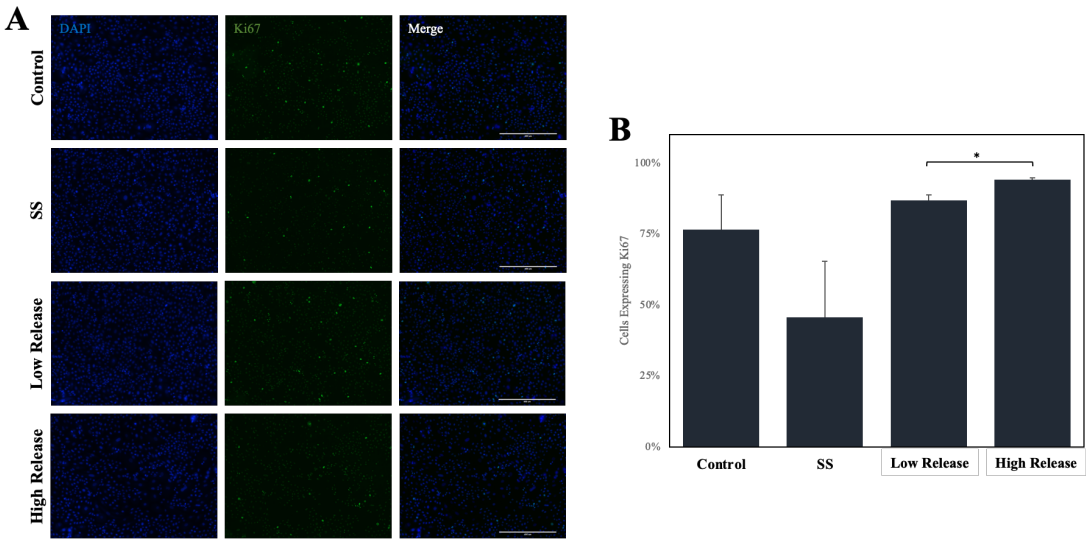

Figure 4.10 | *HeKa Ki67 Expression in Responses to indirect exposure from Low Release and High Release pDA coated coupons.*. Keratinocytes were seeded (10^5 cells/well) and allowed to attach overnight before being exposed to uncoated, Low Release, and High Release stainless steel. (A) A Ki67 assay was then performed and (B) the percentage of cells expressing the proliferative marker Ki67 was determined for each group. There was no significant difference found between the control and all other test groups. However, there was significantly more cells expressing Ki67 in response to the High Release coupons when compared to the Low Release coupons ($p<0.05$). A * indicates a significant difference between two groups ($p<0.05$). [Scale bar = 400um]

3T3-L1

When exposed to H_2O_2 released from pDA coated coupons, there was a significant increase in the number of live cells and area covered in response to the Low Release pDA coating (**Figure 4.11B**). There was significantly more area covered by the cells exposed to the Low Release and High Release pDA surface coatings (**Figure 4.11C**). This can be seen in the formation of a sort of porous network of cells that resembles adipose tissue (**Figure 4.11A**).

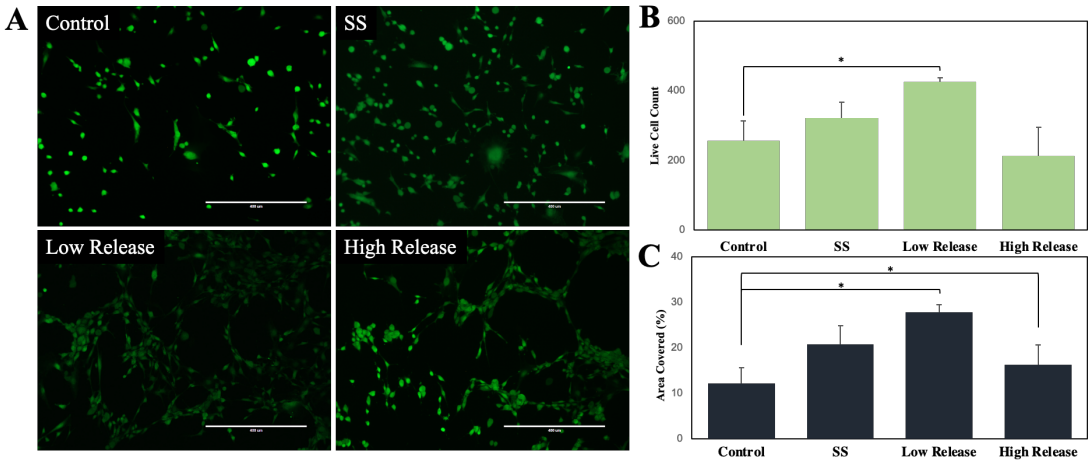

Figure 4.11 | *3T3-L1 Responses to indirect exposure from Low Release and High Release pDA coated coupons.* Pre-adipocytes were seeded then allowed to attach overnight prior to exposure to Low Release and High Release pDA coated coupons. (A) A live/dead assay was performed and (B) cell counts and (C) the area the live cells covered were then calculated. There was a significant increase in the quantity and area covered by cells in response to the Low Release pDA coating. However, when exposed to the High Release pDA coating, there was not a significant increase in the quantity of cells but there was a significant increase in the area covered. The morphology of the cell coverage was also morphologically different when exposed to the pDA coupons. The cells look to have formed a porous network similar to adipose tissue. A * indicates a significant difference (*$p<0.05$). [Scale Bar = 400μm]

4.3.4 Cell Adhesion to the Surface of Medical Grade Stainless Steel

Overall, the adhesion of each tested cell type was not significantly inhibited on medical-grade stainless steel.

L929 Fibroblasts

Cells seeded on medical-grade stainless steel were evaluated for general viability in addition to an available metric of the area covered by live cells. A brushed surface inhibited adhesion of L929 fibroblasts, exhibited by the lowest cell counts and the

smallest area covered by live cells (**Figure 4.12**). There was no significant difference in the number of dead cells on the surface of brushed stainless steel when compared to a standard or mirrored surface finish.

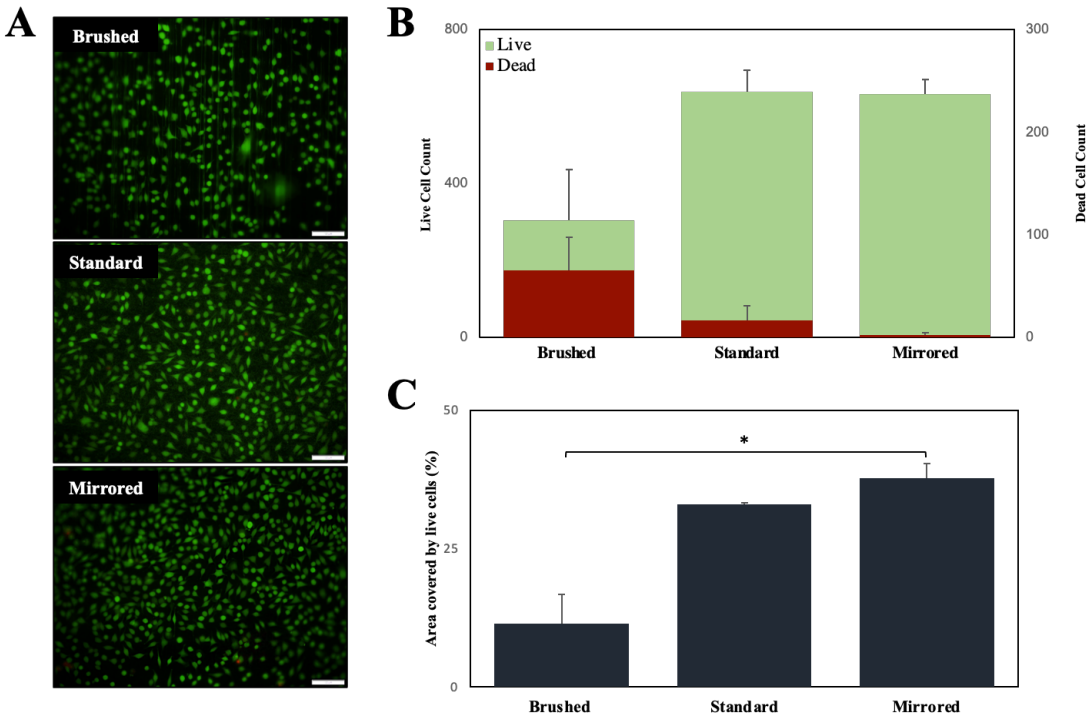

Figure 4.12 | *L929 adhesion to the surface of medical grade stainless steel.* Fibroblasts were seeded on the surface of medical grade stainless steel with a variety of surface roughnesses ($2.5x10^4$ cells/cm^2) and were cultured for 24 hours before a (A) live/dead stain was performed. (B) After 24 hours, there was no significant difference in the quantity of live or dead cells adhered to the various surfaces. (C) However, the cells which were adhered to a brushed surface exhibited a more rounded phenotype as the area covered by live cells was significantly less than a standard or mirrored surface. A * indicates a significant difference ($p<0.05$). [Scale bar = 200μM]

HeKa

Keratinocytes were more sensitive to the underlying substrate roughness than L929 fibroblasts. Compared to a standard surface finish, there was no significant change in cell behavior when changing the underlying substrate roughness (**Figure 4.13B**). However, the roughest surface (brushed finish) has a significantly lower quantity of live cells adhered to the surface when compared to the smoothest surface (mirrored finish). This same trend was not reflected when the area covered by live cells was measured (**Figure 4.13C**) which indicates cells on the mirrored surface were exhibiting a more rounded

morphology while those on the brushed surface exhibited a more spread morphology which can be seen in the live/dead images (**Figure 4.13A**).

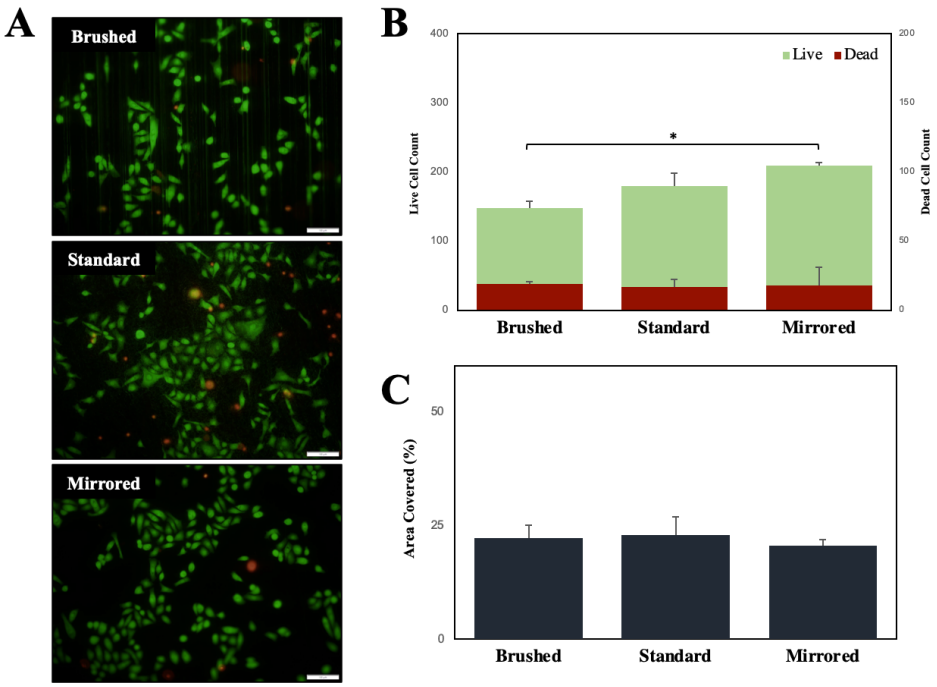

Figure 4.13 | *HeKa keratinocyte adhesion to the surface of medical grade stainless steel.* Keratinocytes were seeded on the surface of medical grade stainless steel ($2.5x10^4$ cells/cm^2) and were incubated for 24 hours prior to a (A) live/dead stain being performed. When (B) cell counts were done there were significantly more live cells on the surface of mirrored stainless steel compared to a brushed surface. There was no difference found between the standard surface and the mirrored or brushed surfaces. When the (C) area covered was evaluated there was no difference found between all surface finishes. A * indicates a significant difference (*$p<0.05$ | **$p<0.01$ | ***$p<0.001$). [Scale bar = 200µM]

3T3-L1

When seeded on the varying surfaces of medical-grade stainless steel, there was no significant difference in the viability of pre-adipocytes (**Figure 4.14B**). The morphology of the pre-adipocytes did significantly change when the underlying substrate roughness was altered. As the surface became more smooth, the cells exhibited a more spread phenotype (**Figure 4.14A**). On the mirrored surface, there are single cells that take up a large proportion of the image. On the brushed surface, cells were more like to spread in the direction of the grain whereas on a mirrored surface the spreading was more random in nature. As the number of cells did not significantly change when the underlying

substrate was altered, the morphological differences led to a significant difference in the area covered by live cells.

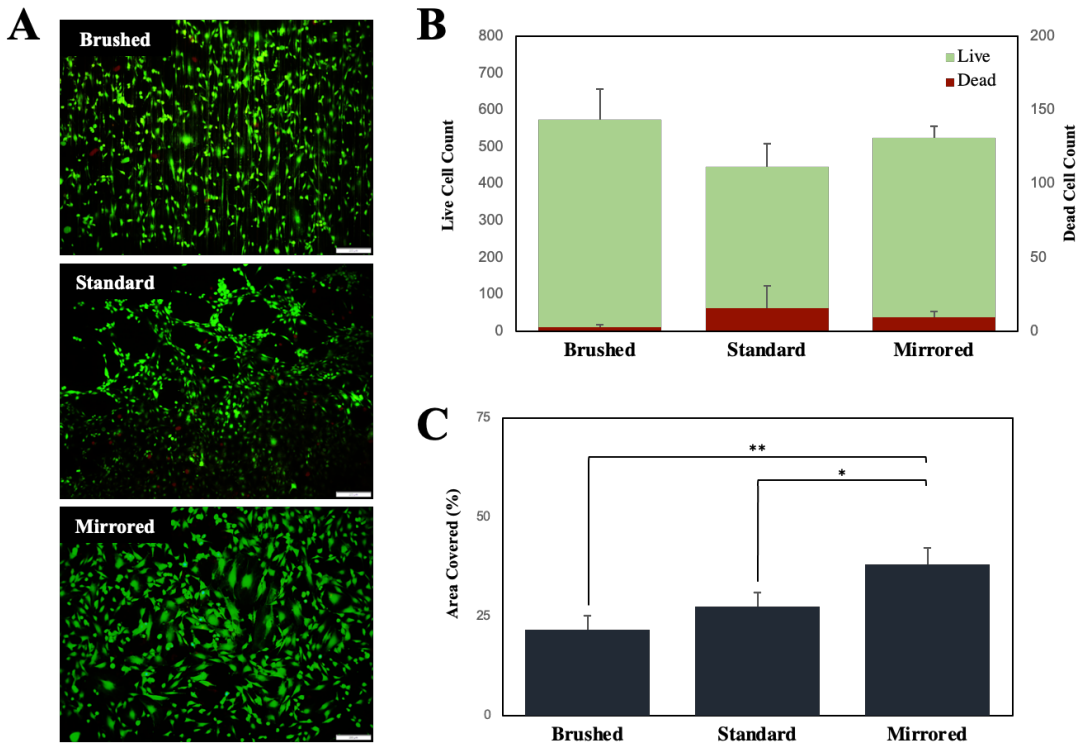

Figure 4.14 | *3T3-L1 Pre-adipocyte adhesion to the surface of medical grade stainless steel.* Pre-adipocytes were seeded on the surface of medical grade stainless steel ($3x10^3$ cells/cm^2) and were incubated for 24 hours prior to a (A) live/dead stain being performed. (B) When cell counts were done, there was no significant difference in the number of live cells or dead cells found between the surface finishes. (C) When the area covered was evaluated there was no difference found between the standard and brushed surface finishes, however, there was a significant increase in the area covered by pre-adipocytes seeded onto a mirrored surface. A * indicates a significant difference (*p<0.05 | **p<0.01 | ***p<0.001). [Scale bar = 200µM]

4.3.5 Cell Adhesion to Medical Grade Stainless Steel with pDA Surface Coatings

The adhesion was evaluated on standard stainless steel and, overall, the addition of the High Release pDA surface coating reduced the number of live cells that were adherent. There were some cell types for which their morphology was not significantly impacted. The impact of the Low Release pDA coatings was dependent on the cell type.

L929 Fibroblasts

When seeded directly onto Low Release pDA surface coatings, there was a significant reduction in cell quantity when compared to an uncoated surface (**Figure 4.15**).

However, there was no decrease in the surface area the cells covered (**Figure 4.15C**). This indicates a more spread morphology of the cells. The same response was also observed for the High Release pDA surface coatings. There was no difference in cellular behavior seen between the Low Release and High Release pDA coatings.

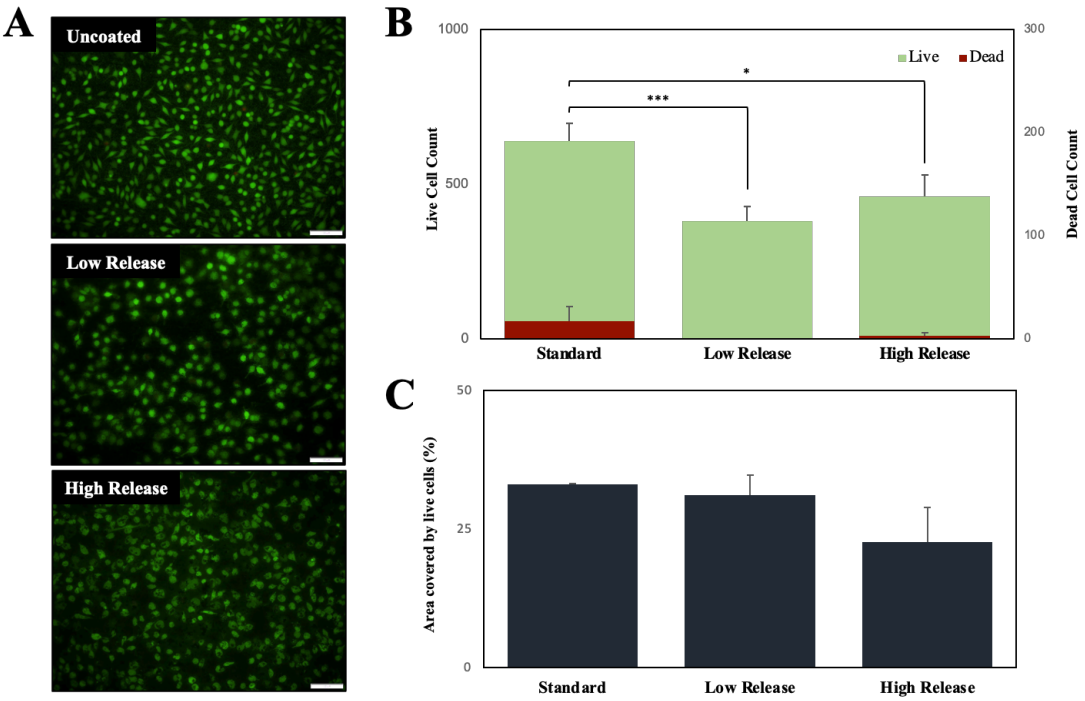

Figure 4.15 | *L929 adhesion to the surface of standard finished medical grade stainless steel with and without pDA surface coatings.* Fibroblasts were seeded on the surface of medical grade stainless steel with and without pDA surface coatings ($2.5x10^4$ cells/cm^2) and were cultured for 24 hours before a (A) live/dead stain was performed. (B) After 24 hours seeded on the surface, there was a significant decrease in the quantity of live cells adhered to the stainless steel when either the Low Release or High Release pDA coating was added. (C) However, there was not a significant difference in the area covered by live cells. This would indicate a larger quantity of live cells on the surface of the pDA coatings exhibited a spread morphology. A * indicates a significant difference (*$p<0.05$ | **$p<0.01$ | ***$p<0.001$). [Scale bar = 200µM]

HeKa

Low Release pDA surface coatings did not significantly alter keratinocyte behavior compared to uncoated standard stainless steel. When the High Release pDA coating was added, there was a significant decrease in both the number of live cells present on the surface of the coupon and the area covered compared to both the control uncoated surface and the Low Release pDA coating (**Figure 4.16**). The cells on both the Low Release pDA

coating and the uncoated surface exhibited a typical morphology for keratinocytes while those seeded on top of the High Release pDA coating were more round (**Figure 4.16A**).

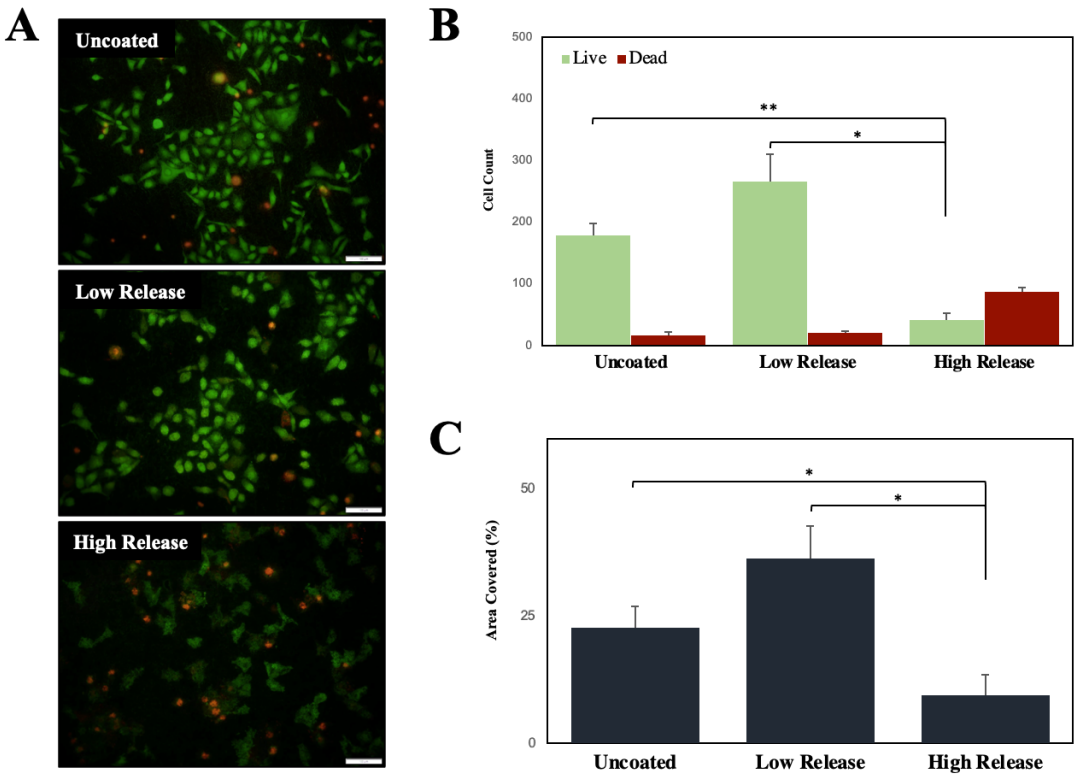

Figure 4.16 | *HeKa adhesion to the surface of standard finished medical grade stainless steel with and without pDA surface coatings.* Keratinocytes were seeded on the surface of medical grade stainless steel with and without pDA surface coatings ($2.5x10^4$ cells/cm^2) and were cultured for 24 hours before a (A) live/dead stain was performed. (B) After 24 hours seeded on the surface, there was no significant difference in the quantity of adherent live cells between the Low Release and uncoated surface. There was a significant decrease in the quantity of adhered live cells in response to the High Release pDA coating when compared to both the uncoated surface and the Low Release pDA coated surface. (C) This same trends were observed for the area covered by these live cells. A * indicates a significant difference (*$p<0.05$ | **$p<0.01$ | ***$p<0.001$). [Scale bar = 200µM]

MeWo

When MeWo cells were seeded directly onto the surface of pDA coated stainless steel, there was a significant decrease in both the quantity of live cells at the surface (**Figure 4.17B**). The cells did not appear to spread when placed on the stiff, uncoated stainless steel surface (**Figure 4.17A**) and the addition of the High Release pDA coating did not improve the morphology. However, there was an observable increase in the quantity of spread cells on the surface of the Low Release pDA coated coupons (**Figure 4.17A**). This

is also reflected by no significant change in the quantity of area covered by the cells while a significant drop in the number of total live cells was observed.

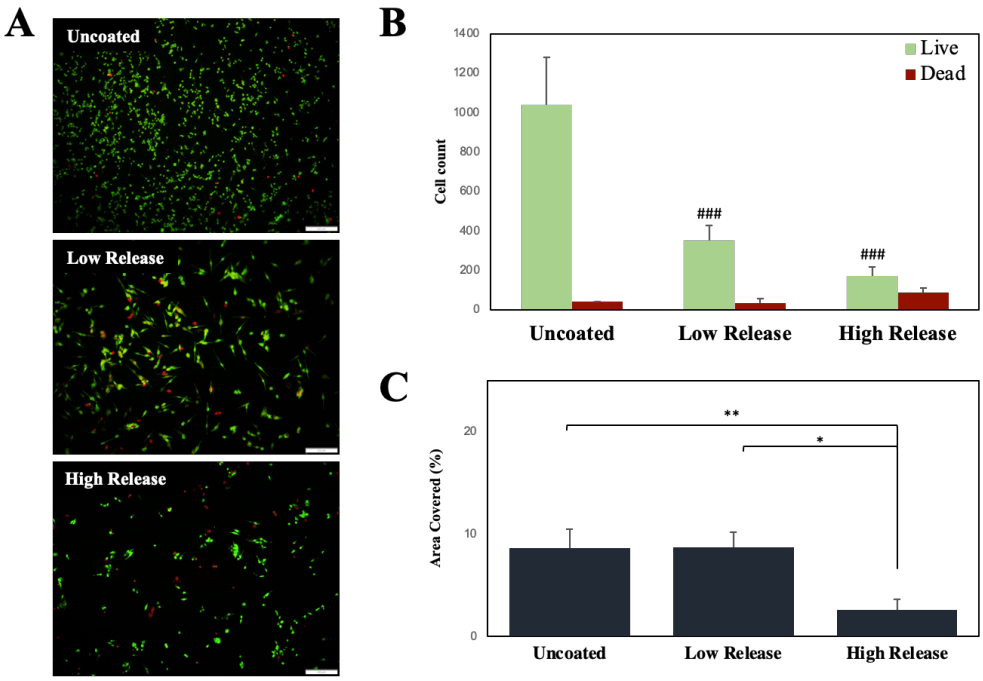

Figure 4.17 | *MeWo adhesion to the surface of standard finished medical grade stainless steel with and without pDA surface coatings.* Malignant melanoma cells were seeded on the surface of medical grade stainless steel with and without pDA surface coatings ($4x10^4$ cells/cm^2) and were cultured for 24 hours before a (A) live/dead stain was performed. (B) After 24 hours seeded on the surface, there was a significant difference in the quantity of adherent live cells between on Low Release and High Release pDA coated surfaces compared to the uncoated surface ($p<0.001$). (C) The area cells covered was not different from the uncoated control on the Low Release surface even though there were less cells overall. There was a significant decline in the area cells covered on the High Release pDA coating compared to both the uncoated and Low Release pDA coated coupons. A * indicates a significant difference (*$p<0.05$ | **$p<0.01$ | ***$p<0.001$). A ### indicates a significant difference from the respective uncoated surface ($p<0.001$). [Scale bar = 200μM]

3T3-L1

When pre-adipocytes were seeded onto the surface of standard stainless steel with pDA coatings there was a significant drop in the number of cells on the surface of High Release pDA coatings (**Figure 4.18B**) with a corresponding drop in the area covered (**Figure 4.18C**). There was not an increase in the number of dead cells, only a decrease in the number of live cells adherent to the surface. There was a lack of a porous structure being formed on the High Release pDA coating while the porous structure was seen on the surface of uncoated and Low Release pDA coated stainless steel (**Figure 4.18A**).

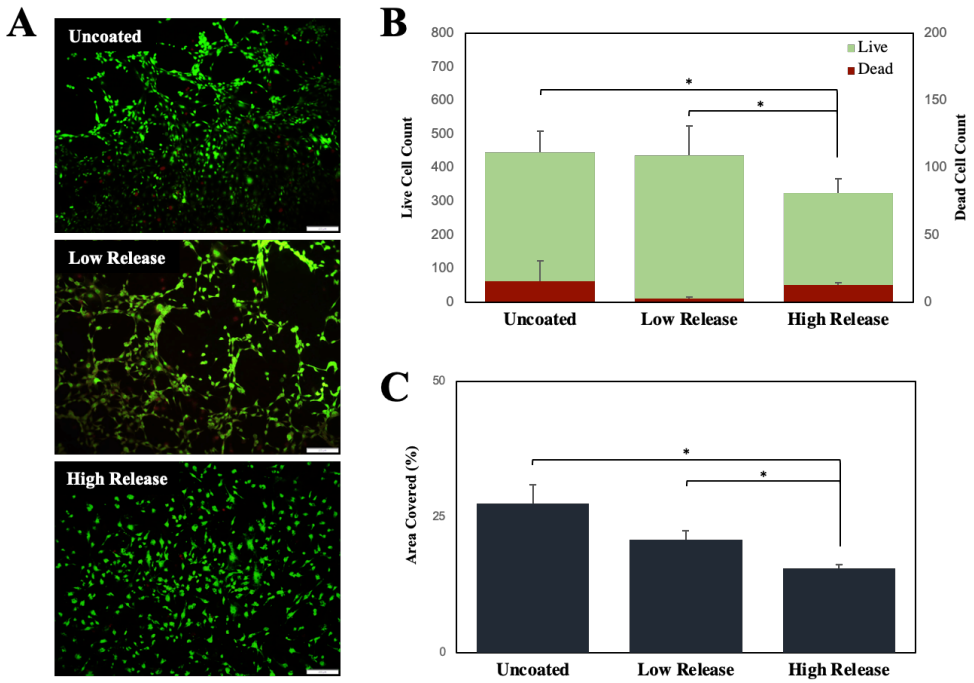

Figure 4.18 | *3T3-L1 Pre-adipocyte adhesion to the surface of medical grade stainless steel with and without pDA surface coatings.* Pre-adipocytes were seeded on the surface of medical grade stainless steel with and without pDA surface coatings ($3x10^3$ cells/cm^2) and were incubated for 24 hours before a (A) live/dead stain being performed. (B) When cell counts were performed, there was a significant decline in the number of live cells on the surface of the stainless steel with the High Release pDA coating. (C) When the area covered was evaluated there was a corresponding decrease in the area covered by live cells on the High Release pDA coatings. There was no significant difference between the uncoated and Low Release pDA coatings. The porous structure formed by the cells on an uncoated surface was seen with the Low Release pDA coating but not the High Release pDA coatings. A * indicates a significant difference (*$p<0.05$ | **$p<0.01$ | ***$p<0.001$). [Scale bar = 200µM]

4.4 Discussion

Hydrogen peroxide is a potent molecule in the wound healing process and has been most commonly used in wound debridement as an antimicrobial agent. The effects of H_2O_2, a ROS, are dose-dependent and can range from a wound healing accelerant at low doses (<1mM) or retardant at high doses (>1mM). The most common dose used in wound debridement is a 3% H_2O_2 solution; the molarity of this solution is approximately 8mM. This has led to poor wound healing outcomes as a result of H_2O_2 usage as an antimicrobial agent. Because the responses, both bacterial and cellular, are dose-dependent there have been many studies looking at what doses promote wound healing mechanisms and what doses induce bactericidal behavior. These doses have almost exclusively been given in a bolus fashion (i.e. all at once). This dosing curve does not

match the dosing that occurs in the natural wound environment (**Figure 4.19**) (Ojha et al., 2008). Due to the short half-life of H_2O_2, maintaining a stable concentration in solution is difficult which makes obtaining the behavior of cells involved in the wound healing cascade in response to physiological doses of H_2O_2 more complex. Through using pDA as a source for the stable generation of H_2O_2 we were able to test the behavior of cells in response to a stable, slowly obtained concentration of H_2O_2 (**Figure 4.2B**) and compare it to their response to bolus doses of H_2O_2.

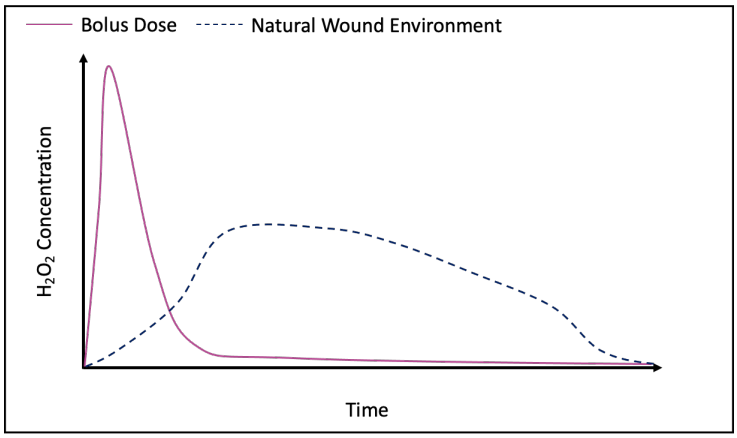

Figure 4.19 | *Concentration of H_2O_2 in solution after a bolus dose and from the natural wound environment.* The concentration of H_2O_2 in solution after a bolus dose (solid pink line) peaks very quickly, however, within a few hours all H_2O_2 is degraded. Whereas, in a natural wound environment, the concentration of H_2O_2 takes up to two days to peak and drops slowly with H_2O_2 still being present after 6 days. (Ojha et al., 2008)

In keratinocytes and malignant melanoma cells, a bolus dose of 200µM was high enough to reduce cell viability while in fibroblasts there was no significant change seen. These cells, when in their natural environment, do not regularly see H_2O_2 in any significant quantity (>50µM). However, when tissue is injured, they do see an increase in H_2O_2 concentration. This concentration increases slowly and when the cells are exposed to this slow increase, we do not see the same decrease in viability. This indicates the method in which a dose of H_2O_2 is administered will affect cell outcomes. This same behavior is seen with other signaling molecules such as nitric oxide. It is known that prolonged exposure to ROS has a detrimental effect on keratinocyte behavior such as migration within the wound site. Other work has shown that in doses less than 700µM the migratory and proliferative capacity of keratinocytes was diminished (O'Toole et al., 1996). This work shares similar results when observing behavior in response to a bolus

dose, however, there was a decrease in viability observed for doses above 100µM. In response to a continuous release, the same effects were not observed. Instead, proliferative capacity increased and viability remained unchanged. Other groups indicate that keratinocytes have increased tolerance to H_2O_2 in solution, with viability not impacted as the concentration of H_2O_2 exceeds 250µM (Loo et al., 2012). A potential difference in results could be attributed to the delay between solution preparation and administration to the cells. In the time between solution preparation and administration, as established in earlier chapters, it is possible the effective concentration of H_2O_2 is significantly reduced. Therefore, a theoretical concentration of 200µM may be effectively reduced to 50µM within 30 min of solution preparation. Evaluation of H_2O_2 stability in cell culture medium supplemented with FBS or calf serum should be evaluated to better understand effective bolus dosing concentrations.

Pre-adipocytes saw an increase in the area covered after exposure to increasing bolus doses of H_2O_2 which is consistent with other work (Lee et al., 2009; Goudarzi et al., 2018a). These cell types require a higher tolerance to H_2O_2 as, during differentiation, they generate their own H_2O_2 to regulate the differentiation process. This same effect was observed when the concentration of H_2O_2 was slowly increased using the pDA coatings. However, there was an additional significant increase in the number of live cells in response to the Low Release pDA coatings. In addition to increasing the quantity and area covered, there was a change in the morphology of the cells in response to the prolonged release of H_2O_2. The pre-adipocytes that were exposed to H_2O_2 from pDA coatings formed a matrix that is reminiscent of adipose tissue (**Figure 4.11A**).

As satellite telemetry tags are made of medical-grade stainless steel, it is important to understand the ability of cells to adhere to the surface. It is possible that increasing the ability for cells to adhere to the stainless steel can increase retention in the blubber as well as reduce negative impacts on the surrounding tissue such as necrosis. The tags have various surface finishes throughout the body of the tag; the tip is polished to a mirrored finish and the back of the body of the tag is patterned with bands to provide a visual for conservationists to indicate how much the tag has been pushed out of the tissue. Pre-adipocytes exhibited a particular sensitivity to the underlying substrate roughness while keratinocytes exhibited a slight increase in the number of live cells adhered to the surface when the roughness was decreased to a mirror polish. As this increase in the number of

live cells did not correspond with an increase in the area covered, it was concluded that cells were exhibiting a more rounded morphology. The environment in which satellite telemetry tags are used is high in fat (blubber) and, while after injury the presence of adipocytes dramatically declines, the ability to promote pre-adipocyte proliferation and adhesion can potentially improve wound healing outcomes and subsequently increase tag retention.

When Low Release pDA coatings were added to the surface of standard finish medical grade stainless steel, there was no significant difference in the adhesion of all cell types. When High Release pDA coatings were added, for most cell types tested, there was a significant decline in the number of adherent cells and the area covered. Fibroblasts did not show a significant change over the uncoated stainless steel (**Figure 4.15B**) and pre-adipocytes lost the porous structure that was present on both the uncoated and Low Release surfaces (**Figure 4.18A**). While there is a loss in cell viability when directly seeded onto the surface of High Release pDA coatings, the viability is not lost when given a little distance (~1mm). As High Release pDA coatings have the ability to reduce bacterial adhesion (see chapter 3), it is unsurprising that they would also reduce cellular adhesion.

4.5 CONCLUSION

Hydrogen peroxide generated by pDA surface coatings has the ability to reduce bacterial adhesion without compromising overall cell viability. The release of H_2O_2 from pDA surface coatings does not significantly reduce viability when cells are exposed indirectly. The High Release pDA coatings significantly inhibited the adhesion on the surface of medical grade stainless steel for all tested cell types while the Low Release pDA coatings inhibited adhesion for fibroblasts and MeWo cell lines. These same doses of H_2O_2 have the ability to prevent bacterial adhesion to the surface of medical-grade stainless steel. This makes the pDA surface coatings a promising approach to improve wound healing outcomes while reducing the chances of biofilm formation.

4.6 REFERENCES

Bae, Y.S., Lee, J.H., Choi, S.H., Kim, S., Almazan, F., Witztum, J.L., et al. (2009). Macrophages generate reactive oxygen species in response to minimally oxidized low-density lipoprotein: toll-like receptor 4- and spleen tyrosine kinase-dependent activation of NADPH oxidase 2. *Circ Res* 104(2)**,** 210-218, 221p following 218. doi: 10.1161/CIRCRESAHA.108.181040.

Balasubramanian, S., and Eckert, R.L. (2007). Keratinocyte proliferation, differentiation, and apoptosis--differential mechanisms of regulation by curcumin, EGCG and apigenin. *Toxicology and applied pharmacology* 224(3)**,** 214-219. doi: 10.1016/j.taap.2007.03.020.

Bruce-Allen, L.J., and Geraci, J.R. (1985). Wound Healing in the Bottlenose Dolphin (Tursiops truncatus). *Canadian Journal of Fisheries and Aquatic Sciences* 42(2)**,** 216-228. doi: 10.1139/f85-029.

Buck, T., Hack, C.T., Berg, D., Berg, U., Kunz, L., and Mayerhofer, A. (2019). The NADPH oxidase 4 is a major source of hydrogen peroxide in human granulosa-lutein and granulosa tumor cells. *Scientific Reports* 9(1)**,** 3585. doi: 10.1038/s41598-019-40329-8.

Camussi, G., Deregibus, M.C., Bruno, S., Cantaluppi, V., and Biancone, L. (2010). Exosomes/microvesicles as a mechanism of cell-to-cell communication. *Kidney international* 78(9)**,** 838-848.

Chen, J.D., Kim, J.P., Zhang, K., Sarret, Y., Wynn, K.C., Kramer, R.H., et al. (1993). Epidermal growth factor (EGF) promotes human keratinocyte locomotion on collagen by increasing the alpha 2 integrin subunit. *Exp Cell Res* 209(2)**,** 216-223. doi: 10.1006/excr.1993.1304.

Cozzi, B., Huggenberger, S., and Oelschläger, H. (2017). General appearance and hydrodynamics (including skin anatomy). *Anatomy of Dolphins. Academic Press, London***,** 21-31.

Forman, H.J., and Torres, M. (2001). Redox signaling in macrophages. *Mol Aspects Med* 22(4-5)**,** 189-216. doi: 10.1016/s0098-2997(01)00010-3.

Geraci, J., and Bruce-Allen, L. (1987). Slow process of wound repair in beluga whales, Delphinapterus leucas. *Canadian Journal of Fisheries and Aquatic Sciences* 44(9)**,** 1661-1665.

Gethin, G. (2007). The significance of surface pH in chronic wounds. *Wounds uk* 3(3)**,** 52.

Giacometti, L. (1967). The skin of the whale (Balaenoptera physalus). *The Anatomical Record* 159(1)**,** 69-75.

Gibbs, S., Silva Pinto, A.N., Murli, S., Huber, M., Hohl, D., and Ponec, M. (2000). Epidermal growth factor and keratinocyte growth factor differentially regulate epidermal migration, growth, and differentiation. *Wound Repair Regen* 8(3)**,** 192-203. doi: 10.1046/j.1524-475x.2000.00192.x.

Goudarzi, F., Mohammadalipour, A., Bahabadi, M., Goodarzi, M.T., Sarveazad, A., and Khodadadi, I. (2018a). Hydrogen peroxide: a potent inducer of differentiation of human adipose-derived stem cells into chondrocytes. *Free Radic Res* 52(7)**,** 763-774. doi: 10.1080/10715762.2018.1466121.

Goudarzi, F., Mohammadalipour, A., Bahabadi, M., Goodarzi, M.T., Sarveazad, A., and Khodadadi, I. (2018b). Hydrogen peroxide: a potent inducer of differentiation of human adipose-derived stem cells into chondrocytes. *Free Radical Research* 52(7)**,** 763-774. doi: 10.1080/10715762.2018.1466121.

Guo, R., Hao, J., Ma, D., Li, H., Liao, K., and Wang, Y. (2020). Persistent proliferation of keratinocytes and prolonged expression of pronociceptive inflammatory mediators might be associated with the postoperative pain in KK mice. *Molecular Pain* 16**,** 1744806920927284. doi: 10.1177/1744806920927284.

Hayyan, M., Hashim, M.A., and AlNashef, I.M. (2016). Superoxide Ion: Generation and Chemical Implications. *Chemical Reviews* 116(5)**,** 3029-3085. doi: 10.1021/acs.chemrev.5b00407.

Hong, W.X., Hu, M.S., Esquivel, M., Liang, G.Y., Rennert, R.C., McArdle, A., et al. (2014). The Role of Hypoxia-Inducible Factor in Wound Healing. *Advances in wound care* 3(5)**,** 390-399. doi: 10.1089/wound.2013.0520.

Jennewein, C., Tran, N., Paulus, P., Ellinghaus, P., Eble, J.A., and Zacharowski, K. (2011). Novel Aspects of Fibrin(ogen) Fragments during Inflammation. *Molecular Medicine* 17(5)**,** 568-573. doi: 10.2119/molmed.2010.00146.

Juven B, and M.D., P. (1996). Antibacterial Effects of Hydrogen Peroxide and Methods For Its Detection and Quantitationt. *Journal of Food Protection* 59**,** 8.

Krock, B.L., Skuli, N., and Simon, M.C. (2011). Hypoxia-induced angiogenesis: good and evil. *Genes & cancer* 2(12)**,** 1117-1133. doi: 10.1177/1947601911423654.

Lee, H., Lee, Y.J., Choi, H., Ko, E.H., and Kim, J.W. (2009). Reactive oxygen species facilitate adipocyte differentiation by accelerating mitotic clonal expansion. *J Biol Chem* 284(16)**,** 10601-10609. doi: 10.1074/jbc.M808742200.

Leveen, H.H., Falk, G., Borek, B., Diaz, C., Lynfield, Y., Wynkoop, B.J., et al. (1973). Chemical acidification of wounds. An adjuvant to healing and the unfavorable action of alkalinity and ammonia. *Ann Surg* 178(6)**,** 745-753. doi: 10.1097/00000658-197312000-00011.

Linley, E., Denyer, S.P., McDonnell, G., Simons, C., and Maillard, J.Y. (2012). Use of hydrogen peroxide as a biocide: new consideration of its mechanisms of biocidal action. *J Antimicrob Chemother* 67(7)**,** 1589-1596. doi: 10.1093/jac/dks129.

Loo, A.E.K., Wong, Y.T., Ho, R., Wasser, M., Du, T., Ng, W.T., et al. (2012). Effects of hydrogen peroxide on wound healing in mice in relation to oxidative damage. *PloS one* 7(11)**,** e49215.

Mannaioni, P.F., Di Bello, M.G., and Masini, E. (1997). Platelets and inflammation: role of platelet-derived growth factor, adhesion molecules and histamine. *Inflamm Res* 46(1)**,** 4-18. doi: 10.1007/pl00000158.

Niethammer, P., Grabher, C., Look, A.T., and Mitchison, T.J. (2009). A tissue-scale gradient of hydrogen peroxide mediates rapid wound detection in zebrafish. *Nature* 459(7249)**,** 996-999.

O'Toole, E.A., Goel, M., and Woodley, D.T. (1996). Hydrogen peroxide inhibits human keratinocyte migration. *Dermatol Surg* 22(6)**,** 525-529. doi: 10.1111/j.1524-4725.1996.tb00368.x.

Ojha, N., Roy, S., He, G., Biswas, S., Velayutham, M., Khanna, S., et al. (2008). Assessment of wound-site redox environment and the significance of Rac2 in cutaneous healing. *Free Radical Biology and Medicine* 44(4)**,** 682-691. doi: https://doi.org/10.1016/j.freeradbiomed.2007.10.056.

Pędziwiatr, P., Mikołajczyk, F., Zawadzki, D., Mikołajczyk, K., and Bedka, A. (2018). Decomposition of hydrogen peroxide - kinetics and review of chosen catalysts. *Acta Innovations* (26)**,** 45-52. doi: 10.32933/ActaInnovations.26.5.

Reeb, D., Best, P.B., and Kidson, S.H. (2007). Structure of the integument of southern right whales, Eubalaena australis. The Anatomical Record: Advances in Integrative Anatomy and Evolutionary Biology: Advances in Integrative Anatomy and Evolutionary Biology 290(6)**,** 596-613.

Robson, S.C., Shephard, E.G., and Kirsch, R.E. (1994). Fibrin degradation product D-dimer induces the synthesis and release of biologically active IL-1 beta, IL-6 and plasminogen activator inhibitors from monocytes in vitro. *Br J Haematol* 86(2)**,** 322-326. doi: 10.1111/j.1365-2141.1994.tb04733.x.

Roy, S., Khanna, S., Nallu, K., Hunt, T.K., and Sen, C.K. (2006). Dermal wound healing is subject to redox control. *Molecular therapy : the journal of the American Society of Gene Therapy* 13(1)**,** 211-220. doi: 10.1016/j.ymthe.2005.07.684.

Ruthenborg, R.J., Ban, J.-J., Wazir, A., Takeda, N., and Kim, J.-W. (2014). Regulation of wound healing and fibrosis by hypoxia and hypoxia-inducible factor-1. *Molecules and cells* 37(9)**,** 637-643. doi: 10.14348/molcells.2014.0150.

Su, C.-Y., Hughes, M.W., Liu, T.-Y., Chuong, C.-M., Wang, H.-V., and Yang, W.-C. (2022). Defining Wound Healing Progression in Cetacean Skin: Characteristics of Full-Thickness Wound Healing in Fraser’s Dolphins (Lagenodelphis hosei). *Animals* 12(5)**,** 537.

Tan, H.-Y., Wang, N., Li, S., Hong, M., Wang, X., and Feng, Y. (2016). The Reactive Oxygen Species in Macrophage Polarization: Reflecting Its Dual Role in Progression and Treatment of Human Diseases. *Oxidative Medicine and Cellular Longevity* 2016**,** 2795090. doi: 10.1155/2016/2795090.

Turley, J.M., Falk, L.A., Ruscetti, F.W., Kasper, J.J., Francomano, T., Fu, T., et al. (1996). Transforming growth factor beta 1 functions in monocytic differentiation of hematopoietic cells through autocrine and paracrine mechanisms. *Cell Growth Differ* 7(11)**,** 1535-1544.

Wahl, S.M., Hunt, D.A., Wakefield, L.M., McCartney-Francis, N., Wahl, L.M., Roberts, A.B., et al. (1987). Transforming growth factor type beta induces monocyte chemotaxis and growth factor production. *Proceedings of the National Academy of Sciences of the United States of America* 84(16)**,** 5788-5792. doi: 10.1073/pnas.84.16.5788.

Wolberg, A.S., and Campbell, R.A. (2008). Thrombin generation, fibrin clot formation and hemostasis. Transfusion and apheresis science : official journal of the World Apheresis Association : official journal of the European Society for Haemapheresis 38(1)**,** 15-23. doi: 10.1016/j.transci.2007.12.005.

Chapter 5

Effect of Chronic ROS Exposure on Complex Wound Healing Mechanisms

The previous chapter explored the behavior of four cell types in response to bolus versus continuous delivery of H_2O_2. The chapter expands on the effects of H_2O_2 released from polydopamine coatings and exogenously delivered in discrete doses on model cell types to affect complex wound healing mechanisms. Cetaceans potentially employ two advanced mechanisms: (1) an increase in endogenous dermcidin and (2) de-differentiation of adipocytes. A malignant melanoma cell line will be used to explore the expression of the AMP dermcidin. The impact sustained release of H_2O_2 has on adipocyte differentiation will be analyzed using 3T3-L1 pre-adipocytes.

The material in this chapter is currently part of a manuscript in preparation for submission in the Fall of 2022.

5.1 Background

The wound healing mechanisms between mammals are highly variable both between species and within a species. The importance of the presence of adipocytes and other cellular mechanisms behind their extraordinary wound healing capabilities has not been fully explored in cetaceans or humans. In addition to the lack of understanding of the role adipocytes play in the cetacean wound healing cascade, the role hypoxia or oxidative stress plays in controlling the generation of angiogenic and adipogenic factors is not well understood either. Oxidant homeostasis, or a balance in redox control, plays an important role in rapid dermal healing in humans (Roy et al., 2006; Ojha et al., 2008; Sen and Roy, 2008). The shift of homeostasis results in oxidative stress or hypoxic stress, which can induce the formation of a chronic wound (Schreml et al., 2010; Hong et al., 2014). Wound healing is a dynamic process that can be described with different but overlapping phases, including inflammation, proliferation, and tissue remodeling. In humans, the inflammation phase is initiated by infiltration of immune cells, including neutrophils and macrophages, at the wound site (Ninan et al., 2015). This results in the production of large amounts of ROS (Bae et al., 2009).

ROS are essential in the differentiation of M2 macrophages, which induce tissue regeneration and anti-inflammatory responses (Rendra et al., 2019). When the levels of ROS are then reduced, cellular migration and proliferation are encouraged. ROS are highly reactive chemical species containing oxygen (O_2) and are divided into two different groups: superoxide ($O_2^{\cdot -}$) and hydroxyl radical ($OH^{\cdot}$) and non-radical species such as hydrogen peroxide (H_2O_2). The presence of H_2O_2 can induce differentiation of keratinocytes which causes the restoration of the epidermal barrier (Roy et al., 2006; Lisse et al., 2016). Topical administration of H_2O_2 has been shown to promote wound healing in an impaired healing animal model (Loo et al., 2012), while complete removal has been shown to significantly delay the wound healing process (Nicholson et al., 1998). It is currently unknown how large a role ROS play in dermal wound healing for cetaceans; however, there are two potential mechanisms in which they may employ complex wound healing pathways: (1) the expression of the antimicrobial peptide (AMP) dermcidin, which has been observed to protect against oxidative stress and (2) the dedifferentiation of adipocytes into myofibroblasts through lipolysis.

Dermcidin is a well-known broad-spectrum antimicrobial peptide commonly found in eccrine sweat glands and is highly effective against gram-negative and gram-positive bacteria species (Stewart et al., 2007; Senyürek et al., 2009; Burian and Schittek, 2015). It has also been an effective antiviral in high concentrations (Ahmed et al., 2019). Chapter 1 detailed the exact mechanism that dermcidin employs against bacteria. However, it is unknown how dermcidin acts to protect against ROS and hypoxia. The entire dermcidin peptide contains 110 amino acids. There are four basic regions of the

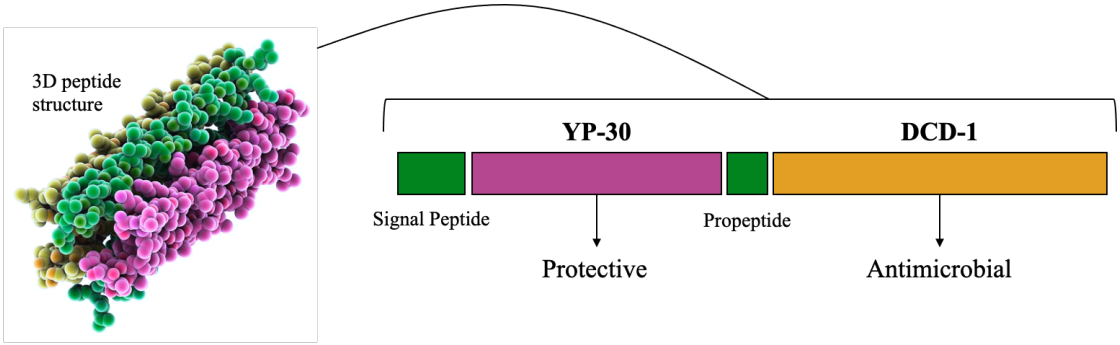

Figure 5.1 | *Dermcidin molecule 3D structure with corresponding peptide sequence.* The molecules 3D structure is composed of four distinct regions: (1) a signal peptide, (2) a YP-30 peptide which is responsible for the protective nature, (3) a propeptide, and (4) the DCD-1 peptide which is responsible for the antimicrobial character. The total length of the molecule is 110 amino acids.

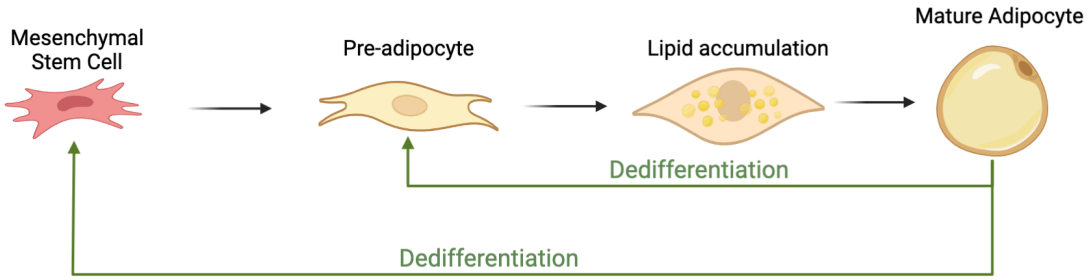

Figure 5.2 | *Differentiation of adipocytes from Mesenchymal stem cells.* The differentiation of adipocytes typically begins with mesenchymal stem cells. The first signs of differentiation occur after a decision has been made by the pre-adipocytes and lipid accumulation is observed. Once fully differentiated, the adipocyte has the ability to dedifferentiate into one of the precursor cell types (either a pre-adipocyte or a mesenchymal stem cell). The dedifferentiation into a mesenchymal stem cells occurs less frequently. (Image created using BioRender)

peptide: (1) signal peptide [19 amino acids], (2) YP-30 peptide [30 amino acids], (3) propeptide [13 amino acids], (4) DCD-1 polypeptide [47 amino acids] (**Figure 5.1**) (Senyürek et al., 2009). The DCD-1 peptide has been the primary region of dermcidin responsible for the antimicrobial effects (Paulmann et al., 2012). There have been multiple cancer cell types that have evolved to express dermcidin (Stewart et al., 2007; Bancovik et al., 2015; Lager et al., 2021). Cells that express this peptide have a greater chance of survival and a higher proliferative character. Even though cetaceans lack sweat glands, the exact origin of their dermcidin expression is still unknown. It could potentially be a key factor in the way cells protect themselves against hypoxia during a dive (Kershaw et al., 2018). To explore the ability of H_2O_2 to increase the expression of endogenous dermcidin, a model cell type will be used in this work. This model cell type - a cell line derived from malignant melanoma cancer (MeWo) - has been previously shown to increase the expression of dermcidin RNA in response to high doses of H_2O_2 (3% solution).

Another potential wound healing mechanism that cetaceans may employ is the dedifferentiation of adipocytes back into their precursor cell types (pre-adipocyte and mesenchymal stem cells) and the subsequent re-differentiation into myofibroblasts (**Figure 5.2**) (Marangoni et al., 2015; Wang et al., 2018). Adipocytes are a plastic cell type that can grow or shrink in response to their surrounding environment and nutrition levels. In addition to fat and nutrient storage, adipocytes are known to play a role in

thermal regulation and have been hypothesized to play a role in the wound healing process in humans and cetaceans (Kvadsheim et al., 1996; Bagge, 2011). Adipocytes can play a role in the inflammatory phase of wound healing by releasing pro-inflammatory cytokines (Cao et al., 2008). Because of this effect, it would potentially be beneficial to reduce the number of adipocytes in the wound environment to prevent the creation of a chronic wound. However, the presence of adipocytes is observed most strongly in the later stages of wound healing when the collagen matrix which would support the growth of adipose tissue is sufficiently regenerated (Su et al., 2022). In the last decade, adipocytes have been observed to dedifferentiate into progenitor cells, which can re-differentiate into various cell types. These cell types include cardiomyocytes (Jumabay et al., 2009) and myofibroblasts (Marangoni et al., 2015). It is thought that through dedifferentiation adipocytes can further assist in the healing of large wounds. As adipocytes use ROS to regulate their differentiation process, it is possible the release of ROS from an outside source could influence the differentiation and subsequent de-differentiation of adipocytes to improve wound healing outcomes. H_2O_2 has been shown to impact the differentiation outcomes of adipose derived stem cells into adipocytes (Tormos et al., 2011; Ho et al., 2013; Goudarzi et al., 2018), however, it is currently unknown whether or not H_2O_2 delivered in a continuous manner can further improve differentiation but also induce dedifferentiation.

As established in chapter 2, pDA surface coatings have the ability to deliver doses of H_2O_2 is a highly controlled manner over a prolonged period of time. As H_2O_2 is an inherently unstable molecule, it has proven difficult to evaluate the effect a stable solution concentration of H_2O_2 would have on wound healing mechanisms as well as how cells will react to protect against prolonged, sustained exposure to a ROS.

5.2 Materials and Methods

Malignant Melanoma (MeWo) (ATCC HTB-65) were cultured using EMEM (ATCC 30-2003) supplemented with 10% FBS (Sigma Aldrich, St. Louis MO). The seeding density used unless otherwise indicated was $4x10^4$ cells/cm^2.

Pre-adipocytes (3T3-L1) (ATCC CL-173) pre-adipocytes were cultured using DMEM supplemented with 15% Fetal Calf Serum (ATCC 30-2030). The seeding density used unless otherwise indicated was $3x10^3$ cells/cm^2.

5.2.1 Dermcidin Expression in Response to Bolus H_2O_2 Dosing

MeWo cells were seeded on the bottom of a 12 well plate and were allowed to attach for 24 hours prior to exposure. After this period, cells were exposed to a dose of H_2O_2 for one or two hours. Cells were then harvested and an ELISA (BioRad) was used to measure quantity of dermcidin. The doses of H_2O_2 used were 50µM, 1mM, and 8mM.

5.2.2 Dermcidin Expression in Response to Prolonged Exposure to H_2O_2 from pDA Surface Coatings

MeWo cells were seeded on the bottom of a 12 well plate and were allowed to attach for 24 hours prior to exposure to H_2O_2. After this period, cells were exposed to Low Release and High Release pDA coated stainless steel (316L) coupons (0.031cm^2) for 24 hours. Cells were then harvested and an ELISA (BioRad) was used to measure quantity of dermcidin. Cell lysate was not stored longer than 24 hours at 4°C prior to use in the ELISA. Expression was normalized relative to the control (no H_2O_2 exposure) to evaluate the effect of both bolus doses and continuous exposure.

5.2.3 Adipocyte Differentiation after Pre-Exposure to H_2O_2

Differentiation Protocol

3T3-L1 pre-adipocytes were seeded directly onto the bottom of a 12 well plate and were allowed to grow until 70% confluence. When the cells were confluent, they were exposed to either a bolus dose of H_2O_2 (50µM, 100µM, or 200µM) or to pDA coated coupons using the Low Release or High Release coating conditions (see Chapter 2 for methods used to create these pDA coatings). The exposure occurred over a 24 hour period before the differentiation process began.

To differentiate the pre-adipocytes, an MDI induction media was made using complete DMEM as a base. IBMX, dexamethasone, and insulin were added to a final concentration of 0.5mM, 1µM, and 10µg/mL respectively. The cells were exposed to the MDI induction medium for 3 days. On day 3, the MDI induction media was removed and cells were incubated in insulin media (10µg/mL in complete DMEM) for an additional 3 days. On day 6, the insulin media was removed and cells were incubated in complete DMEM for an additional 24-48 hours (see **Figure 5.3A** for the visual timeline).

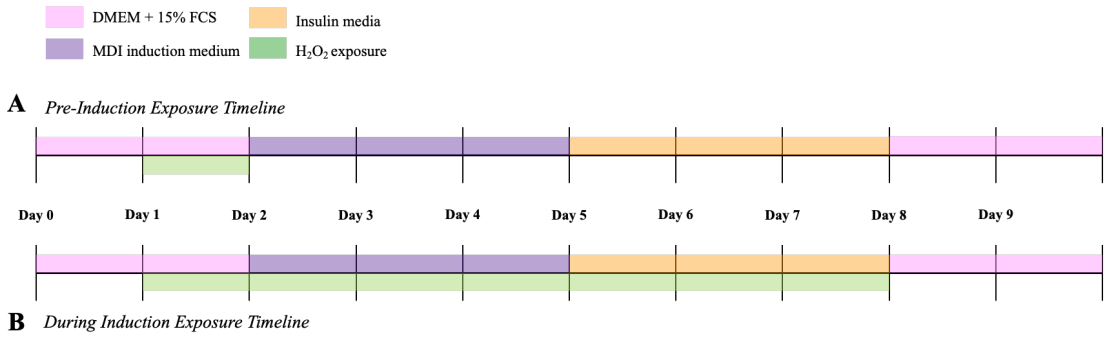

Figure 5.3 | *Timeline for differentiation of 3T3-L1 pre-adipocytes in the presence of H_2O_2 released from pDA surface coatings.* (A) The timeline for differentiation when 3T3-L1 pre-adipocytes were exposed to Low Release and High Release pDA coatings (seen as a green bar) prior to induction of differentiation with MDI medium (seen as a purple bar). After the induction media was allowed to sit for three days, it was replaced with insulin media for days 5-8 before replacement with normal growth media. (B) The timeline for differentiation when 3T3-L1 pre-adipocytes were exposed to Low Release and High Release pDA coatings during the differentiation process. Cells were exposed to pDA coatings similar to those in timeline A, however, the pDA coated coupons were not removed when induction began and remained in place until after the insulin media was removed and replaced with normal growth media. At the end of differentiation an oil red O stain was performed and cells were imaged (Day 10).

Oil Red O Stain

An Oil Red O stain was used to determine which cells were successfully differentiated. Cells were fixed to the bottom of the plate using a 10% formalin solution. After 3 hours of fixing, the cells were washed twice in diH_2O. After washing, cells were incubated in 60% isopropanol for 5 min at room temperature. The isopropanol solution was then discarded, and 0.5mL of Oil Red O working solution was added to each well and allowed to sit for 20min at room temperature. The cells were then washed twice using diH_2O until no excess stain was seen. Hematoxylin (Gill's #2) was used as a counterstain, and cells were imaged using an EVOS microscope.

5.2.4 Adipocyte Differentiation with Prolonged Exposure to H_2O_2 throughout Differentiation Process

Differentiation Protocol

3T3-L1 pre-adipocytes were seeded directly onto the bottom of a 12 well plate and were allowed to grow until 70% confluence. When the cells were confluent, they were exposed to either a bolus dose of H_2O_2 (50µM, 100µM, or 200µM) or to pDA coated coupons

using the Low Release or High Release coating conditions (see Chapter 2 for methods used to create these pDA coatings). The exposure occurred over 24 hours before the differentiation process began.

An MDI induction media was made using complete DMEM as a base to differentiate the pre-adipocytes. IBMX, dexamethasone, and insulin were added to a final concentration of 0.5mM, 1µM, and 10µg/mL, respectively. The cells were exposed to the MDI induction medium for three days. On day 3, the MDI induction media was removed, and cells were incubated in insulin media (10µg/mL in complete DMEM) for an additional three days. On day 6, the insulin media was removed, and cells were incubated in complete DMEM for an extra 24-48 hours (see **Figure 5.3B** for the visual timeline).

Oil Red O Stain

An Oil Red O stain was used to determine which cells were successfully differentiated. Cells were fixed to the bottom of the plate using a 10% formalin solution. After 3 hours of fixing, the cells were washed twice in diH_2O. After washing, cells were incubated in 60% isopropanol for 5 min at room temperature. The isopropanol solution was then discarded, and 0.5mL of Oil Red O working solution was added to each well and allowed to sit for 20min at room temperature. The cells were then washed twice using diH_2O until no excess stain was seen. Hematoxylin (Gill's #2) was used as a counterstain, and cells were imaged using an EVOS microscope.

5.3 RESULTS

5.3.1 DERMCIDIN EXPRESSION IN RESPONSE TO BOLUS H_2O_2 DOSING

When MeWo cells were exposed to an exogenous dose of H_2O_2 (either 50µM, 1mM, or 8mM) for one hour, there was a significant increase in the expression of dermcidin (320% increase when compared to controls) (**Figure 5.4**). There was significantly more expression found with a lower dose of H_2O_2 (320% increase when exposed to 50µM compared to a 220% increase when exposed to 1mM). After two hours, there was no significant difference between the doses. However, there was significantly more dermcidin expression than there was in the first hour (**Figure 5.4**).

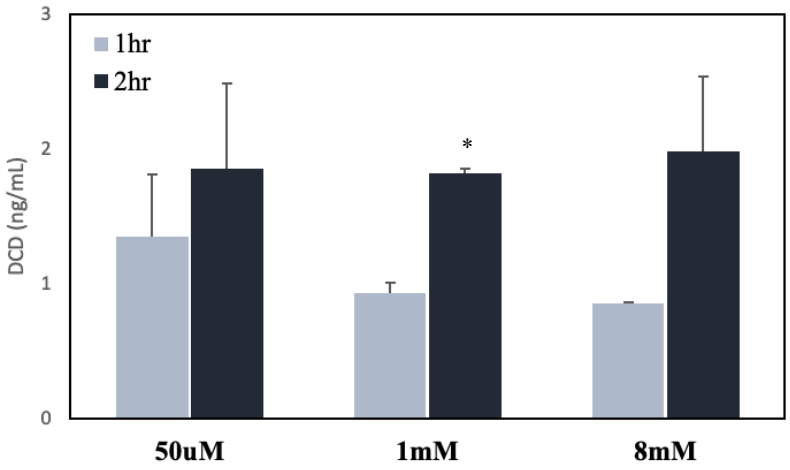

Figure 5.4 | *Dermcidin expression after exposure to bolus doses of H_2O_2.* MeWo cells were exposed to a dose of H_2O_2 for either one hour or two hours and then the expression of dermcidin within the cell was evaluated. There was only a significant increase in dermcidin expression at the 1mM concentration ($p<0.05$), however there was an increase in expression seen with all doses after two hours. A * indicates a significant difference from the respective 1 hour time point ($p<0.05$).

5.3.2 Dermcidin Expression in Response to Prolonged Exposure to H_2O_2 from pDA Surface Coatings

When exposed to a continuous dose of H_2O_2 over 24 hours, the expression of dermcidin was not increased as much as it was with a bolus dose (20% increase when exposed to Low Release pDA coatings vs. 320% increase when exposed to a 50µM bolus dose) (**Figure 5.5**). Between the pDA coatings, there was an increase in expression when the concentration of H_2O_2 increased; however even with the High Release coatings, there was only a 70% increase in expression (**Figure 5.5**).

5.3.3 Adipocyte Differentiation after Pre-Exposure to H_2O_2

When pre-adipocytes were exposed to a dose of 50µM or 100µM, there was no significant impact on the differentiation behavior. However, when exposed to a dose of 200µM, there was a significant reduction in the percentage of pre-adipocytes that underwent differentiation (**Figure 5.6C**). When exposed to a stable concentration of H_2O_2 from pDA coated coupons (Low Release and High Release), there was no change in the number of pre-adipocytes that underwent differentiation (**Figure 5.6D**). The morphology of the differentiated cells was also observably different between the control group and those exposed to higher quantities of H_2O_2. The cells that differentiated after exposure to

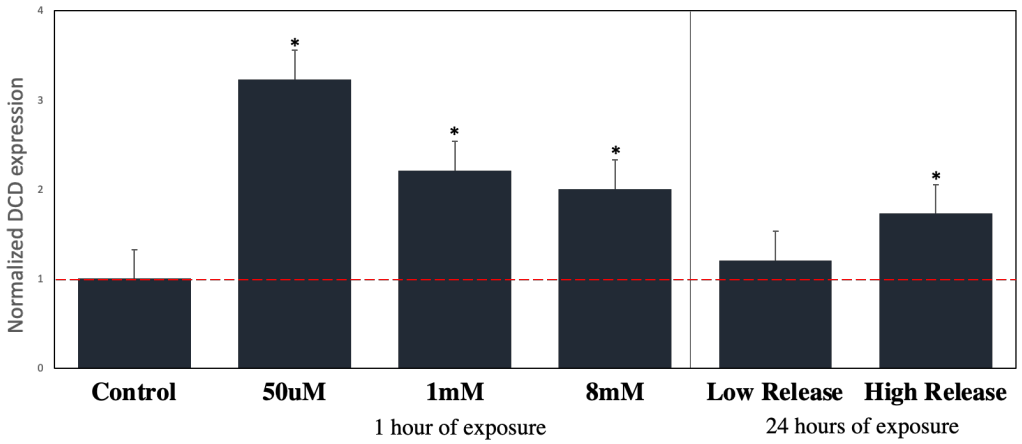

Figure 5.5 | *Dermcidin expression from MeWo cells after exposure to H_2O_2 either from a bolus dose or from pDA surface coatings*. Cells were either exposed to a bolus dose of H_2O_2 for one hour or continuous release from pDA coated coupons for 24 hours. The values are normalized to the expression from controls (i.e., no exposure to H_2O_2). There was significantly more release from cells after a bolus dose compared to the control (no exposure) cells ($p<0.05$). However, there was only a slight increase in expression from cells exposed to pDA coated coupons when compared to the controls. This increase was not significantly different from the controls when exposed to the Low Release pDA coatings, however it was significant when exposed to the High Release pDA coatings. A * indicates a significant difference compared to the control ($p<0.05$).

High Release pDA coatings exhibited a more spread morphology (**Figure 5.6B**) compared to those differentiated without H_2O_2.

5.3.4 Adipocyte Differentiation with Prolonged Exposure to H_2O_2 throughout Differentiation Process

Pre-adipocytes differentiated in the presence of a low, stable concentration of H_2O_2 exhibited no significant change in the proportion of cells that differentiated (**Figure 5.7**). When the solution concentration was increased, there was a corresponding increase in the proportion of differentiated cells (**Figure 5.7C**). The difference in differentiation behavior was only observed when the concentration of H_2O_2 in solution was altered during differentiation. There was no difference in differentiation behavior when cells were exposed to a stable concentration in solution before differentiation.

The morphology of adipocytes was also noticeably different when differentiated in the presence of H_2O_2. More cells exhibited a fibroblast-like morphology in response to High Release pDA surface coatings both pre-induction and during differentiation, but the same spreading effect was seen with Low Release pDA coatings when exposed during differentiation (**Figure 5.7B**). There is still lipid accumulation in the more fibroblast-like

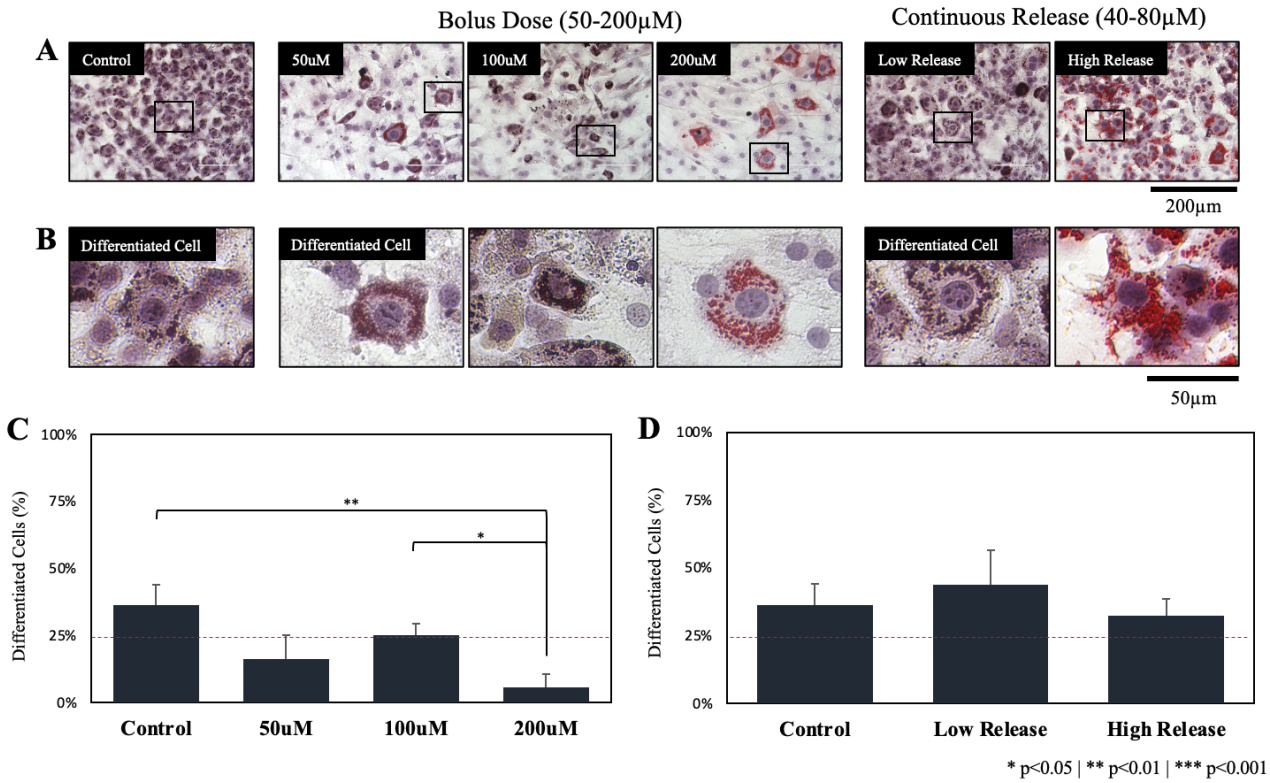

Figure 5.6 | *Differentiation behavior of 3T3-1L adipocytes when previously exposed to H_2O_2.* Undifferentiated pre-adipocytes were exposed to either an exogenous dose of H_2O_2 or pDA coated medical-grade stainless steel coupons for 24 hours. After exposure, cells were differentiated over a 10-day period and the quantity of differentiated adipocytes was evaluated using an oil-red O stain. It was found that the addition of an exogenous dose of 200µM significantly inhibited the differentiation of pre-adipocytes into adipocytes when compare to the control ($p<0.01$). There was no impact on the quantity of cells differentiated when exposed to either a 50 or 100µM bolus dose or either pDA coating. A * indicates a significant difference (*$p<0.05$ | **$p<0.01$ | ***$p<0.001$). The red dashed line crosses at 25% differentiation and is there to be used as a benchmark for comparison between panel C and D. Cell nuclei are stained dark purple and lipid droplets contain the Oil red O stain. A differentiated cell will contain multiple lipid droplets.

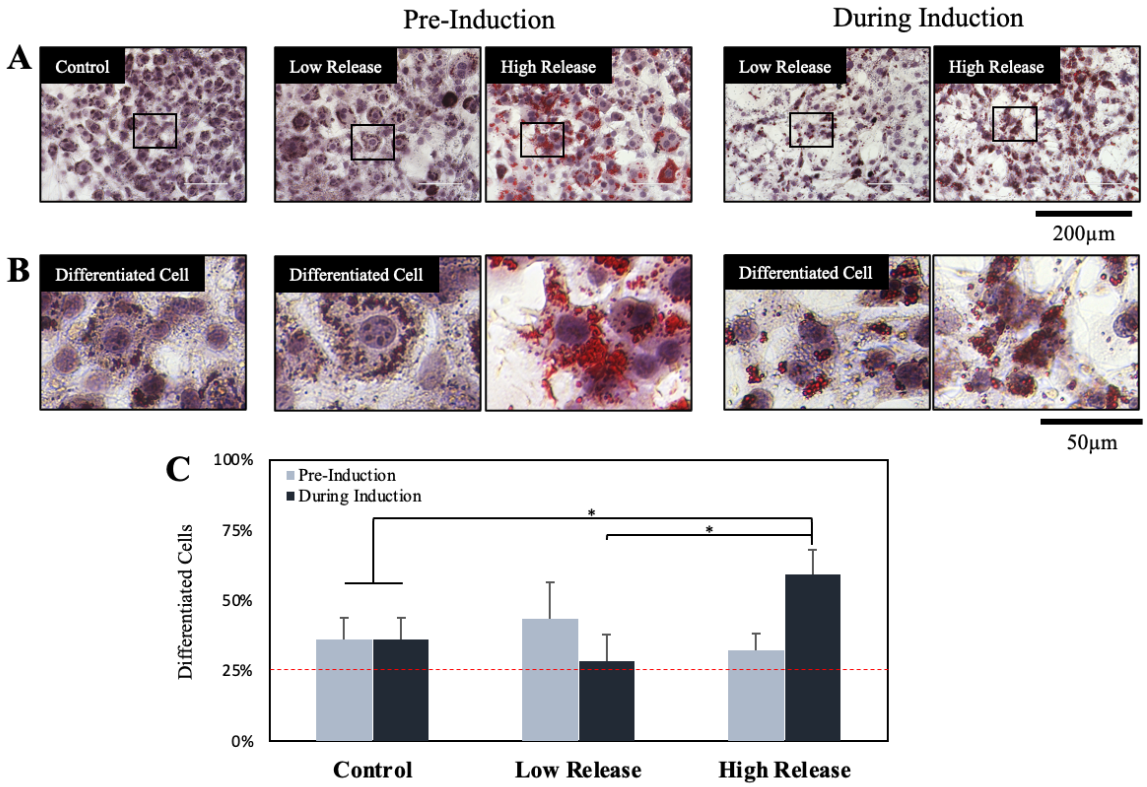

Figure 5.7 | *Differentiation behavior of 3T3-1L adipocytes when exposed to pDA coatings during the differentiation process.* Undifferentiated pre-adipocytes were exposed Low Release and High Release pDA coated medical-grade stainless steel coupons during the differentiation process. The quantity of differentiated adipocytes was evaluated using an oil-red O stain. The addition of the Low Release pDA coatings did not significantly impact the differentiation behavior of pre-adipocytes. However, the addition of the High Release pDA coated coupons significantly increased the percent of pre-adipocytes that differentiated into adipocytes compared to both the control and Low Release samples. A * indicates a significant difference (*$p<0.05$ | **$p<0.01$ | ***$p<0.001$). The red dashed line crosses at 25% differentiation and is there to be used as a benchmark for comparison between Pre-Induction values and During Induction values in panel C. Cell nuclei are stained dark purple and lipid droplets contain the Oil red O stain. A differentiated cell will contain multiple lipid droplets.

cells indicating differentiation is either starting to occur or has already occurred.

5.4 DISCUSSION

The wound healing capability of cetaceans has been an area of interest for decades; however due to the difficulty surrounding the logistics and ethics of study with these large endangered mammals, it is still not well understood. There have only been three major studies of the histology during the wound healing process, but there have been many studies evaluating the composition of blubber. Blubber has been well known to store evidence of pollution and indicate the overall health of the individual. The antimicrobial peptide dermcidin has been found in the blubber during a compositional analysis of the fat from humpback whales. This peptide has been well known to reduce the chances of infection in humans, but the source for dermcidin in humans is eccrine sweat glands. As whales lack sweat glands, it is unknown what cell produces the peptide. The primary role of the peptide is to act as an antimicrobial, however, the peptide has been found to play a role as a protective agent against oxidative stress. This mechanism is primarily through the presence of the YP-30 domain (**Figure 5.1**) which is still active when attached to the DCD-1 domain. Part of this study explored the ability of MeWo cells, which have been shown to produce dermcidin, to increase their expression of dermcidin in response to oxidative stress induced by the ROS H_2O_2. This was done using two delivery methods: (1) an exogenously delivered bolus dose or (2) a continuous dose released from pDA surface coatings on medical-grade stainless steel.

MeWo cells were previously established to be highly sensitive to bolus doses of H_2O_2 (see chapter 4). The expression of dermcidin in other work was evaluated using RT-PCR techniques to evaluate the increase in RNA expression after oxidative stress (Rieg et al., 2004). However, the increase in RNA expression as a result of oxidative stress may not directly correlate to quantity of dermcidin peptides expressed within the cell (de Sousa Abreu et al., 2009). As we were attempting to evaluate the increase in expression of dermcidin peptides in response to oxidative stress, we used an ELISA to evaluate the quantity of dermcidin peptides expressed within the cell. We first evaluated the expression soon after a bolus dose was delivered; When a bolus dose of H_2O_2 was delivered to MeWo cells the expression of dermcidin increased three-fold in the first hour after exposure when compared to the controls (**Figure 5.4**). This increase in expression continued into the two-hour mark, however, there was no difference between the doses.

There was a significant loss of viability with bolus doses higher than 50µM (see chapter 4) so time points greater than 2 hours at these high concentrations would most likely show no additional increase as the cells would be dead. After establishing that insulting MeWo cells with H_2O_2 can induce an increase in dermcidin expression, cells were then exposed to a continuous concentration. This was done by exposing cells to Low Release and High Release pDA surface coatings. These coatings did not previously induce high levels of cell death (see chapter 4) and to get a cumulative exposure level similar to that of the bolus doses the MeWo cells would need to be exposed for approximately 24 hours. We found that after 24 hours of exposure to Low Release and High Release pDA coatings there was a slight increase in the endogenous expression of dermcidin (**Figure 5.5**). There was a greater quantity of dermcidin expressed in response to the High Release coating compared to the Low Release coating, however, the difference in cell death at these concentrations was not significantly different (see chapter 4). This likely means the dermcidin which was expressed in response to a slowly increasing concentration was more able to protect the cells from the subsequent oxidative stress which was induced by a stable concentration of H_2O_2. As it is still unknown what exact mechanism these cells use to create dermcidin endogenously it is possible that creating this molecule takes substantial energy from the cell and, when forced to produce it quickly, can prove to be too great a cost resulting in subsequent cell death (Reimertz et al., 2003; Iurlaro and Muñoz-Pinedo, 2016). As wounds in terrestrial mammals slowly generate their own low concentrations of ROS to improve the recruitment of immune cells as well as act as a barrier to prevent bacterial adhesion, it is also possible cetaceans utilize similar mechanisms to prevent infection and promote wound healing. The ROS potentially generated in the blubber of cetaceans can act to stimulate the production of dermcidin in response to a wound or a long dive resulting in hypoxic tissue environments. The dermcidin produced in cetaceans most likely has a primary function to prevent infection at the wound site but may also act to keep the process limits to the margins of the wound, effectively acting to protect surrounding cells against excess oxidative stress. This excess oxidative stress can also trigger additional phenotypic and morphologic changes in various cell types which can inhibit wound repair.

As blubber is primarily made of fatty tissue, a major component of wound repair for cetaceans is adipogenesis which occurs in later stages of wound healing (Su et al., 2022).

During adipogenesis, pre-adipocytes will differentiate into adipocytes which will subsequently fill with oils. If this process goes unchecked, adipocytes can overfill and the resulting pressure induced on neighboring adipocytes can cause necrosis to take place. To prevent an overabundance of adipocytes from forming, during differentiation adipocytes generate endogenous concentrations of ROS which can act as negative feedback to stop the differentiation process. This indicates using ROS can help to either increase the proportion of pre-adipocytes that differentiate into adipocytes or to decrease the time it takes to do so. There is also evidence that insulting differentiating adipocytes with an exogenous dose of H_2O_2 for up to two hours increases DNA damage and reduces the overall viability of human adipose-derived mesenchymal stem cells (Valverde et al., 2018) so the dose administered needs to be tailored to the application. Our results indicate that the viability of pre-adipocytes is not reduced when insulted with an exogenous bolus dose of H_2O_2 prior to differentiation (see chapter 4) rather, there is a marked increase in the proliferation of pre-adipocytes in the presence of H_2O_2. This indicates the resulting behavior of pre-adipocytes to H_2O_2 is dependent on the time and duration in which H_2O_2 is applied during the differentiation process.

To understand this behavior we applied an insult of H_2O_2 both during the entirety of the differentiation process as well as prior to the beginning of differentiation. We found when applying insults of H_2O_2 in a bolus fashion there was a significant decrease in the number of pre-adipocytes that underwent differentiation (**Figure 5.6**). This behavior was only significant with a 200µM bolus dose and was not observed when H_2O_2 was introduced in a gradual manner, mimicking a H_2O_2 gradient similar to a wound site. As the concentration present in the wound environment has been observed to be approximately 300µM, it is possible that a bolus dose of 200µM may have simulated a fresh wound environment where differentiation would not be appropriate.

When H_2O_2 was held at a stable concentration throughout the differentiation process there was a threshold that not only increased the proportion of cells that underwent differentiation (evidenced by the accumulation of lipid droplets) but also a significant alteration in the morphology of differentiated cells (**Figure 5.7B**). This altered morphology resembled the initial fibroblast-like morphology typical of pre-adipocytes however the presence of lipid droplets was still observed. When adipocytes dedifferentiate they revert back to their original fibroblast morphology while, in the early

stages of dedifferentiating, retaining lipid droplets generated during the initial differentiation process. It is possible the stable concentration of H_2O_2 generated by our High Release pDA coatings encouraged the dedifferentiation of adipocytes, however, further studies are needed to both confirm the dedifferentiation as well as explore potential re-differentiation into cell types which may improve wound healing outcomes.

5.5 CONCLUSION

The wound healing process in cetaceans is complex and occurs rapidly. It is possible the presence of the antimicrobial peptide dermcidin as well as the large quantity of adipose tissue contribute to this outcome. Oxidative stress and the presence of ROS are two components that cetaceans utilize during the wound healing process. It has previously been difficult to recreate the wound environment to explore the effect oxidative stress and ROS have on more complex wound healing mechanisms as the half-life of most ROS is less than 2 hours in solution. Our pDA surface coatings have the ability to generate the ROS H_2O_2 and maintain physiologic concentrations for a prolonged period of time (>24 hours) which makes it possible to observe concentration-dependent cellular behavior. This ability has allowed us to observe the potential mechanism used to increase the expression of the antimicrobial peptide dermcidin without compromising tissue viability. At physiologic concentrations generated by pDA surface coatings, an increase in the expression of dermcidin was seen without an increase in cell death. These same concentrations also contributed to an increase in the number of differentiated pre-adipocytes and potentially led to the dedifferentiation of adipocytes, however, dedifferentiation in response to ROS still needs to be explored further.

5.6 REFERENCES

Ahmed, A., Siman-Tov, G., Hall, G., Bhalla, N., and Narayanan, A. (2019). Human Antimicrobial Peptides as Therapeutics for Viral Infections. *Viruses* 11(8)**,** 704. doi: 10.3390/v11080704.

Bae, Y.S., Lee, J.H., Choi, S.H., Kim, S., Almazan, F., Witztum, J.L., et al. (2009). Macrophages generate reactive oxygen species in response to minimally oxidized low-density lipoprotein: toll-like receptor 4- and spleen tyrosine kinase-dependent activation of NADPH oxidase 2. *Circ Res* 104(2)**,** 210-218, 221p following 218. doi: 10.1161/CIRCRESAHA.108.181040.

Bagge, L. (2011). Thermal and Phase-Change Properties of the Blubber of Shortfinned Pilot whales (Globicephala macrorhynchus) and Pigmy Sperm Whales (Kogia breviceps). Master of Science, Univeristy of North Carolina Wilmington.

Bancovik, J., Moreira, D.F., Carrasco, D., Yao, J., Porter, D., Moura, R., et al. (2015). Dermcidin exerts its oncogenic effects in breast cancer via modulation of ERBB signaling. *BMC cancer* 15**,** 70-70. doi: 10.1186/s12885-015-1022-6.

Burian, M., and Schittek, B. (2015). The secrets of dermcidin action. *Int J Med Microbiol* 305(2)**,** 283-286. doi: 10.1016/j.ijmm.2014.12.012.

Cao, H., Gerhold, K., Mayers, J.R., Wiest, M.M., Watkins, S.M., and Hotamisligil, G.S. (2008). Identification of a lipokine, a lipid hormone linking adipose tissue to systemic metabolism. *Cell* 134(6)**,** 933-944. doi: 10.1016/j.cell.2008.07.048.

de Sousa Abreu, R., Penalva, L.O., Marcotte, E.M., and Vogel, C. (2009). Global signatures of protein and mRNA expression levels. *Molecular BioSystems* 5(12)**,** 1512-1526. doi: 10.1039/B908315D.

Goudarzi, F., Mohammadalipour, A., Bahabadi, M., Goodarzi, M.T., Sarveazad, A., and Khodadadi, I. (2018). Hydrogen peroxide: a potent inducer of differentiation of human adipose-derived stem cells into chondrocytes. *Free Radic Res* 52(7)**,** 763-774. doi: 10.1080/10715762.2018.1466121.

Ho, P.-J., Yen, M.-L., Tang, B.-C., Chen, C.-T., and Yen, B.L. (2013). H2O2 accumulation mediates differentiation capacity alteration, but not proliferative decline, in

senescent human fetal mesenchymal stem cells. *Antioxidants & redox signaling* 18(15)**,** 1895-1905. doi: 10.1089/ars.2012.4692.

Hong, W.X., Hu, M.S., Esquivel, M., Liang, G.Y., Rennert, R.C., McArdle, A., et al. (2014). The Role of Hypoxia-Inducible Factor in Wound Healing. *Advances in wound care* 3(5)**,** 390-399. doi: 10.1089/wound.2013.0520.

Iurlaro, R., and Muñoz-Pinedo, C. (2016). Cell death induced by endoplasmic reticulum stress. *The FEBS Journal* 283(14)**,** 2640-2652. doi: https://doi.org/10.1111/febs.13598.

Jumabay, M., Matsumoto, T., Yokoyama, S., Kano, K., Kusumi, Y., Masuko, T., et al. (2009). Dedifferentiated fat cells convert to cardiomyocyte phenotype and repair infarcted cardiac tissue in rats. *J Mol Cell Cardiol* 47(5)**,** 565-575. doi: 10.1016/j.yjmcc.2009.08.004.

Kershaw, J.L., Botting, C.H., Brownlow, A., and Hall, A.J. (2018). Not just fat: investigating the proteome of cetacean blubber tissue. *Conserv Physiol* 6(1)**,** coy003. doi: 10.1093/conphys/coy003.

Kvadsheim, P.H., Folkow, L.P., and Blix, A.S. (1996). Thermal conductivity of minke whale blubber. *Journal of Thermal Biology* 21(2)**,** 123-128. doi: 10.1016/0306-4565(95)00034-8.

Lager, T.W., Conner, C., Keating, C.R., Warshaw, J.N., and Panopoulos, A.D. (2021). Cell surface GRP78 and Dermcidin cooperate to regulate breast cancer cell migration through Wnt signaling. *Oncogene* 40(23)**,** 4050-4059. doi: 10.1038/s41388-021-01821-6.

Lisse, T.S., King, B.L., and Rieger, S. (2016). Comparative transcriptomic profiling of hydrogen peroxide signaling networks in zebrafish and human keratinocytes: Implications toward conservation, migration and wound healing. *Scientific Reports* 6(1)**,** 20328. doi: 10.1038/srep20328.

Loo, A.E.K., Wong, Y.T., Ho, R., Wasser, M., Du, T., Ng, W.T., et al. (2012). Effects of hydrogen peroxide on wound healing in mice in relation to oxidative damage. *PloS one* 7(11)**,** e49215.

Marangoni, R.G., Korman, B.D., Wei, J., Wood, T.A., Graham, L.V., Whitfield, M.L., et al. (2015). Myofibroblasts in murine cutaneous fibrosis originate from adiponectin-

positive intradermal progenitors. *Arthritis Rheumatol* 67(4)**,** 1062-1073. doi: 10.1002/art.38990.

Nicholson, N.C., Ramp, W.K., Kneisl, J.S., and Kaysinger, K.K. (1998). Hydrogen peroxide inhibits giant cell tumor and osteoblast metabolism in vitro. *Clinical orthopaedics and related research* (347)**,** 250-260.

Ninan, N., Thomas, S., and Grohens, Y. (2015). Wound healing in urology. *Adv Drug Deliv Rev* 82-83**,** 93-105. doi: 10.1016/j.addr.2014.12.002.

Ojha, N., Roy, S., He, G., Biswas, S., Velayutham, M., Khanna, S., et al. (2008). Assessment of wound-site redox environment and the significance of Rac2 in cutaneous healing. *Free Radical Biology and Medicine* 44(4)**,** 682-691. doi: https://doi.org/10.1016/j.freeradbiomed.2007.10.056.

Paulmann, M., Arnold, T., Linke, D., Özdirekcan, S., Kopp, A., Gutsmann, T., et al. (2012). Structure-activity analysis of the dermcidin-derived peptide DCD-1L, an anionic antimicrobial peptide present in human sweat. *The Journal of biological chemistry* 287(11)**,** 8434-8443. doi: 10.1074/jbc.M111.332270.

Reimertz , C., Kögel , D., Rami , A., Chittenden , T., and Prehn , J.H.M. (2003). Gene expression during ER stress–induced apoptosis in neurons : induction of the BH3-only protein Bbc3/PUMA and activation of the mitochondrial apoptosis pathway. *Journal of Cell Biology* 162(4)**,** 587-597. doi: 10.1083/jcb.200305149.

Rendra, E., Riabov, V., Mossel, D.M., Sevastyanova, T., Harmsen, M.C., and Kzhyshkowska, J. (2019). Reactive oxygen species (ROS) in macrophage activation and function in diabetes. *Immunobiology* 224(2)**,** 242-253. doi: 10.1016/j.imbio.2018.11.010.

Rieg, S., Garbe, C., Sauer, B., Kalbacher, H., and Schittek, B. (2004). Dermcidin is constitutively produced by eccrine sweat glands and is not induced in epidermal cells under inflammatory skin conditions. *Br J Dermatol* 151(3)**,** 534-539. doi: 10.1111/j.1365-2133.2004.06081.x.

Roy, S., Khanna, S., Nallu, K., Hunt, T.K., and Sen, C.K. (2006). Dermal wound healing is subject to redox control. *Molecular therapy : the journal of the American Society of Gene Therapy* 13(1)**,** 211-220. doi: 10.1016/j.ymthe.2005.07.684.

Schreml, S., Szeimies, R., Prantl, L., Karrer, S., Landthaler, M., and Babilas, P. (2010). Oxygen in acute and chronic wound healing. *British Journal of Dermatology* 163(2)**,** 257-268.

Sen, C.K., and Roy, S. (2008). Redox signals in wound healing. *Biochimica et Biophysica Acta (BBA) - General Subjects* 1780(11)**,** 1348-1361. doi: https://doi.org/10.1016/j.bbagen.2008.01.006.

Senyürek, I., Paulmann, M., Sinnberg, T., Kalbacher, H., Deeg, M., Gutsmann, T., et al. (2009). Dermcidin-derived peptides show a different mode of action than the cathelicidin LL-37 against Staphylococcus aureus. *Antimicrob Agents Chemother* 53(6)**,** 2499-2509. doi: 10.1128/aac.01679-08.

Stewart, G.D., Lowrie, A.G., Riddick, A.C., Fearon, K.C., Habib, F.K., and Ross, J.A. (2007). Dermcidin expression confers a survival advantage in prostate cancer cells subjected to oxidative stress or hypoxia. *Prostate* 67(12)**,** 1308-1317. doi: 10.1002/pros.20618.

Su, C.-Y., Hughes, M.W., Liu, T.-Y., Chuong, C.-M., Wang, H.-V., and Yang, W.-C. (2022). Defining Wound Healing Progression in Cetacean Skin: Characteristics of Full-Thickness Wound Healing in Fraser’s Dolphins (Lagenodelphis hosei). *Animals* 12(5)**,** 537.

Tormos, K.V., Anso, E., Hamanaka, R.B., Eisenbart, J., Joseph, J., Kalyanaraman, B., et al. (2011). Mitochondrial complex III ROS regulate adipocyte differentiation. *Cell metabolism* 14(4)**,** 537-544.

Valverde, M., Lozano-Salgado, J., Fortini, P., Rodriguez-Sastre, M.A., Rojas, E., and Dogliotti, E. (2018). Hydrogen Peroxide-Induced DNA Damage and Repair through the Differentiation of Human Adipose-Derived Mesenchymal Stem Cells. *Stem Cells International* 2018**,** 1615497. doi: 10.1155/2018/1615497.

Wang, Q.A., Song, A., Chen, W., Schwalie, P.C., Zhang, F., Vishvanath, L., et al. (2018). Reversible De-differentiation of Mature White Adipocytes into Preadipocyte-like Precursors during Lactation. *Cell Metab* 28(2)**,** 282-288.e283. doi: 10.1016/j.cmet.2018.05.022.

Chapter 6

Conclusions and Future Directions

6.1 Summary and Key Findings

Satellite telemetry tags are an essential tool used to track the wellbeing of large marine mammals. These tags penetrate through the dermis, home to a diverse microbiome, and implant into the underlying blubber tissue (Robbins et al., 2013; Kershaw et al., 2018). The tags are meant to remain implanted for upwards of a year. However, due to the transdermal nature of the implant, this gives the bacteria living in the skin microbiome ample opportunity to adhere to the stainless steel and migrate into the tissue. Antibiotic surface coatings have been used to prevent the adhesion and proliferation of bacteria within the wound (IWC, 2020). Still, the growing concern for resistance to the antibiotics forming has led to a push in non-antibiotic-based approaches at mitigating the chances of infection (Dowding, 1977; Livermore, 2000; Shaikh et al., 2015).

Hydrogen peroxide has been shown to be effective as a biocide and plays a crucial role in wound healing (Juven B and M.D., 1996; Goudarzi et al., 2018). In a typical wound environment, there will be a concentration gradient of H_2O_2 generated to prevent bacterial adhesion to the tissue and promote local wound healing mechanisms like the migration of keratinocytes and an increase in the expression of angiogenic factors (Niethammer et al., 2009). However, creating a method for controlled delivery of H_2O_2 has proven to be difficult due to the short half-life of the ROS. A molecule that has been found to generate H_2O_2 during polymerization is pDA (Tyo et al., 2019). Polydopamine can form a surface coating on both organic and inorganic substrates through the formation of covalent bonds (Ryu et al., 2018). These bonds can prevent delamination from sheer forces which makes pDA based surface coatings a good candidate to use on satellite telemetry tags. This work presents an antimicrobial pDA surface coating as a potential solution to prevent bacterial adhesion and subsequent infection on medical grade stainless steel satellite telemetry tags. The pDA coatings were able to generate continuous release of H_2O_2 in a physiologically relevant range that is tailorable based on the coating conditions. These coatings were also able to prevent bacterial adhesion of relevant bacterial strains to the surface of medical grade stainless steel regardless of surface finish. When evaluated for their cytotoxic character, it was found that the coatings

that released the highest quantity of H_2O_2 reduced the number of surface adherent live cells. However, when indirectly exposed to the H_2O_2 generated from the High Release pDA coatings, the effects were not as toxic. These coatings were also able to increase the quantity of the AMP dermcidin, which can further protect the cetacean against infection and protect the local cells against oxidative stress. Furthermore, the differentiation of pre-adipocytes into adipocytes indicates a later stage of healing in cetacean dermal wounds. The ability to increase the presence of adipocytes can improve wound healing through the subsequent generation of structurally important collagen. The pDA surface coatings increased the number of pre-adipocytes and the proportion of pre-adipocytes that differentiated into adipocytes. Adipocytes have been known to de-differentiate to their precursor cell types in response to the change in pH of the wound environment. This de-differentiation can lead to re-differentiate into more relevant cell types based on the type of wound (e.g., cardiomyocyte for tissue repair after myocardial infarction). A sign of de-differentiation in adipocytes is their morphology: the more spread the cell, the higher the likelihood of de-differentiation (Jumabay et al., 2009). This change in morphology was also observed when pre-adipocytes were differentiated in the presence of pDA surface coatings and continuous H_2O_2 release. Key findings from each chapter included in this work were:

6.1.1 Chapter 2

Coating conditions were critical in controlling the release from pDA surface coatings on medical-grade (316L) stainless steel.

- The pH and temperature, independently, did not significantly impact the release profile of the pDA coatings. However, when both the pH and temperature in which the coatings were created were elevated (pH 8.5 at 35°C), there was a significant increase in the quantity of H_2O_2 generated by the surface coatings.
- All pDA coatings significantly increased the hydrophilicity of the stainless steel surface and had similar chemical compositions.
- pDA coatings that released more significant quantities of H_2O_2 were found to have a lower degree of polymerization, which correlates to larger amounts of unoxidized OH groups.

- Sterilization methods did not significantly impact the release quantity from pDA surface coatings.
- The pDA surface coatings were able to be stored for up to three weeks before a 50% reduction in H_2O_2 release was observed. However, the most significant loss of release occurs in the first five days regardless of being stored in an inert environment.

6.1.2 Chapter 3

When exposed to model bacteria strains, the pDA surface coatings significantly reduced the quantity of adhered bacteria to the surface of medical-grade stainless steel with varying surface roughness.

- *E. coli* adhesion was reduced by up to 70% on a stainless steel coupon with a standard surface finish coated with the High Release pDA surface coating. The reduction with the addition of the Low Release pDA coating depended on the surface finish of the coupon.
- *S. epi* adhesion was not affected when the Low Release pDA surface coating was added to stainless steel coupons; however, adhesion was increased with the High Release pDA coating.
- *P. cryo* adhesion was reduced by adding the High Release pDA surface coating on stainless steel on all tested surface finishes.
- *T. skag* adhesion was reduced by adding the Low Release and High Release pDA surface coatings on all tested surface finishes.

6.1.3 Chapter 4

Model cells exposed to bolus and continuous doses of H_2O_2 exhibited a difference in cytotoxic behavior. Overall, cells were able to withstand greater cumulative amounts of H_2O_2 when the concentration in solution was gradually increased over a prolonged period.

- L929 fibroblasts exhibited a slight drop in viability when exposed to a bolus dose of H_2O_2 of 200µM. Still, they did not show a decrease in viability when exposed to either the Low Release pDA coatings or the High Release pDA coatings.
- HeKa cells, when exposed to a bolus dose greater than 50µM, exhibited a significant decrease in viability. Similar to L929 fibroblasts, HeKa cells did not show this same

drop in viability when insulted with a continuous concentration of H_2O_2 from Low Release or High Release pDA coatings.

- When exposed to a bolus dose of H_2O_2, pre-adipocytes increased in number when exposed to larger quantities. When exposed to the Low Release pDA coatings, there was an increase in the number of live cells; however, the same increase was not observed when exposed to the High Release pDA coating.

6.1.4 Chapter 5

The prolonged exposure to a stable concentration of H_2O_2 in solution can induce the expression of the antimicrobial peptide dermcidin and promote differentiation of pre-adipocytes.

- More endogenous dermcidin was present in response to a bolus dose of H_2O_2; however, MeWo cells' viability after a bolus dose was significantly impaired. When exposed to a prolonged release of H_2O_2 via the Low Release and High Release pDA coatings, there was a slight elevation in the endogenous dermcidin present after 24 hours. However, the survival of the cells was significantly greater after exposure to the pDA coatings compared to bolus doses.
- H_2O_2 delivered in a bolus dose prior to differentiation decreased the proportion of pre-adipocytes that successfully differentiated.
- Differentiation after exposure to a stable concentration of H_2O_2 generated from Low Release and High Release pDA coatings was not significantly increased or reduced.
- Differentiation was increased when pre-adipocytes were exposed to continuous H2O2 concentrations generated from High Release pDA surface coatings.

6.2 Limitations

The main factor limiting the scope of this work is the lack of cetacean-derived cell lines and bacteria species found in the healthy microbiome on cetacean skin. As cetaceans live their entire lives underwater, the cells located in blubber tissue are more likely to experience prolonged hypoxic periods. This fact and the fact that reactions to H_2O_2 are cell-dependent make it highly probable that the difference in species will confer a difference in tolerance to oxidative stress. In addition to the differences for cell types within the tissue, the bacteria located on the material's surface may also exhibit varying

tolerances to H_2O_2 generated from pDA surface coatings. The tested aquatic bacteria were isolated from either Siberian permafrost (*Psychrobacter cryohalolentis*) or the pelagic zone in the ocean (*Tenacibaculum skagerrakense*).

A second limitation centers on this work only taking place using medical-grade stainless steel. The sensitive nature of pDA coating deposition makes it highly dependent on the underlying substrate surface chemistry. A second prominently used metal in conservation practices is titanium. The release profile from pDA coatings on medical-grade stainless steel is unlikely to be identical on titanium. Therefore, for a coating to be employed in the field, it would need to be optimized based on the substrate to be coated.

6.3 Future Directions

Field Applications

The High Release pDA surface coatings developed in this work were deployed into right whales off the coast of Argentina in the summer of 2021. While it is difficult to evaluate the efficacy of the pDA coatings in preventing bacterial adhesion in the field due to low rates of baseline infection, the effect on the visual appearance of the wound could indicate the health of the surrounding tissue. In addition to visual analysis, the pDA surface coatings could be applied to less permanent devices such as biopsy darts or LIMPET tags.

Effects of chronic exposure to H_2O_2

Due to the short half-life of H_2O_2, creating a material capable of maintaining a stable concentration in solution is complex. This work has developed a material that can act as a vehicle to generate H_2O_2 in significant quantities over a prolonged period and maintain a stable solution concentration below 500μM. This makes pDA a good vehicle for delivering H_2O_2 to various cell types that play crucial roles in wound healing so that chronic responses to oxidative stress from ROS can be evaluated. It is possible that the de-differentiation of adipocytes can be triggered through chronic oxidative stress, as seen in chapter 5.

Functionalization

In addition to evaluating the effects these coatings have in cetacean conservation applications, these coatings could also act as a priming layer to improve the attachment of

AMPs. The AMP dermcidin is effective against both gram-positive and gram-negative bacteria and as an effective antiviral. Functionalizing pDA surface coatings with this AMP would further the antimicrobial character while maintaining any benefits the prolonged release of H_2O_2 would have on surrounding tissue.

6.3 REFERENCES

Dowding, J.E. (1977). Mechanisms of gentamicin resistance in Staphylococcus aureus. *Antimicrob Agents Chemother* 11(1)**,** 47-50. doi: 10.1128/AAC.11.1.47.

Goudarzi, F., Mohammadalipour, A., Bahabadi, M., Goodarzi, M.T., Sarveazad, A., and Khodadadi, I. (2018). Hydrogen peroxide: a potent inducer of differentiation of human adipose-derived stem cells into chondrocytes. *Free Radic Res* 52(7)**,** 763-774. doi: 10.1080/10715762.2018.1466121.

IWC (2020). Report of the Joint US Office of Naval Research, International Whaling Commission and US National Oceanic and Atmospheric Administration Workshop on Cetacean Tag Development, Tag Follow-up and Tagging Best Practices.

Jumabay, M., Matsumoto, T., Yokoyama, S., Kano, K., Kusumi, Y., Masuko, T., et al. (2009). Dedifferentiated fat cells convert to cardiomyocyte phenotype and repair infarcted cardiac tissue in rats. *J Mol Cell Cardiol* 47(5)**,** 565-575. doi: 10.1016/j.yjmcc.2009.08.004.

Juven B, and M.D., P. (1996). Antibacterial Effects of Hydrogen Peroxide and Methods For Its Detection and Quantitationt. *Journal of Food Protection* 59**,** 8.

Kershaw, J.L., Botting, C.H., Brownlow, A., and Hall, A.J. (2018). Not just fat: investigating the proteome of cetacean blubber tissue. *Conserv Physiol* 6(1)**,** coy003. doi: 10.1093/conphys/coy003.

Livermore, D.M. (2000). Antibiotic resistance in staphylococci. *International Journal of Antimicrobial Agents* 16**,** 3-10. doi: https://doi.org/10.1016/S0924-8579(00)00299-5.

Niethammer, P., Grabher, C., Look, A.T., and Mitchison, T.J. (2009). A tissue-scale gradient of hydrogen peroxide mediates rapid wound detection in zebrafish. *Nature* 459(7249)**,** 996-999.

Robbins, J., Zerbini, A.N., Gales, N., Gulland, F.M., Double, M., Clapham, P.J., et al. (2013). Satellite tag effectiveness and impacts on large whales: preliminary results of a case study with Gulf of Maine humpback whales. *Paper SC/65a/SH05 presented to the IWC Scientific Committee*.

Ryu, J.H., Messersmith, P.B., and Lee, H. (2018). Polydopamine Surface Chemistry: A Decade of Discovery. *ACS Applied Materials & Interfaces* 10(9)**,** 7523-7540. doi: 10.1021/acsami.7b19865.

Shaikh, S., Fatima, J., Shakil, S., Rizvi, S.M., and Kamal, M.A. (2015). Antibiotic resistance and extended spectrum beta-lactamases: Types, epidemiology and treatment. *Saudi J Biol Sci* 22(1)**,** 90-101. doi: 10.1016/j.sjbs.2014.08.002.

Tyo, A., Welch, S., Hennenfent, M., Kord Fooroshani, P., Lee, B.P., and Rajachar, R. (2019). Development and Characterization of an Antimicrobial Polydopamine Coating for Conservation of Humpback Whales. *Frontiers in Chemistry* 7(618). doi: 10.3389/ fchem.2019.00618.

Appendix A

Reprinting Permissions

As all the data in this work was published through open-source publications there is no additional permission required to reprint. Permission was granted from the publishing author and the work was appropriately cited.

APPENDIX B

CHAPTER 2 SUPPLEMENTARY FIGURES

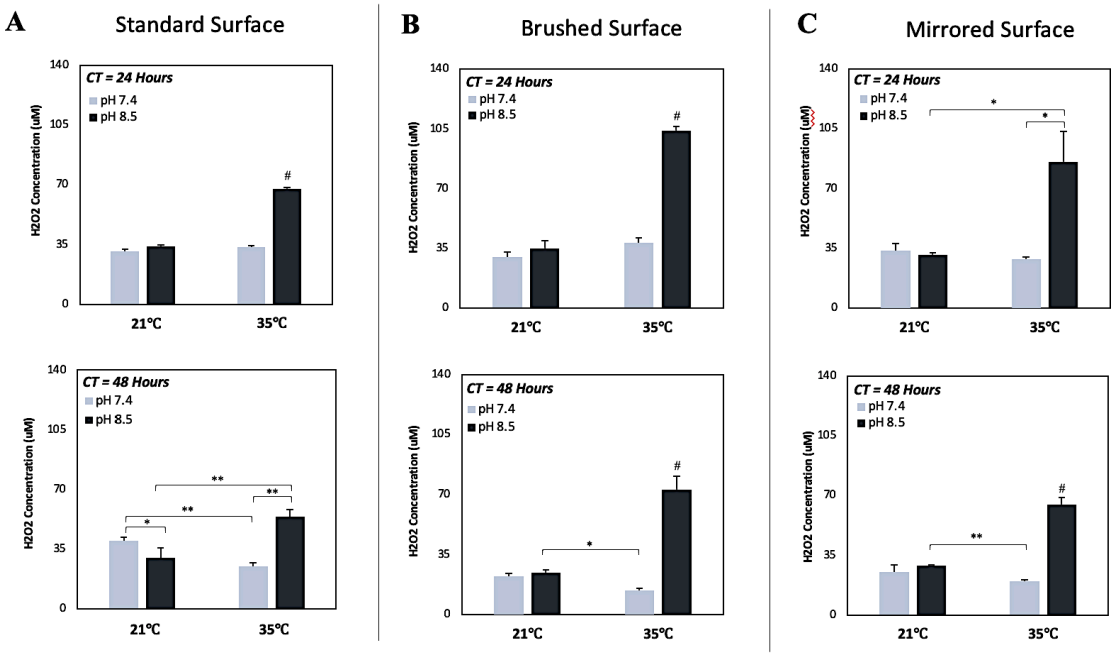

Figure B.1 | *Hydrogen peroxide solution concentration after a 24-hour period on various surface finishes.* Hydrogen peroxide release measured over a 24-hour period on samples with a coating time (CT) of 24 and 48-hours for (A) standard, (B) brushed, and (C) mirrored surface finishes. # indicates a significant differences from all other conditions ($p<0.05$); individual significant differences are indicated by a * ($p<0.05$) or ** ($p<0.01$).

Appendix C

Chapter 3 Supplementary Figures

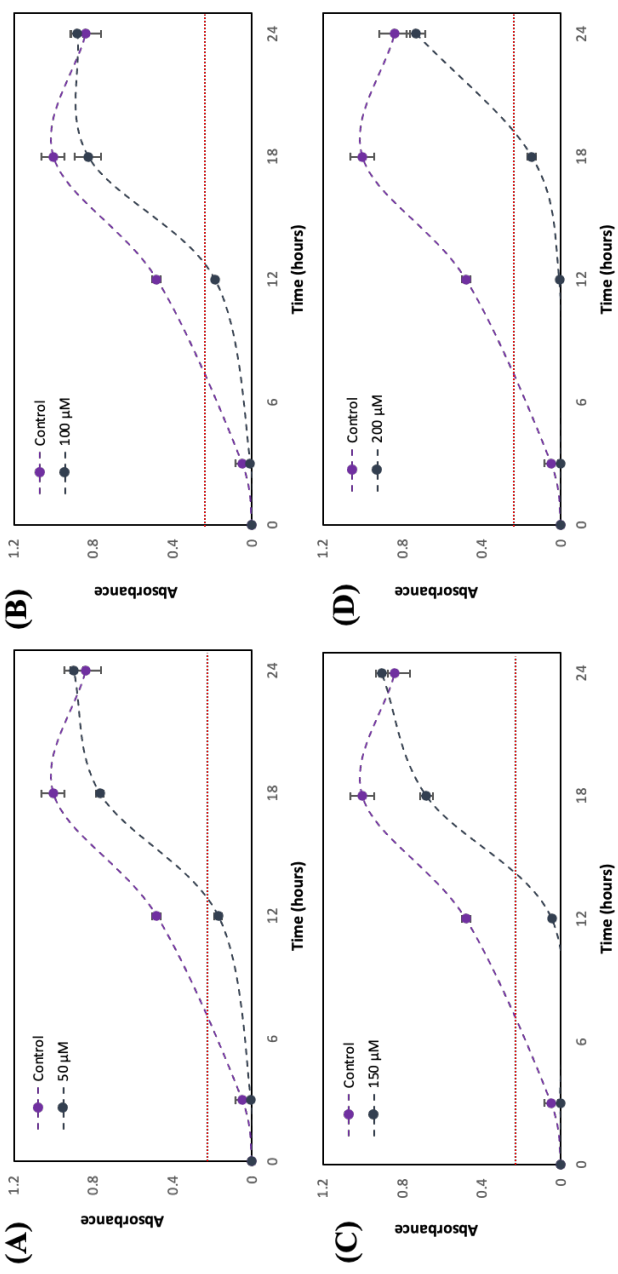

Figure C.1 | *S. epi growth over a 24-hour period with different initial doses of hydrogen peroxide. S. epi* bacteria growth was measured using absorbance readings at 400nm with different initial doses of H_2O_2. The control was used to determine typical bacterial growth without the presence of H_2O_2. (a) Growth was slowed with the addition of a 50µM dose. No additional inhibition was observed with doses of (b) 100µM and (c) 150µM. (d) At 200µM dosing, bacteriostatic conditions were achieved for 18 hours. The red line represents a threshold used to indicate bacteriostatic behavior (absorbance = 0.20).

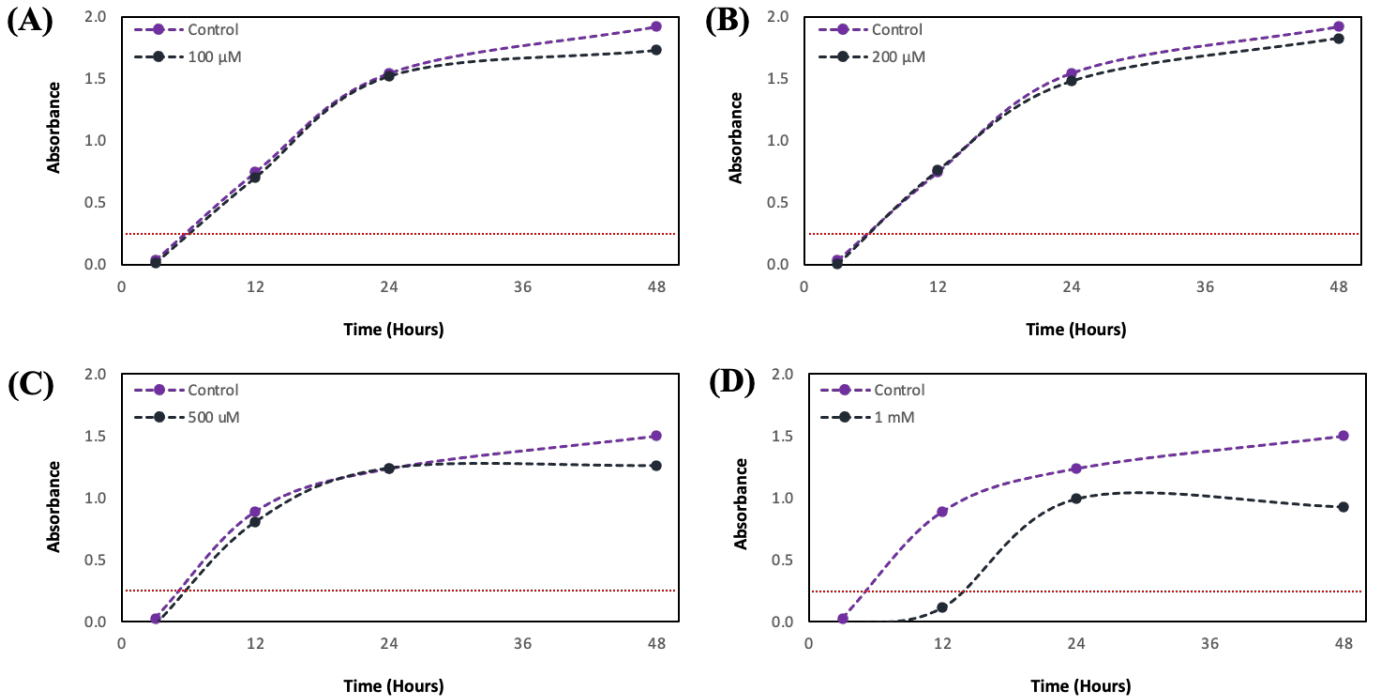

Figure C.2 | *E. coli growth over a 48-hour period with different initial doses of hydrogen peroxide. E. coli* bacterial growth was measured using absorbance readings at 400nm with different initial doses of H_2O_2. The control for this experiment was typical bacterial growth without the presence of H_2O_2. There was induction of bacteriostatic behavior is any dose less than 1mM. 1mM of H_2O_2 induced bacteriostatic behavior for 12 hours and reduced overall bacterial growth over a 48-hour period. The red line represents a threshold used to indicate bacteriostatic behavior (absorbance = 0.20).

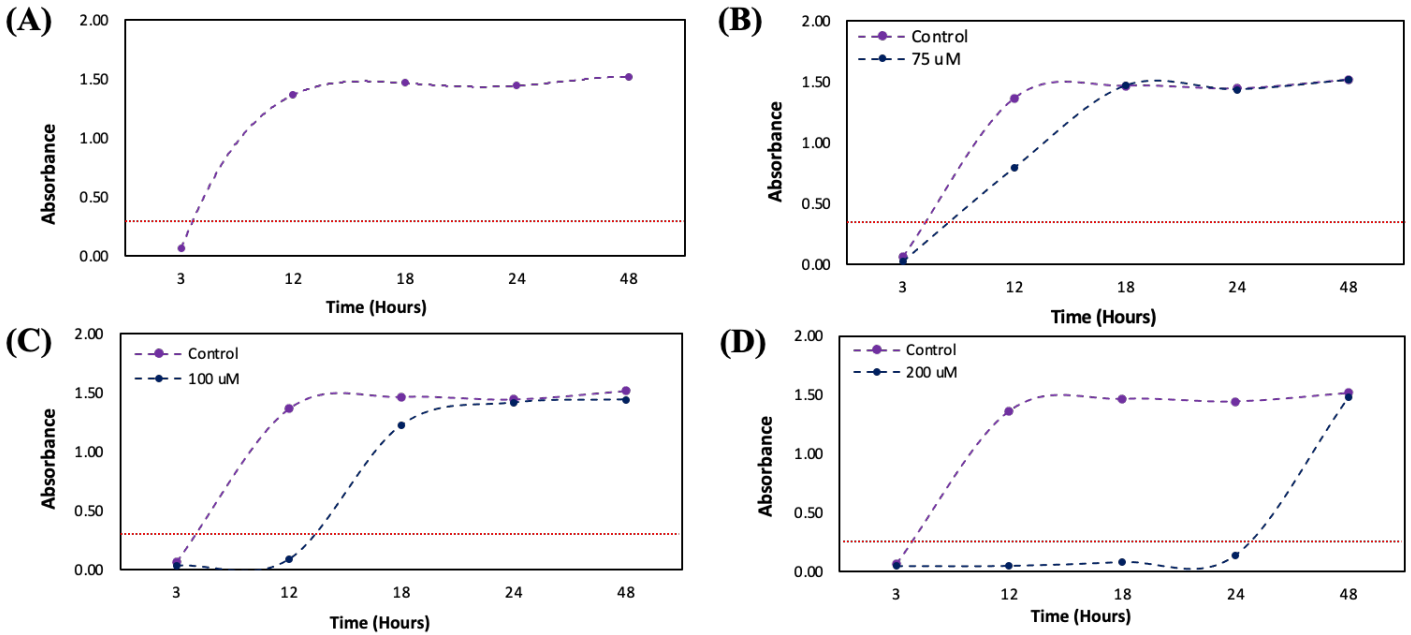

Figure C.3 | *P. cryo growth over a 48-hour period with different initial doses of hydrogen peroxide. P. Cryohalolentis* bacteria growth was measured using absorbance readings at 400nm with different initial doses of H_2O_2. (A) The control was used to determine typical bacterial growth. (B) Growth was first slowed at a dose of 75µM. (C) At 100µM dosing, bacteriostatic conditions were achieved. (D) At 200µM bacteriostatic conditions were maintained for 24 hours.

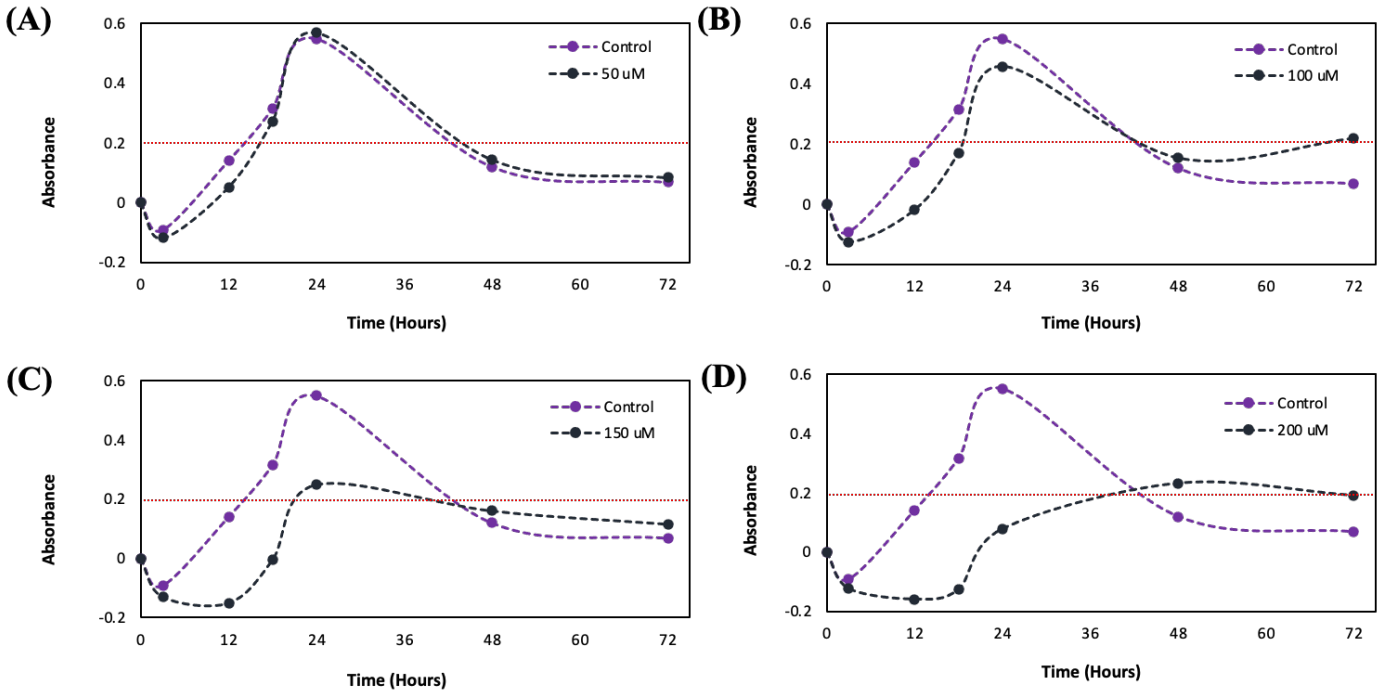

Figure C.4 | *T. skag growth over a 72-hour period with different initial doses of hydrogen peroxide. T. skag* bacterial growth was measured using absorbance readings at 400nm with different initial doses of H_2O_2. The control was used to determine typical bacterial growth without the presence of H_2O_2. A dose greater than 100µM was required to begin to induce any significant alterations in the growth profile of *T. skag*. A dose of 150µM of H_2O_2 induced a bacteriostatic response for 18 hours, an increase of that dose to 200µM extended the bacteriostatic behavior to 24 hours. The red line represents the threshold used to indicate bacteriostatic behavior (absorbance = 0.20).

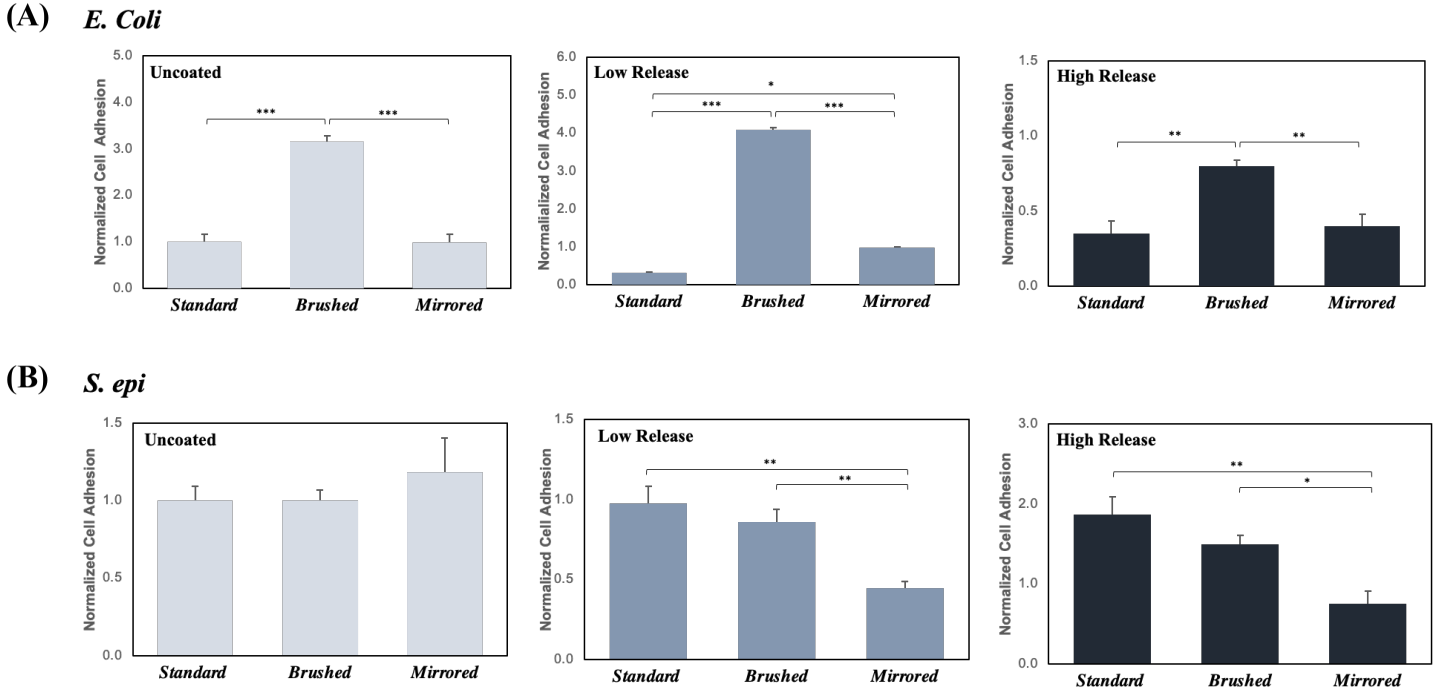

Figure C.5 | *Adhesion of terrestrial bacteria to the surface of 316 SS coupons with varying surface finishes.* Coupons with varying surface finishes (Standard [Ra = 0.635µm], Brushed [Ra =0.813µm], and Mirrored [Ra = 0.15µm]) were coated using both the Low Release (pH 7.4, 21°C) and High Release (pH 8.5, 35°C) coating conditions then incubated in a bacterial solution for 24 hours and adhesion was evaluated. (A) Adhesion of *E. coli* was evaluated after coupons were incubated for 6 hours. With and without pDA coatings an increased adhesion was observed on the brushed surface finish when compared to both the standard and mirrored surfaces. The only other difference between surface finishes was observed with the Low Release coupons; there was significantly more adhesion on the mirrored surface when compared to the standard surface. (B) The mirrored coupons with both the Low Release and High Release pDA coatings significantly reduced bacterial adhesion while there was no reduction in adhesion observed on the uncoated mirrored surface when compared to the standard surface finish. A * is used to indicate a significant difference (* $p<0.05$ | ** $p<0.01$ | *** $p<0.001$).

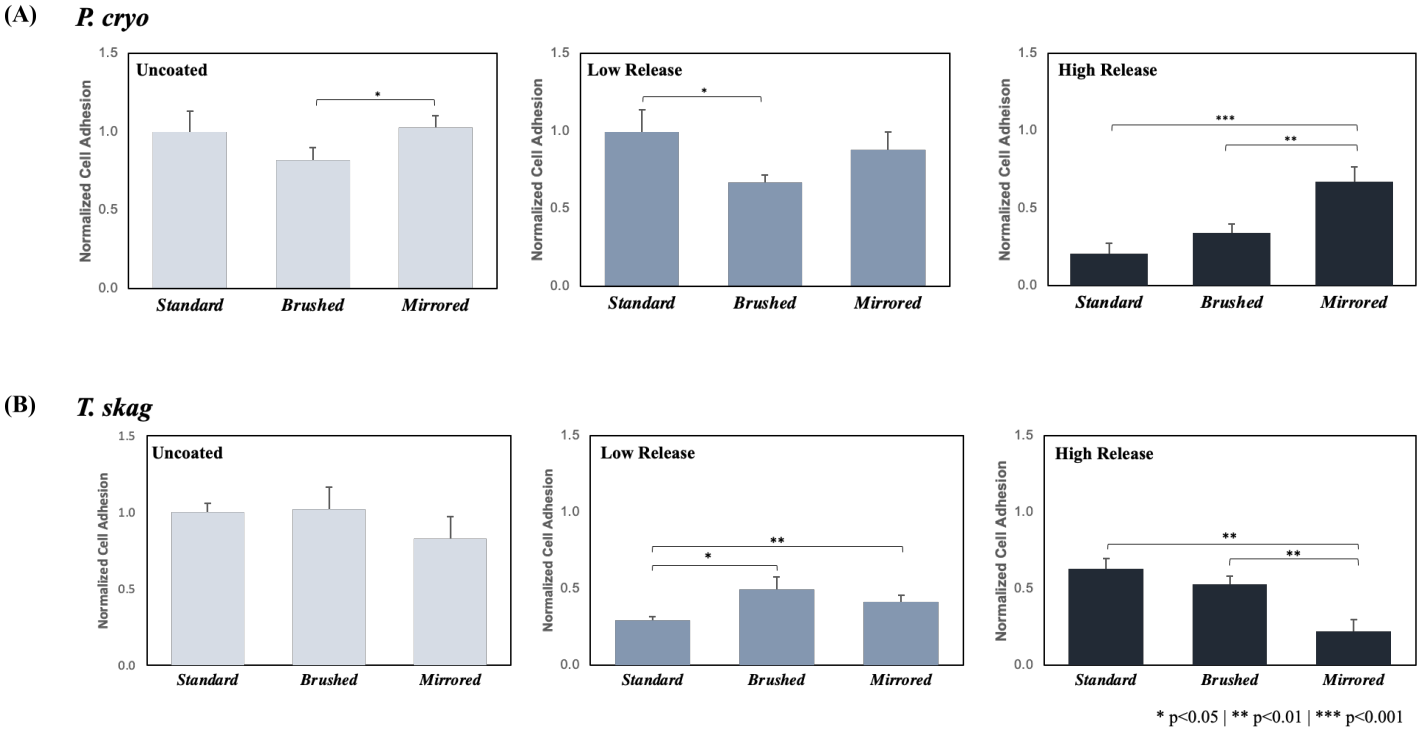

Figure C.6 | *Adhesion of aquatic bacteria to the surface of 316 SS coupons with varying surface finishes.* (A) There was a significant difference between uncoated brushed and mirrored coupons and Low Release standard and brushed coupons. The mirror finish coupons that were coated with the High Release pDA coatings exhibited significantly more bacterial adhesion when compared to the standard and brushed finished coupons with the same pDA coating. However, the increase in adhesion over the other surface finishes does not correspond to an increase when compared to the respective uncoated mirrored surface. (B) There was a significant reduction in adhesion on mirrored surfaces with the addition of the High Release pDA surface coating when compared to brushed and standard surface finishes. There was also significantly more adhesion on mirrored and brushed surfaces when compared to a standard surface for Low Release pDA coatings. There was no statistically significant difference between the bacterial adhesion on the uncoated surfaces regardless of surface finish.

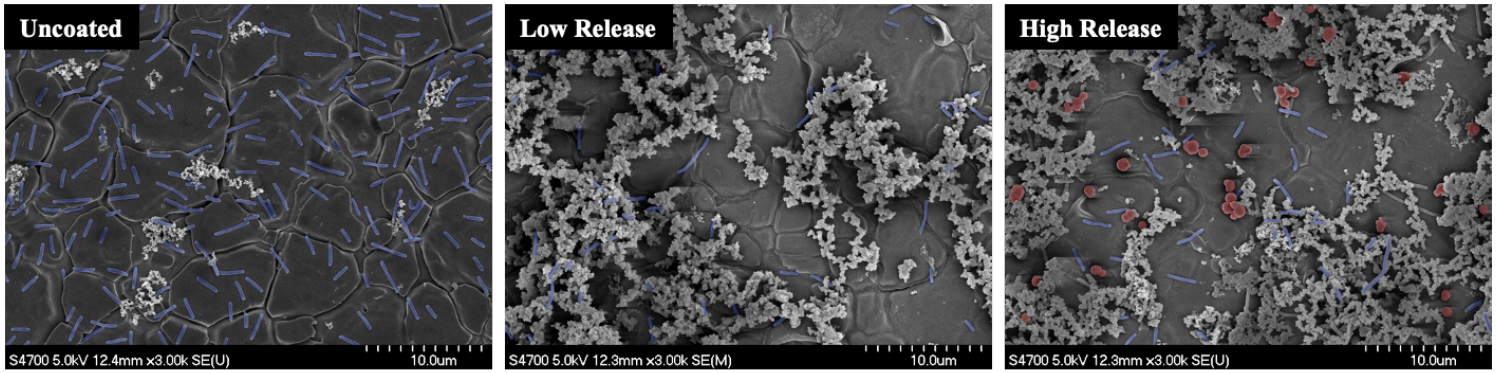

Blue = Exponential growth
Red = Stagnant growth

Figure C.7 | *Representative images of T. skag on the surface of stainless steel coupons with a standard surface finish.* Coupons a standard surface finish [Ra = 0.635µm] were coated using both the Low Release (pH 7.4, 21°C) and High Release (pH 8.5, 35°C) coating conditions. The coupons were then incubated for 24 hours in a solution of *T. skag* and the adhesion was evaluated. On the uncoated and Low Release pDA coated surfaces, all bacteria were in the exponential growth phase (indicated by the rodlike/spindly morphology – highlighted in blue). On the High Release pDA coated surface, there was an increase in the proportion of bacteria which were in the stagnant growth phase (indicated by the round/globular morphology – highlighted in red).